SRS-TR148
11 August 1967

EFFECT OF BIAS ERRORS ON INTERPLANETARY NAVIGATION AND GUIDANCE SYSTEM PERFORMANCE

Contract No. NAS8-20358

Prepared for
NATIONAL AERONAUTICS AND SPACE ADMINISTRATION
MARSHALL SPACE FLIGHT CENTER
Huntsville, Alabama

PHILCO Ford
PHILCO-FORD CORPORATION
Space & Re-entry Systems Division
Palo Alto, California

EFFECT OF BIAS ERRORS ON INTERPLANETARY NAVIGATION AND GUIDANCE SYSTEM PERFORMANCE

Contract No. NAS8-20358

11 August 1967

Prepared by

Paul J. Rohde

PHILCO-FORD CORPORATION
Space and Re-entry Systems Division
Palo Alto, California

for

National Aeronautics and Space Administration
Marshall Space Flight Center
Huntsville, Alabama

FOREWORD

The research presented in this report was performed for the Astrionics Laboratory of the George C. Marshall Flight Center, Huntsville, Alabama. This report is the final report on the interplanetary navigation and guidance study task under NASA Contract NAS 8-20358. The results presented here extend the scope of the navigation and guidance study completed under Contract NAS 8-11198.

TABLE OF CONTENTS

TABLE OF CONTENTS (Cont'd)

LIST OF ILLUSTRATIONS

LIST OF ILLUSTRATIONS (Cont'd)

LIST OF ILLUSTRATIONS (Cont'd)

LIST OF ILLUSTRATIONS (Cont'd)

LIST OF TABLES

ABSTRACT

The primary objective of the Navigation and Guidance research task of Contract NAS 8-20358 is to critically assess the influence of the constraints imposed on the study performed under Contract NAS 8-11198 on the results obtained. The study has analyzed the influence of bias error sources on the navigation and guidance requirements for a round-trip Mars mission. The equation of motion bias errors considered are: (1) Astronomical Unit Conversion, (2) Solar-Radiation Pressure, (3) Mars' Planetary Mass, and (4) Earth's Planetary Mass. The measurement bias errors considered are: (1) Sextant Angle Measurement Bias, and (2) Onboard Clock Bias. The navigation system used in the analysis consists of a sextant with a 10 arc second accuracy. The measurement data are processed with a Kalman filter.

The theoretical analysis of the effect of bias error sources on the estimation process is presented. Recent theoretical developments are presented that concern three areas of interest in this study. An analysis is presented that shows the error introduced in an estimation process due to neglecting both equation of motion and measurement bias error sources in the modeling of the physical process. A second analysis shows the capability of separating the effects due to bias error sources from those due to random errors. Finally, techniques are presented for efficient parametric analysis by means of matrix manipulations.

Data results are presented that show the effect of bias errors on the navigation and guidance requirements. The results are presented in terms of end point constraint estimate accuracies and velocity requirements, respectively. The only equation of motion bias error that significantly limits the navigation system performance is the uncertainty in the mass of Mars. An uncertainty of 150 km^3/sec^2, produces an uncertainty in the entry altitude at Mars of 4 to 5 km. The two measurement bias errors contribute significant estimation errors when they are neglected. Expanding the state being estimated to include the measurement bias error sources, allows the navigation system to be calibrated with the resulting improved performance.

The midcourse guidance velocity requirements are significantly altered by the equation of motion errors. The trajectory deviations due to the bias errors cannot be accurately estimated until the final portion of the trajectory at which time they must then be corrected by the guidance system. An example cited for an Earth-Mars trajectory shows an increase in the velocity requirements from 23 meters/second with no equation of motion errors to 41 meters/second with uncertainties in the A.U. conversion and Mars' planetary mass.

SECTION I

INTRODUCTION

1.1 GENERAL OBJECTIVES AND SCOPE

The primary objective of the Navigation and Guidance research task of Contract NAS-8-20358 is to critically assess the influence of the constraints imposed on the study performed under Contract NAS-8-11198 on the results obtained[1]. Research under Contract NAS-8-11198 established the basic requirements for an Advanced Spaceborne Detection, Tracking and Navigation System capable of performing future interplanetary missions. The constraints on the original study that are analyzed in this research report are the following:

(1) The assumption that the only significant error sources are random in nature.

(2) The original choice of 1975 round-trip Mars trajectory.

In order to analyze the influence of these constraints on the previous results, several tasks had to be completed:

(1) Research and analysis of the literature available on the techniques used to estimate the various physical constants that are required to specify an interplanetary trajectory. The uncertainty associated with each of these estimates constitutes a bias error in the equations of motion of a spacecraft.

(2) Determine the types of measurement bias errors to be considered.

---

(1) Superscripts refer to references listed in Section 8.

(3) Derive suitable mathematical models to analyze the influence of the equation of motion and measurement bias errors on the trajectory estimation process.

(4) Develop methods for data presentation which indicate the importance of the bias error sources.

(5) Determine the areas which require future research.

The scope of the study includes an evaluation of the onboard navigation system performance under the influence of the following bias errors.

(1) Equation of Motion Errors

a. Uncertainty in the Astronomical Unit conversion
b. Uncertainty in the Earth's mass
c. Uncertainty in Mars' mass
d. Uncertainty in the solar radiation pressure

(2) Measurement Biases

a. Sextant bias in onboard measurement
b. Time bias in onboard clock

The results that are obtained show the effects of these bias errors on the navigation system performance. In order to make the problem amenable to study, certain restrictions on the scope had to be made.

(1) The covariance matrix of injection errors at Earth is not studied as a parameter. This matrix, which is a function of the time in park orbit at Earth, is intended to be representative of the capabilities of future launch vehicle guidance systems. The primary influence of this matrix is on the magnitude of the midcourse velocity requirements at the first guidance correction.

(2) The study emphasizes the following phases of the mission:

a. Midcourse from Earth to Mars

b. Midcourse from Mars to Earth.

(3) The onboard navigation instrument is a sextant with a random measurement error of 10 arc seconds. The error magnitude is not studied parametrically. This random error is a parameter in the original study. The measurement schedules used are also derived from the original study.

(4) The guidance system analysis is restricted to evaluation of trajectory deviation corrections rather than a statistical analysis. This is due to both theoretical and simulation limitations in the analysis of the effects of bias errors on the guidance system performance.

1.2 STUDY FORMAT

The effect of bias errors on the navigation system performance may vary considerably depending on the mission itself. This study is designed to identify the error sources and show their effect on the system performance for a variety of trajectories.

The study was performed in four basic steps. The results of each step are presented in the order that they were performed.

(1) Analysis of applicable filter theory

(2) Analysis of bias error sources.

(3) Computer simulation.

(4) Generate results.

Section 2 contains a description of the theoretical aspects of Kalman filtering with bias errors present in the system. There are several new

and interesting developments presented that are incorporated in the study. These developments concern the following areas of interest.

(1) The effects of neglecting bias errors.

(2) Separable properties of bias error effects from the effects of random errors.

(3) Computer end of run observations that greatly simplify parametric type analyses.

Section 3 presents a description of the bias errors that are considered in the study. A particular emphasis is placed on the equations of motion parameters. The uncertainty in the astronomical unit conversion is discussed in detail and a model described for analyzing its effect on an interplanetary trajectory.

The digital computer simulations that are utilized in the study are described in Section 4.

The results of the parametric analyses for the outbound and return trajectories are presented in Section 5.

The tables and figures that are discussed in the report are presented at the end of the report.

SECTION 2

THEORETICAL ANALYSIS OF OPTIMAL ESTIMATION PROCESS

The function of the navigation system, as defined in this report, is to obtain an estimate of vehicle state based on either direct observations of the vehicle (Earth-based tracking) or observations of celestial bodies whose positions are known (on-board tracking). The purpose of this section is to describe the error analysis techniques that have been used to study the effects measurement and equation of motion parameter uncertainties on the vehicle state estimation process.

The following presentation of the orbit estimation process is based on the filtering theory of Kalman[2] and the orbit determination application by Schmidt[3,4,5]. The theory for including measurement and equation of motion bias type errors into the optimal orbit estimation process is presented in References 1 and 6. These references show three different techniques by which the bias errors in the estimation process can be handled. Each technique produces an optimal estimate but under a different assumption concerning the modeling of the dynamic and/or measurement bias error sources. The three techniques are the following.

(1) Neglect - In this case, the state being estimated is simply the three components of vehicle position and velocity. The dynamic and measurement models are assumed to be known perfectly and there are no bias errors in the physical process being analyzed. The effect of uncertainties in system parameters are neglected.

(2) Include - This technique allows for an expansion of the state vector to include specified dynamic and measurement parameters that produce bias error sources. The optimal estimation

process fits the measurement data to the model to obtain a best estimate of the vehicle state and the system parameters simultaneously.

(3) Consider - With this type of analysis, the measurement and dynamic parameters are not included in the state vector being estimated but the effects of the uncertainties in these parameters are considered in the estimation process. An optimal estimate of the state is obtained under the constraint that specified unsolved for system parameters have constant uncertainties (standard deviations) associated with their fixed estimates.

Each of these techniques has both favorable and unfavorable aspects. If the bias errors are neglected, the state vector is reduced in dimension and correspondingly the number of computations required in the estimation process is reduced. Alternately, the removal of bias errors from a problem in which they can significantly influence the results being obtained causes the state estimates that are obtained to have optimistic uncertainties attached to them. The implication here is that an analysis must be made to establish the relative importance of measurement and dynamic bias error sources to a particular orbit estimation process. On the basis of this analysis, the method for treating each of the error sources can be established. The allowable total size of the state vector would be limited by the computer capability either ground or onboard in terms of its size and speed. Within these limitations, the filtering techniques used for the various bias errors sources in the order of decreasing importance would be to include, consider, and neglect them.

The second part of this section describes some recent developments on techniques for efficient parametric analysis of navigation system performance. The theory is based primarily on the fine work of Gunckel[7]. The techniques apply to two areas: the effect of bias errors that are not included in the optimal filter, and the effect of varying the initial

state variable (bias error) uncertainty covariance matrix. The important feature of these techniques is that they are applied to the data obtained at the conclusion of a single computer run of an orbit determination simulation. The parametric analysis is accomplished by means of matrix manipulations of the end point data and thereby eliminates the need for making a large number of computer analysis runs when scanning a range of parametric values of the initial error variances.

2.1 SYSTEM DESCRIPTION

The Kalman filter optimal estimation process is based on minimizing a loss function for a linear dynamical system. In order to get a linear system of equations for the orbit determination process, a linearization is performed about the "best estimate" of the state of the nonlinear system.

The equations of motion of the spacecraft may in general be written as a set of nonlinear differential equations of the form

$$\dot{X} = F(X, U, T) \qquad (2\text{-}1)$$

The n dimensional vector, X, defines the vehicle state, U is an ℓ dimensional vector of control and forcing functions. Uncertainties in the functions, U, will be referred to as "equation of motion bias errors". The observations or measurements are in general related to the state X by

$$Y = G(X, V, t) + q(t) \qquad (2\text{-}2)$$

The m dimensional vector, V, defines the measurement parameters and q is the random measurement noise. Uncertainties in the vector, V, will be referred to as "measurement bias errors." Linearization of equations 2-1 and 2-2 about a nominal trajectory yields the following.

$$\dot{x} = \left(\frac{\partial F}{\partial X}\right) x + \left(\frac{\partial F}{\partial U}\right) u \equiv A(t)\, x + B(t)\, u \qquad (2\text{-}3)$$

$$y = \left(\frac{\partial G}{\partial X}\right) x + \left(\frac{\partial G}{\partial V}\right) v + q \equiv H(t)\, x + D(t)\, v + q(t) \qquad (2\text{-}4)$$

The solution of (2-3), for constant controls over the interval $t_1 \leq t \leq t_2$, may be expressed as

$$x(t_2) = \varphi(t_2, t_1)\, x(t_1) + \varphi_u(t_2, t_1)\, u(t_1) \qquad (2\text{-}5)$$

where φ is the nxn state transition matrix that relates a deviation in the state at t_1 to a deviation at t_2, and φ_u is an $n \times \ell$ matrix that relates the deviation in the state at t_2 to a unit variation in the control at t_1. The elements of φ and φ_u are referred to as sensitivity coefficients. In general φ and φ_u are computed by numerical integration of the variational equations with appropriate initial conditions.

The solution of the linearized differential equations of spacecraft motion (equation 2-5) and the state measurements or observations (equation 2-4) represent the physical process shown in Figure 2-1. The figure is drawn with fat lines to represent the fact it is a matrix block diagram. The three procedures that are used to model and estimate the bias errors shown in Figure 2-1 are discussed in the next sections.

2.2 KALMAN FILTER THEORY

Derivations of the optimal Kalman filter for different dynamic and measurement models are presented in many references.[1-8] The theory presented in the following paragraphs will draw heavily from techniques used in References 6, 7, and 8.

2.2.1 Bias Errors Neglected

The navigation analysis performed during the initial study[1] neglected the effects of the bias errors, u and v, shown in Figure 2-1. The optimal filter for the case of neglecting these errors will be derived below[8]. The derivation will be followed by an analysis[7] of the error in the estimate due to the fact the bias error sources are neglected in the filter.

The recursive linear estimation problem may be stated as follows. Given the physical process shown in Figure 2-1 determine an estimate, $\hat{x}_n(t)$, of the state at t that is a linear combination of an estimate at $t-1$ and the measurement data y. The estimate must be "best" in the sense that the expected value of the sum of the squares of the error in the estimate is a minimum (minimum variance estimate). That is, $\hat{x}_n(t)$ is to be chosen so that

$$E\left[\left(\hat{x}_n(t) - x(t)\right)^T \left(\hat{x}_n(t) - x(t)\right)\right]^* = \text{minimum} \qquad (2\text{-}6)$$

The dynamics of the system are described by the homogeneous linear difference equation

$$x(t) = \Phi(t, t-1)\, x(t-1) \qquad (2\text{-}7)$$

The measurements, y, are linearly related to the state and corrupted by additive noise.

$$y(t) = H(t)\, x(t) + q(t) \qquad (2\text{-}8)$$

The Kalman filter equation shall be derived for the model described by equations (2-7) and (2-8).

---

* E[ ] means expected value of bracketed quantity.

The form of a linear estimation equation can be hypothesized from the physical characteristics of the system. The state evolves according to (2-7) so, given an estimate $\hat{x}_n$ at t-1, it is reasonable to predict the estimate at t as

$$\hat{x}(t) = \varphi(t, t-1)\, \hat{x}_n(t-1) \qquad (2\text{-}9)$$

when no information is available. A measurement at t can be used to modify the estimate. Based on $\hat{x}(t)$ and (2-8), one would expect the measurement value at t to be $H(t)\, \hat{x}(t)$. An error in the estimate is reflected by an error in this expected measurement value.

$$e(t) = y(t) - H(t)\, \varphi(t, t-1)\, \hat{x}_n(t-1) \qquad (2\text{-}10)$$

The estimate is to be a linear function of the new measurements. Define an unknown "gain" matrix, K(t), such that the new estimate $\hat{x}_n$ at t after inclusion of the observation is given by

$$\hat{x}_n(t) = \hat{x}(t) + K(t) \left[y(t) - H(t)\, \hat{x}(t) \right] \qquad (2\text{-}11)$$

The linear filter described by equations (2-9) and (2-11) is shown in block form in Figure 2-2.

The matrix K(t) shall be determined so that $E\left[\left(\hat{x}_n(t) - x(t)\right)^T \left(\hat{x}_n(t) - x(t)\right)\right]$ is minimized. It shall be referred to as the weighting or gain matrix.

Let

$$\tilde{x}_n(t) = \hat{x}_n(t) - x(t) \qquad (2\text{-}12)$$

then

$$E\left[\left(\hat{x}_n(t) - x(t)\right)^T \left(\hat{x}_n(t) - x(t)\right)\right] = E\left[\tilde{x}_n(t)^T \tilde{x}_n(t)\right] \quad (2\text{-}13)$$

This can be rewritten as

$$E\left[\tilde{x}_n(t)^T \tilde{x}_n(t)\right] = \text{trace } E\left[\tilde{x}_n(t)\, \tilde{x}_n(t)^T\right] \quad (2\text{-}14)$$

where the trace is defined as the sum of the diagonal elements of a matrix. Define the matrix $P_n(t)$ as

$$P_n(t) \equiv E\left[\tilde{x}_N(t)\, \tilde{x}_n(t)^T\right] \quad (2\text{-}15)$$

Now, form $\tilde{x}_n(t)$ using equation (2-11)

$$\begin{aligned}\tilde{x}_n(t) &= \left[\varphi(t,t\text{-}1)\, \hat{x}(t\text{-}1) + K(t)\left(y(t) - H(t)\, \varphi(t,t\text{-}1)\, \hat{x}(t\text{-}1)\right)\right] - \varphi(t,t\text{-}1)\, x(t\text{-}1) \\ &= \varphi(t,t\text{-}1)\, \tilde{x}(t\text{-}1) - K(t)\, H(t)\, \varphi(t,\, t\text{-}1)\, \hat{x}(t\text{-}1) + K(t)\left(H(t)\, x(t) + q(t)\right) \\ &= \left(I - K(t)\, H(t)\right)\, \varphi(t,\, t\text{-}1)\, \tilde{x}(t\text{-}1) + K(t)\, q(t) \quad (2\text{-}16)\end{aligned}$$

From equation (2-16) the $P_n(t)$ matrix can now be formed

$$\begin{aligned}P_n(t) &= E\left\{\left[(I - KH)\, \varphi(t,\, t\text{-}1)\, \tilde{x}_n(t\text{-}1) + Kq\right]\left[(I\text{-}KH)\, \varphi(t,t\text{-}1)\, \tilde{x}_n(t\text{-}1) + Kq\right]^T\right\} \\ &= (I - KH)\, \varphi(t,t\text{-}1)\, E\left[\tilde{x}_n(t\text{-}1)\, \tilde{x}_n(t\text{-}1)^T\right]\, \varphi^T(t,\, t\text{-}1)\, (I - H^T K^T) \\ &\quad + K\, E\left[q\, \tilde{x}_n(t\text{-}1)^T\right]\, \varphi^T(t,\, t\text{-}1)\, (I - H^T K^T) \\ &\quad + (I - KH)\, \varphi(t,\, t\text{-}1)\, E\left[\tilde{x}_n(t\text{-}1)\, q^T\right]\, K^T + K\, E\left[q\, q^T\right] K^T \quad (2\text{-}17)\end{aligned}$$

By definition

$$E\left[q(t)\ q^T(t)\right] = Q(t)$$

$$E\left[\tilde{x}_n(t-1)\ \tilde{x}_n(t-1)^T\right] = P_n(t-1)$$

$$E\left[q(t)\ q^T(t-1)\right] = 0$$

$$E\left[q(t)\ \tilde{x}_n^T(t-1)\right] = 0 = E\left[\tilde{x}_n(t-1)\ q(t)^T\right]$$

Therefore $P_n(t)$ can be rewritten

$$P_n(t) = (I - KH)\ P(t)\ (I - KH)^T + KQK^T \qquad (2\text{-}18)$$

where

$$P(t) = \varphi(t,\ t\text{-}1)\ P_n(t-1)\ \varphi^T(t,\ t\text{-}1) \qquad (2\text{-}18a)$$

Expanding (2-18) gives

$$P_n(t) = P(t) - KHP(t) - P(t)H^TK^T + K(HP(t)\ H^T + Q)\ K^T \qquad (2\text{-}19)$$

The matrix $P(t)$ does not depend upon $K(t)$, so it is unaffected by the selection of $K(t)$. The matrix $(HP(t)\ H^T + Q)$ is symmetric and nonnegative-definite, so it can be written as the product of a matrix $S(t)$ and its transpose (i.e., a matrix square root).

$$S(t)S(t)^T = HP(t)H^T + Q \qquad (2\text{-}20)$$

The last three terms of (2-19) have the form of a quadratic matrix polynominal in terms of the unknown $K(t)$. Introduce (2-20) into (2-19) and

hypothesize the existence of a matrix $R(t)$ such that

$$P_n(t) = P(t) + (KS - R)(KS - R)^T - RR^t \qquad (2\text{-}21)$$

This procedure is the matrix equivalent of completing the square of a quadratic polynominal. Assuming that $S(t)S(t)^T$ is positive definite, it follows directly that

$$R(t) = P(t)\, H^T \left(S(t)^{-1}\right)^T \qquad (2\text{-}22)$$

Only the product term in (2-21) involves the gain matrix $K(t)$. The product of a matrix and its transpose is nonnegative-definite, so the trace of $P_n(t)$ is minimized by choosing

$$K(t)S(t) = P(t)\, H(t)^T \left(S(t)^{-1}\right)^T \qquad (2\text{-}23)$$

Thus the optimal gain matrix is

$$K(t) = P(t)\, H^T(t) \left[H(t)\, P(t)\, H^T(t) + Q(t)\right]^{-1} \qquad (2\text{-}24)$$

Substituting (2-24) and (2-22) into (2-21) shows that the convariance matrix $P_n(t)$ for the optimal gain is

$$P_n(t) = P(t) - P(t)\, H^T(t) \left[H(t)\, P(t)\, H^T(t) + Q\right]^{-1} H(t)\, P(t) \qquad (2\text{-}25)$$

Equations (2-9), (2-11), (2-18a), (2-18), and (2-24) constitute the Kalman filter for the model described by Equations (2-7) and (2-8). These equations are summarized below.

The time propagation of the state estimate is given by equation (2-9).

$$\hat{x}(t) = \varphi(t,t-1)\ \hat{x}_n(t-1)$$

The updating of the state estimate for a measurement is given by equation (2-11).

$$\hat{x}_n(t) = \hat{x}(t) + K(t)\left[y(t) - H(t)\ \hat{x}(t)\right]$$

The time propagation of the covariance matrix is given by equation (2-18a).

$$P(t) = \varphi(t,\ t-1)\ P_n(t-1)\ \varphi(t,\ t-1)^T$$

The updating of the covariance matrix for a measurement is given by equation (2-18).

$$P_n(t) = (I - KH)\ P(t)\ (I - KH)^T + KQK^T$$

The optimal filter gain is given by equation (2-24).

$$K(t) = P(t)\ H(t)^T\left[H(t)\ P(t)\ H(t)^T + Q(t)\right]^{-1}$$

2.2.1.1 Effect of Neglecting Bias Errors. The bias errors, u and v, shown in Figure 2-1 were neglected in the derivation of the optimal filter in the previous section. This section will present an analysis, due to Gunkel[7], of the error in estimate caused by neglecting these bias errors.

Two different types of bias error sources are shown in Figure 2-1, state vector perturbation biases, u, and measurement biases, v. State vector

biases might include uncertainties in planetary gravitational constants and solar pressure acceleration. Measurement biases could include any of a number of instrument imperfections.

The analysis of the effect of these error sources is accomplished by an application of linear superposition. The system and optimal estimation process models are linear dynamical systems. Therefore, the effect of any additional inputs can be found by ignoring the effects of any of the original inputs (the random noise q(t)).

Equation of Motion Biases. The effect of the equation of motion biases is shown in the following equations

$$x_{\mu}(t) = \varphi(t, t-1)\, x_{\mu}(t-1) + \varphi_{\mu}(t, t-1)\, u \tag{2-26}$$

$$\hat{x}_{n\mu}(t) = \left[I - K(t)H(t)\right] \varphi(t, t-1)\, x_{n\mu}(t-1) + K(t)H(t)\, x_{\mu}(t) \tag{2-27}$$

where the subscript μ is used to identify the value of the state vector resulting from the input μ.

Equations (2-26) and (2-27) can be obtained either by examining Figures 2-1 and 2-2 or by using the model equations given in the previous section.

The estimation error resulting from μ is found by taking the difference between (2-27) and (2-26) to give

$$\tilde{x}_{n\mu}(t) = \hat{x}_{n\mu}(t) - x_{\mu}(t) = \left[I - K(t)H(t)\right]\left[\varphi(t,t-1)\, \tilde{x}_{n\mu}(t-1) - \varphi_{\mu}(t,t-1)\mu\right] \tag{2-28}$$

One of the primary objectives of this study, is to determine the sensitivity of the estimation error to changes in the state vector biases. These sensitivities are found by partial differentiation of (2-28). Defining the sensitivity matrix,* $C_u(t)$, as

$$C_\mu(t) = \frac{\partial \tilde{x}_{n_\mu}(t)}{\partial u}$$

and then differentiating (2-28) gives

$$C_\mu(t) = \left[I - K(t)H(t)\right] \left[\phi(t, t-1)\, C_u(t-1) - \phi_u(t, t-1)\right] \qquad (2\text{-}29)$$

The bias errors being analyzed are generally the result of an error in estimate of one or more physical constants in the equations of motion. The expected value of the error in estimate of the constants is zero.

$$E(u) = 0 \qquad (2\text{-}30)$$

Due to the uncertainty in the estimates being used for the constants, u, there is a covariance matrix associated with the estimate.

$$E(uu^T) \equiv M \qquad (2\text{-}31)$$

The uncertainties in the equation of motion constants (2-31) can be transformed into the covariance matrix of error in estimate of the state by means of (2-29).

---

*The matrix has been defined as C(t) because an interesting relationship exists between this sensitivity matrix and the correlation matrix between the vehicle state and the system biases. This relationship will be shown in Section 2.2.3.

$$P_u(t) = C_u(t)\, M\, C_u(t)^T \qquad (2\text{-}32)$$

where: $P_u(t)$ is the covariance matrix of the error in estimate of the state due to the uncertainties in the equations of motion that have been neglected.

Measurement Bias Errors. The effects of measurement biases can be determined in a similar manner. The dynamical equations are

$$y_v(t) = D(t)\, v \qquad (2\text{-}33)$$

$$\tilde{x}_{nv}(t) = \left[I - K(t)H(t)\right] \Phi(t, t\text{-}1)\, \tilde{x}_{nv}(t\text{-}1) + K(t)D(t)v \qquad (2\text{-}34)$$

The sensitivity $C_v(t)$ is

$$C_v(t) = \frac{\partial \tilde{x}_{nv}(t)}{\partial v} = \left[I - K(t)H(t)\right] \Phi(t, t\text{-}1)\, C_v(t\text{-}1) + K(t)D(t) \qquad (2\text{-}35)$$

As in the case of equation of motion errors, the expected value of v is zero but there is an associated error in this estimate.

$$E(v) = 0 \qquad E(vv^T) = W \qquad (2\text{-}36)$$

The uncertainty in the estimate of the measurement biases, W, can be reflected in an error in estimate of the state with the use of (2-35).

$$P_v(t) = C_v(t)\, W\, C_v(t)^T \qquad (2\text{-}37)$$

where $P_v(t)$ is the covariance matrix of the error in estimate of the state due to neglecting the measurement bias uncertainties.

The total error in estimate of the state must realistically include the effects shown by equations (2-32) and (2-37) in addition to that shown by (2-25) which is the result of initial state uncertainty and random noise in the observations.

$$P_T(t) = P(t) + P_u(t) + P_v(t) \qquad (2\text{-}38)$$

where $P_t(t)$ is the total state uncertainty including the effects of neglected bias errors.

Portions of the data presented in later sections were obtained by the techniques just presented. These data show the effects of the bias errors that had been neglected in the previous study[1].

2.2.2 Bias Errors Included (Parameter Estimation)

The bias error parameters, u and v, can be included as additional elements of the state vector and estimated along with the vehicle state. The physical process for the inclusion of the bias errors in the state is shown in Figure 2-3.

The dynamics equations for the system may be written in terms of partitioned matrices as

$$\begin{pmatrix} x(t) \\ u \\ v \end{pmatrix} = \begin{pmatrix} \Phi(t, t-1) & \Phi_u(t, t-1) & 0 \\ 0 & I & 0 \\ 0 & 0 & I \end{pmatrix} \begin{pmatrix} x(t-1) \\ u \\ v \end{pmatrix} \qquad (2\text{-}39)$$

or by definition

$$z(t) = \varphi_z(t,t-1)z(t-1) \qquad (2\text{-}39a)$$

and

$$y_z(t) = \begin{pmatrix} H(t) & 0 & D(t) \end{pmatrix} \begin{pmatrix} x(t) \\ u \\ v \end{pmatrix} + q(t) \qquad (2\text{-}40)$$

and by definition

$$y_z(t) = H_z(t)\, Z(t) + q(t) \qquad (2\text{-}40a)$$

These equations have the same form as (2-7) and (2-8) and yield the same solution for the optimal filter as shown in Figure 2-2.

The filter equations and optimal gain are presented below.

$$\hat{z}(t) = \varphi_z(t, t-1)\, \hat{z}_n(t-1) \qquad (2\text{-}41)$$

$$P_z(t) = \varphi_z(t, t-1)\, P_{zn}(t-1)\, \varphi_z^T(t, t-1) \qquad (2\text{-}42)$$

$$\hat{z}_n(t) = \hat{z}(t) + K_z(y_z - \hat{y}_z) \qquad (2\text{-}43)$$

$$P_{zn}(t) = P_z(t) - K_z\, H_z\, P_z(t) \qquad (2\text{-}44)$$

where the optimal gain, $K_z(t)$ is

$$K_z(t) = P_z H_z^T (H_z P_z H_z^T + Q)^{-1} \qquad (2\text{-}45)$$

Equations (2-41) and (2-42) are for updating the state and covariance matrix between the observations, (2-43) and (2-44) are for the improvement in estimate and the covariance matrix of the error in estimate as a result of the observation $y_z(t)$.

With this expanded state definition one may include as many unknowns (in principle) as he desires. The expanded state being estimated increases the computer storage requirements and the time required to perform the computation.

2.2.3 Bias Error Considered

The bias error treatment described in this section is due to Schmidt[6]. An optimum estimation process is desired that includes the effects of bias error parameters on the state estimation process but constrains these parameter estimates and their uncertainties to remain constant.

From the previous derivation, it is apparent that no theoretical difficulties are introduced by parameter estimation. There may be practical difficulties since one may not be able to obtain a solution that converges when a large number of unknowns are introduced. This can occur when the unknowns are not linearly independent for the number of significant figures retained in the numerical calculations. Also the computer size can be excessive when a large number of unknown parameters are added.

For these reasons one would like to include the effects of unknown parameters in the sense that they deteriorate the estimate of state, without actually carrying through all the calculations for estimating them. The manner in

which this is done will be described subsequently for: (1) equation of motion bias errors and (2) measurement biases.

The analysis will be performed independently for the two bias error sources with the random noise, $q(t)$, neglected in both cases. This type of analysis invokes the principle of superposition in a linear system. The following analysis will be directed at three areas of interest: (1) obtaining an expression for the optimum gain, $K(t)$, when the bias error effects are considered, (2) showing the separability of the total error covariance matrix into a part due to random errors and parts due to each of the bias error sources, and (3) show the relationship that exists between the correlation matrix of the state and bias errors and the partial sensitivity matrix obtained in Section 2.2.1.1.

The physical process being analyzed is shown in Figure 2-1 and the linear filter is shown in Figure 2-2. The filter gain, $K(t)$, is to be selected so that it is optimum in the sense of a minimum variance filter with the effects of the bias errors, u and v, considered. The bias errors are assumed to be defined by the following statistical quantities.

$$E(u) \equiv \hat{u} \equiv 0 \qquad E(uu^T) = M \tag{2-46}$$

$$E(v) \equiv \hat{v} = 0 \qquad E(vv^T) = W \tag{2-47}$$

Equation of Motion Errors. The following equations describe the dynamics of the system and the estimation process with the equation of motion bias errors.

$$x(t) = \varphi(t, t-1)\, x(t-1) + \varphi_u(t, t-1)u \tag{2-48}$$

$$\hat{x}_n(t) = \left[I - KH\right]\left[\varphi(t, t-1)\, \hat{x}_n(t-1) + KH\, x(t)\right] \tag{2-49}$$

The optimum filter gain is to be selected so that $E\left[\left(x(t) - \hat{x}_n(t)\right)^T \left(x(t) - \hat{x}_n(t)\right)\right]$ is minimized.

Let

$$\tilde{x}_n(t) \equiv x(t) - \hat{x}_n(t) \tag{2-50}$$

then

$$E\left[\left(x(t) - \hat{x}_n(t)\right)^T \left(x(t) - \hat{x}_n(t)\right)\right] \equiv E\left[x_n(t)^T \tilde{x}_n(t)\right] \tag{2-51}$$

or

$$E\left[\tilde{x}_n(t)^T \tilde{x}_n(t)\right] = \text{Trace } E\left[\tilde{x}_n(t)\, \tilde{x}_n^T(t)\right] \equiv \text{Trace } \left[P_n(t)\right] \tag{2-52}$$

now form $\tilde{x}_n(t)$,

$$\tilde{x}_n(t) = \left[I - KH\right]\left[\varphi(t, t-1)\, \tilde{x}_n(t-1) + \varphi_u(t, t-1)u\right] \tag{2-53}$$

From this the covariance matrix of the error in estimate, $P_n(t)$ can be formed as defined by (2-52).

$$P_n(t) = E\left\{\left[I - KH\right]\left[\varphi(t, t-1)\, \tilde{x}_n(t-1) + \varphi_u(t, t-1)u\right]\left[\varphi(t, t-1)\, \tilde{x}_n(t-1) + \varphi_u(t, t-1)\, u\right]^T \left[I - KH\right]^T\right\} \tag{2-54}$$

$$P_n(t) = [I-KH]\left\{\varphi E\left[\tilde{x}_n(t-1)\tilde{x}_n^T(t-1)\right]\varphi^T + \varphi E\left[\tilde{x}_n(t-1)u^T\right]\varphi_u^T + \varphi_u E\left[u\, \tilde{x}_n^T(t-1)\right]\varphi^T + \varphi_u E\left[uu^T\right]\varphi_u^T\right\}\left[I - KH\right]^T \tag{2-55}$$

At this point it is very useful to define several of the statistical correlation terms that are in (2-55).

Let

$$C_u(t) = E\left[\tilde{x}(t)\ u^T\right] \qquad C_{un}(t) = E\left[\tilde{x}_n(t)\ u^T\right] \tag{2-56}$$

using the dynamic equation (2-48)

$$C_u(t) = E\left\{\left[\Phi(t,\ t\text{-}1)\ \tilde{x}_n(t\text{-}1) + \Phi_u(t,\ t\text{-}1)\ u\right]u^T\right\} \tag{2-57}$$

or using (2-56) and (2-46)

$$C_u(t) = \Phi(t,\ t\text{-}1)\ C_{un}(t\text{-}1) + \Phi_u(t,\ t\text{-}1)\ M \tag{2-58}$$

The correlation factor, $C_u(t)$, changes at the time of an observation.

$$C_{un}(t) = E\left[\tilde{x}_n(t)\ u^T\right] \tag{2-59}$$

from (2-53) and (2-58)

$$C_{un}(t) = \left[I - KH\right]C_u(t) \tag{2-60}$$

The correlation matrix (2-60) is of the same form as the sensitivity matrix shown in equation (2-29). If equation (2-60) is post multiplied by M^{-1} the two equations are the same. Interpretation of the correlation matrix as a sensitivity matrix suggests the following separated form for the covariance matrix $P_n(t)$.

let

$$P_n(t-1) = P'_n(t-1) + C_{un}(t-1)\, M^{-1}\, C^T_{un}(t-1) \qquad (2\text{-}61)$$

where

$P_n(t-1)$ is the total state covariance matrix.

$P'_n(t-1)$ is the uncertainty in the state due to the initial covariance matrix, $P(o)$, and random measurement noise.

The second term is the uncertainty in the state due to the uncertainty in the equation of motion parameters.

Returning to equation (2-55) and making the substitutions for the expected values yields the following

$$P_n(t) = \left[I - KH\right]\left\{\varphi\, P_n(t-1)\, \varphi^T + \varphi\, C_{un}(t-1)\, \varphi^T_u + \varphi_u C^T_{un}(t-1)\varphi^T + \varphi_u\, M\, \varphi^T_u \right\}\left[I-KH\right]^T \qquad (2\text{-}62)$$

Using the assumed form of $P_n(t-1)$ in equation (2-61) for $P_n(t-1)$ in (2-62) yields

$$P_n(t) = \left[I - KH\right]\left\{\varphi\, P'_n(t-1)\varphi^T + \varphi\, C_{un}(t-1)M^{-1}C_{un}{}^T(t-1)\varphi^T + \varphi\, C_{un}(t-1)\, \varphi^T_u + \varphi_u C_{un}{}^T(t-1)\, \varphi^T + \varphi_u\, M\, \varphi^T_u\right\}\left[I - KH\right]^T \qquad (2\text{-}63)$$

Evaluation of $C_u(t)\, M^{-1}\, C_u(t)^T$ using (2-58) yields

$$C_u(t)\, M^{-1}\, C^T_u(t) = \varphi\, C_{un}(t-1)\, M^{-1}\, C^T_{un}(t-1)\, \varphi^T + \varphi\, C_{un}(t-1)\, \varphi_u + \varphi_u C^T_{un}(t-1)\, \varphi^T + \varphi_u\, M\, \varphi^T_u \qquad (2\text{-}64)$$

Substituting (2-64) into (2-63) yields

$$P_n(t) = \left[I - KH\right]\left\{P'(t) + C_u(t)\, M^{-1}\, C_u^T(t)\right\}\left[I - KH\right]^T \qquad (2\text{-}65)$$

where

$$P'(t) = \Phi\, P_n'(t-1)\, \Phi^T$$

using (2-60) and (2-18)

$$P_n(t) = P_n'(t) + C_{un}(t)\, M^{-1}\, C_{un}^T(t) \qquad (2\text{-}66)$$

Equation (2-66) which is the recursion of (2-61) shows the feasibility of expressing the total covariance matrix in a separated form. One part is due to the initial covariance matrix, $P(0)$, and the random measurement noise and the other is due to the effect of the bias errors.

The filter gain, $K(t)$, is to be selected to minimize the trace of equation (2-65). The derivation of the solution for $K(t)$ is the same as that presented in Section 2.2.1.

Rewriting (2-65)

$$P_n(t) = (I - KH)\ A(I - KH)^T \qquad (2\text{-}67)$$

where

$$A = P'(t) + C_u(t)\, M^{-1}\, C_u^T(t)$$

or

$$P_n(t) = A - KHA - AH^T K^T + KHAH^T K^T \qquad (2\text{-}68)$$

This equation is exactly of the same form as (2-19) with the following equivalent variables.

$$A \sim P(t) \quad K \sim K \quad H \sim H \quad HAH^T \sim SS^T$$

The solution of (2-68) for the optimal gain is given by (2-23). Making the appropriate substitutions into (2-23) yields

$$K(t)\, S(t) = A(t)\, H^T(t) \left(S(t)^{-1}\right)^T \qquad (2\text{-}69)$$

or the optimal gain when considering the bias error parameters is

$$K(t) = AH^T(HAH^T)^{-1} \qquad (2\text{-}70)$$

where

$$A \equiv P'(t) + C_u(t)\, M^{-1}\, C_u^T(t)$$

Comparing the filter gain obtained while neglecting the bias errors (2-24) with (2-70), indicates that the only change in the gain matrix is due to a change in the form of the covariance matrix, $P(t)$. In the gain computation for the inclusion of the bias error effects, the covariance matrix used is increased by the effect of the parameter uncertainties given by the term $C_u(t)\, M^{-1}\, C_u^T(t)$.

Measurement Bias Errors. The method of considering measurement bias errors in the estimation process can be analyzed in a manner similar to that just described for the equation of motion biases. Linear superposition will be invoked to neglect all inputs other than the measurement biases in this analysis. The physical process and filter being used are shown in Figures 2-1 and 2-2 respectively.

The following equations describe the dynamics of the system and the estimation process with the measurement biases.

$$x(t) = \varphi(t, t-1)\, x(t-1) \tag{2-71}$$

$$y(t) = D(t)v + H\, x(t) \tag{2-72}$$

$$\hat{x}_n(t) = \left[I - KH\right] \varphi(t, t-1)\, \hat{x}_n(t-1) + K\left[D(t)\, v + H\, x(t)\right] \tag{2-73}$$

The error in estimate $\tilde{x}_n(t)$ is the following

$$\tilde{x}_n(t) = x(t) - \hat{x}_n(t) = \left[I - KH\right] \varphi(t, t-1)\, \tilde{x}_n(t-1) - K\, D(t)\, v \tag{2-74}$$

The covariance matrix is

$$P_n(t) = E\left[\tilde{x}_n(t)\, \tilde{x}_n^T(t)\right] = E\left\{\left[(I - KH)\, \varphi(t, t-1)\, \tilde{x}_n(t-1) - K\, D(t)\, v\right] \left[(I - KH)\, \varphi(t, t-1)\, \tilde{x}_n(t-1) - KD(t)\, v\right]^T\right\} \tag{2-75}$$

$$P_n(t) = (I - KH)\,\varphi(t, t-1)\,E\left[\tilde{x}_n(t-1)\,\tilde{x}_n^T(t-1)\right]\varphi^T(t, t-1)\,(I - KH)^T$$
$$- (I - KH)\,\varphi(t, t-1)\,E\left[\tilde{x}_n(t-1)\,v^T\right]D^T K^T \qquad (2\text{-}76)$$
$$- K D E\left[v\,\tilde{x}_n^T(t)\right]\varphi^T(t, t-1)\,(I - KH)^T + K D E\left[(v\,v^T)\right]D^T K^T$$

Let

$$C_v(t) = E\left[\tilde{x}(t)\,v^T\right] \qquad C_{vn}(t) = E\left[\tilde{x}_n(t)v^T\right] \qquad (2\text{-}77)$$

then from equation (2-71)

$$C_v(t) = E\left[\varphi(t, t-1)\,\tilde{x}_n(t-1)\,v^T\right] = \varphi(t, t-1)\,C_{vn}(t-1) \qquad (2\text{-}77a)$$

and from equation (2-74)

$$C_{vn}(t) = E\left\{\left[(I - KH)\,\varphi(t, t-1)\,\tilde{x}_n(t-1)\,v^T - K(t)\,D\,v\right]v^T\right\} \qquad (2\text{-}78)$$

applying (2-77) and (2-46) yield

$$C_{vn}(t) = (I - KH)\,\varphi(t, t-1)\,C_{vn}(t-1) - K(t)\,D(t)\,W \qquad (2\text{-}79)$$

or

$$C_{vn}(t) = (I - KH)\,C_v(t) - K(t)\,D(t)\,W \qquad (2\text{-}80)$$

The covariance matrix will be defined to be made of two parts, one due to the random errors and one due to the biases.

Define

$$P_n(t-1) = P'_n(t-1) + C_{vn}(t-1)\, W^{-1}\, C^T_{vn}(t-1) \qquad (2\text{-}81)$$

and

$$P(t) = \varphi(t, t-1)\, P_n(t-1)\, \varphi(t, t-1) \qquad (2\text{-}82)$$

or using (2-77a)

$$P(t) = P'(t) + C_v(t)\, W^{-1}\, C^T_v(t) \qquad (2\text{-}83)$$

where

$$P'(t) = \varphi(t, t-1)\, P'_n(t-1)\, \varphi^T(t, t-1)$$

Substituting the above definitions of the covariance matrix and the correlation matrices in equation (2-76) yields the following.

$$P_n(t) = (I - KH)\, \varphi(t, t-1)\, P_n(t-1)\, \varphi^T(t, t-1)\, (I - KH)^T - (I - KH)\, C_v(t)\, D^T\, K^T$$

$$- KD\, C^T_v(t)\, (I - KH)^T + KDW\, D^T\, K^T \qquad (2\text{-}84)$$

Substituting (2-82) and (2-83) into (2-84) yields

$$P_n(t) = (I - KH) \left(P'(t) + C_v(t)\, W^{-1}\, C^T_v(t)\right) (I - KH)^T - (I - KH)\, C_v(t)\, D^T\, K^T$$

$$- KD\, C^T_v(t)\, (I - KH)^T + KD\, W\, D^T\, K^T \qquad (2\text{-}85)$$

Using (2-80), the expression $C_{vn}(t)\, W^{-1}\, C_{vn}^T(t)$ may be evaluated

$$C_{vn}(t)\, W^{-1}\, C_{vn}^T(t) = (I - KH)\, C_v(t)\, W^{-1}\, C_v^T(t)\, (I - KH)^T$$
$$- (I - KH)\, C_v(t)\, D^T\, K^T - KD\, C_v^T(t)\, (I - KH)^T$$
$$+ KD\, W\, D^T\, K^T \qquad (2\text{-}86)$$

Substitution of (2-86) into (2-85) yields

$$P_n(t) = P_n'(t) + C_{vn}(t)\, W^{-1}\, C_{vn}(t) \qquad (2\text{-}87)$$

where

$$P_n'(t) = (I - KH)\, P'(t)\, (I - KH)^T$$

Equation (2-87) is the recursion of (2-81) and shows the feasibility of separating the effect of the measurement biases from the effect of random errors. The optimal filter gain, K, is to be selected so the trace of the covariance matrix, $P_n(t)$ is a minimum.

Equation (2-85) can be expanded into the following form.

$$P_n(t) = P'(t) + C_v\, W^{-1}\, C_v^T - K\left\{H\left(P'(t) + C_v\, W^{-1}\, C_v^T\right) + D\, C_v^T\right\}$$
$$- \left\{\left(P'(t) + C_v\, W^{-1}\, C_v^T\right) H^T + C_v\, D^T\right\} K^T$$
$$+ K\left\{H\left(P'(t) + C_v\, W^{-1}\, C_v^T\right) H^T + D\, W\, D + D\, C_v^T\, H^T\right.$$
$$\left. + H\, C_v\, D^T\right\} K^T \qquad (2\text{-}88)$$

or

$$P_n(t) = P'(t) + C_v W^{-1} C_v^T - K A - A^T K^T + K B K^T \qquad (2\text{-}89)$$

where

$$A = H\left(P'(t) + C_v W^{-1} C_v^T\right) + DC_v^T$$

$$B = HP'(t) H^T + \left[D w + H C_v(w^{-1})^T\right]\left[Dw + H C_v(w^{-1})^T\right]^T$$

$$ww^T = W.$$

Equation (2-89) has the same form as (2-19) with the following equivalent variables.

$$I \sim P(t) \qquad A \sim H \qquad K \sim K \qquad B(t) \sim SS^T$$

The solution of (2-89) for the optimal gain is given by (2-23). Making the appropriate substitutions into (2-23) yields

$$K(t)\, S(t) = A^T(t) \left(S(t)^{-1}\right)^T \qquad (2\text{-}90)$$

or the optimal gain when considering the measurement bias error parameters is

$$K(t) = A^T(t)\, B^{-1}(t) \qquad (2\text{-}91)$$

where

$$A^T(t) = \left(P'(t) + C_v W^{-1} C_v^T\right) H^T + C_v D^T$$

$$B^{-1}(t) = \left\{H P'(t) H^T + \left[D w + H C_v (w^{-1})^T\right]\right.$$

$$\left.\left[D w + H C_v (w^{-1})^T\right]^T\right\}^{-1}$$

$$ww^T = W$$

Equation (2-91) is the optimal gain with the measurement bias errors considered.

2.3 PARAMETRIC ERROR ANALYSIS

The error analysis of a space navigation system generally requires that the effects of the error sources on the system performance be examined in a parametric manner. A computer simulation of a space mission is in general quite complex and the quantity of navigation data to be processed can be large. These factors result in a significant amount of computer time being required for one data run with a single set of error parameters (variances). When there is interest in a large range of variances on each of the error parameters this implies a large number of computer runs and the correspondingly large computer run time. An extremely useful error analysis technique would be one by which following a single computer run all the parametric data of interest could be obtained simply by means of matrix manipulations of the covariance matrix rather than additional runs. This section will describe two such parametric analysis techniques that have been utilized in this study. The two techniques used apply to: (1) analysis of the effects of initial uncertainties in error parameters that have been

included in the state and estimated (parameter estimation) and, (2) analysis of the effect of errors that have been neglected from the estimation process.

The parametric analysis techniques being presented were originated by Grunckel[7] and are elaborated on in Reference 9.

2.3.1 Initial State Uncertainties

The change in the state covariance matrix due to the inclusion of an observation is given by (2-44).

$$P_{zn}(t) = P_z(t) - P_z(t)\left(H_z^T \; H_z P_z(t) \; H_z^T + Q\right)^{-1} H_z \; P_z(t) \qquad (2\text{-}92)$$

The diagonal elements of $P_{zn}(t)$ define the variances on the vehicle state estimate, position and velocity, and any bias errors that are being estimated as part of the expanded state vector.

For the case of a scalar problem, (2-92) becomes

$$P_n = \frac{P_o Q}{H^2 P_o + Q} \qquad (2\text{-}93)$$

In a conventional error analysis, where one of the elements of $P_z(t)$ (2-92) may be an equation of motion parameter (mass of a body, A.U. etc.) and a number of navigation observations are made of the vehicle, the effect of changing the initial variances of the bias parameters in the problem would be determined by simulating the mission with new parameters. For the scalar case, this corresponds to changing the initial variance, P_o, by a factor k and making a computer run. The technique being presented here is one in which an additional direct observation of the bias parameter is made at the conclusion of the first computer run.

If the initial parameter variance of interest in the scalar case is

$$P_o' = k P_o \tag{2-94}$$

then a direct observation of the bias parameter with a measurement variance, Q, defined by equating (2-94) and (2-93) will yield the desired initial parameter variance, P_o'.

$$P_n \quad P_o' \quad k P_o \quad \frac{P_o Q}{P_o + Q} \tag{2-95}$$

where

$$H \quad 1$$

Solving for Q yields

$$Q = P_o \left(\frac{k}{1 - k}\right) \tag{2-96}$$

The fact that the direct observation of the bias parameter with the measurement error defined by (2-96) to change an initial variance is not required to be made at the start of the run but can be made last is shown as follows.

The order in which the data are processed is shown below, where y (1) is the direct parameter measurement.

$$\begin{aligned} y(1) &= H(1)\, x(1) + q(1) \\ y(2) &= H(2)\, x(2) + q(2) \\ &\vdots \\ y(t) &= H(t)\, x(t) + q(t) \end{aligned} \tag{2-97}$$

An entirely equivalent set of data would be obtained by processing the direct parameter measurement last.

This gives the following sequence of measurements.

$$\begin{aligned} y(z) &= H(2)\, x(2) + q(2) \\ &\vdots \\ y(t) &= H(t)\, x(t) + q(t) \\ y(1) &= H(1)\, \varphi^{-1}(t,\, 1)\, x(t) + q(1) \end{aligned} \qquad (2\text{-}98)$$

The fact that the order of the observations can be interchanged without changing the final state uncertainty can be easily seen if the observation are all referenced to the same time and the covariance matrix P_n, is written as an inverse information matrix (see Appendix A).

The observation sequence in (2-97) all referenced to time, t, becomes

$$\begin{aligned} y_1(t) &= H(1)\, \varphi^{-1}(t,\, 1)\, x(t) + q(1) \equiv M(1)\, x(t) + q(1) \\ y_2(t) &= H(2)\, \varphi^{-1}(t,\, 2)\, x(t) + q(2) \equiv M(2)\, x(t) + q(2) \\ &\vdots \\ y_t(t) &= H(t)\, \varphi^{-1}(t,\, t)\, x(t) + q(t) \equiv M(t)\, x(t) + q(t) \end{aligned} \qquad (2\text{-}99)$$

Now, using the following inverse form of the covariance matrix

$$P_n(t) = \left\{ \left[P_o(t) \right]^{-1} + H^T Q^{-1} H \right\}^{-1} \qquad (2\text{-}100)$$

and applying it successively to each of the measurements in (2-99) yields

$$P_n(t) = \left\{ \left[P_o(t) \right]^{-1} + \sum_{i=1}^{t} M^T(i)\, Q(i)^{-1}\, M(i) \right\}^{-1} \qquad (2\text{-}101)$$

Clearly, the order of the terms under the summation in (2-101) is not important. Since the order of the observations is not important it is possible to change an initial variance by means of a direct observation of the parameters at the end of a sum.

When the parameter whose initial variance is to be changed is a bias whose value is unknown but constant for the entire mission, the measurement partial is

$$M(t) \equiv H(1)\, \varphi^{-1}(t, 1) = \left[000 \ldots . 1\ 00 \right] \qquad (2\text{-}102)$$

Where it is assumed that the state variable of interest is the i^{th} state variable.

Equation (2-92) which shows the computation of the updated covariance matrix can be simplified by noting

$$P_z(t)\, H_z^T(t) = C_i$$

$$H_z(t)\, P_z(t)\, H_z^T(t) = \sigma_i^2$$

where

$$H_z(t) \equiv M(t) = \left[000 \ldots . 1\ 00 \right]$$

C_i is the ith column of $P_z(t)$ and σ_i^2 is the (i, i) element of $P_z(t)$

Then using (2-92)

$$P_{zn}(t) = P_z(t) - C_i \left(\sigma_i^2 + \frac{k\, \sigma_{xi}^2}{1 - k} \right)^{-1} C_i^T \qquad (2\text{-}103)$$

where

σ_{xi}^2 is the initial uncertainty in the i^{th} state variable

k is the variance scaling desired

Using (2-103) the initial uncertainties can be varied by orders of magnitude with almost no computational penalty.

A special case of equation (2-103) is with k = 0. In this case the initial uncertainty is zero and the state variable is effectively eliminated from the estimation process.

2.3.2 Neglected Bias Errors

The parametric analysis of the effect of bias errors that have been neglected in the estimation process is straight forward. The error sensitivity matrices to equation of motion and measurement biases are shown by (2-29) and (2-35) respectively.

$$C_u(t) = (I - KH) \left[\varphi(t, t\text{-}1)\, C_u(t\text{-}1) - \varphi_u(t, t\text{-}1) \right] \qquad (2\text{-}104)$$

$$C_v(t) = (I - KH)\, \varphi(t, t\text{-}1)\, C_v(t\text{-}1) + K\, D \qquad (2\text{-}105)$$

The covariance matrix of the error in estimate due to neglecting these errors is the following.

$$P(t) = C_u(t)\, E(uu^T)\, C_u^T(t) + C_v(t)\, E(vv^T)\, C_v^T(t) \qquad (2\text{-}106)$$

It can be seen in (2-106) that the contribution of each bias error source adds algebriacally into the total error. Each error source can therefore be examined separately and its effect analyzed merely by scaling the variance of the element up or down. For example, consider the i^{th} element in the equation of motion errors.

$$P_i(t) = C_{iu}(t)\, k\, E(u_i u_i^T)\, C_{iu}^T(t) = C_{iu}\, k\, \sigma_i^2\, C_{iu}^T(t) \qquad (2\text{-}107)$$

where $C_{iu}(t)$ is the i^{th} column of the matrix $C_u(t)$ and k is the desired scaling of the variance of the (i, i) element of $E(uu^T)$.

This type analysis can be done very easily at the end of a run in which the C_u and C_v matrices have been computed.

SECTION 3

ANALYSIS OF BIAS ERROR SOURCES

This section presents a description of the bias error sources that are considered in this study. There are two basic types of bias error sources of interest: (1) equation of motion parameters and (2) measurement parameters. These error sources correspond to the system inputs, u and v, that are used in the analysis in Section 2. These parameters enter the estimation process because even though an estimate is available for each parameter there is some degree of uncertainty associated with it. The use of the term bias error to describe these errors arises from the fact that although the expected difference between the parameter estimate and its true value is zero, the uncertainty in the estimate causes a constant error. The actual difference enters the estimation process as a constant. For example, the estimate of the mass of the earth may be described as follows:

$$E(u_\epsilon) = \hat{k} \quad E\left(u_\epsilon^2 - \bar{u}_\epsilon^2\right) = \sigma_k^2 \qquad (3\text{-}1)$$

$\hat{k}$ = estimate of earth's mass

σ_k^2 = variance in the estimate

The quantity σ_k^2 is a statistical quantity related to the estimation process used to obtain $\hat{k}$. If the true value of the earth's mass is k, then the planetary mass in a trajectory simulation is in error as follows:

$$\epsilon = k - \hat{k} \qquad (3\text{-}2)$$

k = the true value of mass

$\hat{k}$ = the estimated value of mass

ϵ = actual error in estimate

The error, ϵ, would introduce a constant bias in the simulation using $\hat{k}$, it would not exhibit a random variation along the trajectory. This example describes the nature of the bias errors being considered. They are constants in the process being modeled that have been estimated but have a non-zero uncertainty associated with their estimates.

The equation of motion error sources that are included in the analysis are: (1) astronomical unit conversion, (2) mass of the Earth, (3) mass of Mars, and (4) solar radiation pressure. The measurement error sources evaluated are a bias in the on-board sextant measurement and a bias in the onboard clock. The following sections will describe each of these error sources and how they affect the trajectory estimation process. A large part of the information presented in this section is taken from Reference 10, the midterm progress report, entitled, "Influence of Uncertainties In The Astronomical Unit Conversion and Mars Planetary Mass on Earth-Mars Trajectories."

3.1 EQUATION OF MOTION BIASES

The various methods used in estimating the heliocentric and planetary constants are described in References 11 through 16. Tables 3-1, 3-2, and 3-3 summarize the results of several determinations of the ratio of the astronomical unit to laboratory units and the planetary masses of Earth and Mars. The large discrepancy between the radar measurements of the astronomical unit distance and the dynamical method using the asteroid Eros is discussed in Reference 14. The discussion indicates that a plausible explanation of this discrepancy is the existence of systematic ephemeris errors that are not accounted for in the dynamic method.

3.1.1 Astronomical Unit Conversion

The analysis of the astronomical unit (A.U.) presented here and the results in Section 5 are an extension and generalization of the work reported in reference 17 by S. Henrick, et al.

The uncertainty in the ratio of the astronomical unit to a laboratory unit is an important factor in the accuracy with which an interplanetary mission can be performed. Reference 17 demonstrates the importance of using the basic "Gaussian" gravitational constant based on the A. U. and the solar mass in trajectory computations. This is due to the eight or nine figure accuracy[18] to which it is presently known. The same constant expressed in laboratory units is only accurate to three or four figures. The importance of the uncertainty in the ratio to an interplanetary mission is due to the fact that with an ephemeris expressed in terms of the A.U., mission analysis specifications of injection conditions at Earth are in terms of the A.U. The uncertainty in the conversion of the geocentric injection conditions from a working laboratory unit to the astronomical unit results in the Earth escape velocity being in error in units of A.U./Day. Conversely, the uncertainty in the ratio will appear in the initial heliocentric position and velocity of the Earth, the gravitational constant, and in the terminal position and velocity of Mars, if these quantities are converted from astronomical units to kilometers.

The error caused by the ratio uncertainty in the conversion of the trajectory problem totally into A.U.'s is the same as the error in converting the problem to kilometers[17]. This equivalence is shown below. The computer simulation used in the analysis of the uncertainty in the ratio expresses the problem in kilometers. The geocentric hyperbolic excess velocity is assumed to be known precisely and the uncertainty in the ratio occurs in the planetary ephemeris.

The ratio of the A.U. to the equatorial radius is the "solar parallax" expressed in radians (Figure 3-1). Then the desired ratio of the kilometer

to the A.U. embodied in the mean Earth distance, R, is related to the solar parallax as follows:

$$R \doteq \frac{a_\epsilon}{\pi} \tag{3-3}$$

where

a_ϵ = Earth equatorial radius

π = solar parallax

R = Earth-Sun mean distance

The relative uncertainty in the ratio is

$$\frac{\Delta R}{R} = -\frac{\Delta \pi}{\pi} - \frac{\Delta a_\epsilon}{a_\epsilon} \tag{3-4}$$

or neglecting the smaller uncertainty in a_e

$$\frac{\Delta R}{R} = -\frac{\Delta \pi}{\pi} \equiv -\pi' \tag{3-5}$$

The effect of the relative uncertainty, π', in the ratio will appear in the initial geocentric position and velocity of the vehicle if they are expressed in the astronomical unit. The analysis of the error resulting from the conversion of the initial state to astronomical units is presented below.

The Hohmann transfer trajectory geometry is shown in Figure 3-2. The relative error in the major axis, 2a, can be found from the vis-viva integral which may be written:

$$v^2 = 2\mu\left(\frac{1}{r} - \frac{1}{2a}\right) = 2r_\epsilon v_\epsilon^2\left(\frac{1}{r} - \frac{1}{2a}\right) \qquad (3\text{-}6)$$

where

r, v = heliocentric position and velocity of vehicle

r_ϵ, v_ϵ = heliocentric position and velocity of Earth

$r_\epsilon v_\epsilon^2$ = gravitational constant assuming Earth orbit is circular

$2a$ = major axis of transfer

For the Hohmann transfer, the initial heliocentric vehicle state is the following:

$$r = r_\epsilon \qquad v = v_\epsilon + v_\infty \qquad (3\text{-}7)$$

where v_∞ is the velocity of the vehicle at about a million kilometers. In the process of conversion of the problem from kilometers to A.U.'s the position and velocity of the Earth may be assumed to be known accurately in astronomical units.

$$\Delta r = \Delta r_\epsilon = \Delta v_\epsilon = 0 \qquad (3\text{-}8)$$

The heliocentric vehicle velocity is in error due to the fact that v_∞ although known accurately in laboratory units must be converted to A.U.'s using R as a conversion factor.

$$\Delta v = \Delta v_\infty = v_\infty \pi' \qquad (3\text{-}9)$$

Then from equation (3-6),

$$\frac{\Delta(2a)}{(2a)^2} \quad \frac{v\Delta v}{r_\epsilon v_\epsilon^2} \tag{3-10}$$

or using equation (3-9)

$$\frac{\Delta 2(a)}{(2a)} = \frac{2a}{r_\epsilon} \frac{v\ v_\infty}{v_\epsilon^2} \pi' \tag{3-11}$$

The conversion of the problem from A.U. to kilometers yields the following expression[17] for $\frac{\Delta 2a}{2a}$ that differs from equation (3-11).

$$\frac{\Delta 2a}{2a} = \left[\frac{2a}{r_\epsilon} \frac{v\ v_\infty}{v_\epsilon^2} - 1\right] \pi' \tag{3-12}$$

This is the uncertainty in Δa expressed in kilometers, leaving the position of Mars as an uncertainty. Since the position of Mars is well known in astronomical units, the uncertainty should be sought in $\Delta(2a/R)$ not $\Delta(2a)$. Then equation (3-12) becomes

$$\frac{\Delta\left(\frac{2a}{R}\right)}{\left(\frac{2a}{R}\right)} = \left(\frac{\Delta 2a}{2a} - \frac{\Delta R}{R}\right) = \frac{2a}{r_\epsilon} \frac{v\ v_\infty}{v_\epsilon^2} \pi' \tag{3-13}$$

which is in agreement with equation (3-11).

Using approximate Hohmann transfer numbers, equations (3-11) and (3-12) are evaluated to use as a point of reference for the data that follow.

$$\frac{2a}{r_\epsilon} = \frac{5}{2} \qquad \frac{v}{v_\epsilon} = \frac{13}{12} \qquad \frac{v_\infty}{v_\epsilon} = \frac{1}{12} \qquad 2a = 375 \cdot 10^6 \text{ km}$$

$$\frac{2a}{r_\epsilon} \frac{v\, v_\infty}{v_\epsilon^2} = .226$$

Letting $\pi' = .67 \cdot 10^{-5}$ ($\Delta R \approx -1000$ km)

From equation (3-11) the uncertainty in the semi-major axis of the transfer is the following.

$$\Lambda(2a) = (.226)\ (.67 \cdot 10^{-5})\ (375 \cdot 10^6)$$

$$\Lambda(2a) = 560 \text{ km}$$

$$\Lambda(a) = 280 \text{ km}$$

The uncertainty in the semi-major axis from equation (3-12) which leaves the position of Mars as an uncertainty is the following

$$\Lambda(2a) = (.226\text{-}1)\ (.67 \cdot 10^{-5})\ (375 \cdot 10^6)$$

$$\Delta(2a) = -1940 \text{ km}$$

$$\Delta(a) = -970 \text{ km}$$

The Hohmann transfer example case is illustrated in Figure 3-3. The figure shows the significance of the "two uncertainties" in the transfer major axis.

The computer simulation used to analyze the effect of the A.U. conversion uncertainty on the interplanetary trajectory is described in Section 4.

3.1.2 Planetary Mass

The target approach phase of an interplanetary trajectory is a target centered hyperbola (Figure 3-4). The characteristics of this trajectory are determined by the vehicle velocity state relative to the target at the time the "sphere of influence"[19] is reached and the planetary mass of the target body. The vehicle velocity state relative to the target at this time is determined by the particular heliocentric transfer trajectory that is used. The following is an analysis of the effect of a planetary mass uncertainty on an approach trajectory. The analysis follows that presented in Reference 20.

The error in planetary mass is related to an error in the semi-major axis of the approach hyperbola through the vis-viva equation.

$$a = \frac{\mu}{v_\infty^2} \tag{3-14}$$

where

a = semi-major axis

μ = planetary mass

v_∞ = hyperbolic excess velocity

or

$$\frac{\Delta\mu}{u} = \frac{\Delta a}{a} \tag{3-15}$$

The angle between the approach and regression asymptotes, δ, is related to the approach trajectory as follows.

$$\delta = 2 \cos^{-1}\left(\frac{1}{\epsilon}\right) = 2 \cos^{-1}\left(\frac{\mu}{\mu + r_p v_\infty^2}\right) \tag{3-16}$$

where

ϵ = eccentricity

r_p = periapsis radius

Figure 3-5 presents the scattering angle at Mars as a function of distance of closest approach and the hyperbolic excess velocity. Deviations in δ due to the uncertainty in the planetary mass may be obtained as follows. The $\vec{B}$ vector[21] magnitude is maintained constant i.e.;

$$|\vec{B}| \equiv b = a\sqrt{|(1-\epsilon^2)|} \tag{3-17}$$

Then from equations (3-16) and (3-17)

$$\sin\left(\frac{\delta}{2}\right) \Delta\delta = -\frac{2\Delta\epsilon}{\epsilon^2} \tag{3-18}$$

and

$$0 = 2a(1-\epsilon^2)\,\Delta a - 2a^2\,\epsilon\Delta\epsilon$$

or

$$\Delta\epsilon = \frac{(1-\epsilon^2)}{a\epsilon}\Delta a = \frac{b^2\Delta a}{a^3\epsilon} \tag{3-19}$$

Substituting equation (3-18) into (3-19) yields

$$\Delta\delta = -\frac{2b^2\Delta a}{(a\epsilon)^3 \sin\frac{\delta}{2}} = -\left(\frac{b}{a}\right)^2\left(\frac{2}{\epsilon^3 \sin\frac{\delta}{2}}\right)\frac{\Delta\mu}{\mu} \tag{3-20}$$

$$\Delta\delta = -\frac{2b}{a\epsilon^2}\frac{\Delta\mu}{\mu} = -\frac{2ab}{a^2+b^2}\frac{\Delta\mu}{\mu}$$

in terms of v_∞ equation (3-20) becomes

$$\Delta\delta = - \frac{2b}{v_\infty^2} \left[\frac{\Delta\mu}{\mu^2/v_\infty^4 + b^2} \right] \qquad (3\text{-}21)$$

Figure 3-6 presents the deviations in the scattering angle at Mars as a function of v_∞ and distance of closest approach. The planetary mass uncertainty, $\frac{\Delta\mu}{\mu}$, is 0.0047. These data were obtained by taking the difference between a nominal scattering angle and scattering angles obtained when using perturbed values of the planetary gravitational constant, μ, in a conic trajectory program. The difference results obtained in this manner for the stated planetary mass deviation agree quite well with the linear deviation expressed by equation (3-21).

The importance of these scattering angle deviations on a Earth return trajectory is expressed by the sensitivity of the Earth close approach distance to the scattering angle at Mars. This sensitivity for typical Mars-Earth trajectories ranges from one hundred thousand to a million kilometers for one degree variation in the scattering angle.

The deviation in Mars close approach distance as a function of planetary mass and close approach distance (RCA) is shown in Figure 3-7. The data in Figure 3-7 indicate that an uncertainty in the planetary mass of the order shown in Table 3-3 causes close approach deviations from ±2 km for a high energy trajectory to ±15 km for a very low energy trajectory. The deviations on the low energy trajectory increase to ±35 km for a close approach distance of 50,000 km. These data show that the planetary mass uncertainty is an important factor for missions requiring terminal accuracies on the order of 15 km and less.

The entry corridor at Mars with a 5 mb atmosphere is approximately 20 km[22] or ±10 km from a nominal trajectory. This indicates that for an atmospheric entry mission, a low energy approach trajectory could have significant deviations due to the uncertainty in the planetary mass. The statistical

significance attached to the uncertainties shown in Table 3-3 is also a factor in determining the need for approach guidance corrections on the higher energy trajectories. If it is assumed that the uncertainties shown in the table represent one sigma values; then the deviations in Figures 3-6 and 3-7 represent the maximum deviations to be expected in 68% of the cases for a selected uncertainty. It would then require the deviation numbers to be increased by a factor of 3 to include 99% of the cases. The uncertainties in Table 3-3 have been treated as one sigma values in the analysis.

The deviation in close approach distance at Earth as a function of planetary mass deviation and approach energy is shown in Figure 3-8. These data indicate that the deviations are less than ±1 Km for the planetary mass uncertainties shown in Table 3-2. This indicates that for an entry mission at Earth the planetary mass uncertainty is not a very significant factor. The data shown in Reference 23 indicates that the entry corridor at Earth is 21 Km for a vehicle with a L/D ratio of one and a speed of 18 km/sec.

3.1.3 Solar Radiation Pressure

In the trajectory analysis of a spacecraft, a knowledge of the environmental forces acting on the vehicle is required. An important component of the spacecraft environmental force is that due to radiation. While radiation is generally considered as a mode of energy transfer, it is well known that momentum is also transferred by radiation. The forces resulting from this momentum transfer can have an important influence on the trajectory of a spacecraft.

Several papers have appeared dealing with the effects of solar radiation pressure in regard to space vehicles[24,25]. The theoretical basis of radiation pressure and methods for exact determination of the force acting on a body in a stream of radiation are discussed in Reference 26. Figure 3-9 shows the solar radiation pressure variation as a function of distance from the sun.

The primary interest in this study centers on the effects of uncertainties in the solar radiation force acting on the vehicle. The analysis presented in Section 5 treats the solar radiation force uncertainty as a bias error. The analysis examines the ensemble behavior of the vehicle state through the state convariance matrix. This analysis requires the use of the control sensitivity matrix, $\Phi_u(t_2,t_1)$, as described in Section 2. This matrix is obtained by integration of the variational equations. These equations are described in Section 3.1.4. The solar pressure enters the equations of motion as follows.

The equation of motion of the spacecraft may be written as follows:

$$\dot{X} = F(X, U, t) \tag{3-22}$$

where

$$X = \begin{bmatrix} R \\ V \end{bmatrix}$$

Using the partitioned form of equation (3-22)

$$\ddot{R} = F'(R, V, U, t) \tag{3-23}$$

The function F' may be written as follows:

$$F' = -\mu_{CB} \frac{R}{r^3} - \sum_{i=1}^{N} \mu_i \left(\frac{\Delta_i}{\delta_i^3} + \frac{R_i}{r_i^3} \right) + \sum_{j=1}^{k} P_j \tag{3-24}$$

where

r is the magnitude of R, the vector from the central body to the vehicle.

μ_{CB} is the gravitational mass of the central body.

μ_i is the gravitational mass of the i^{th} body.

r_i is the magnitude of R_i, the vector from the central body to the i^{th} body.

δ_i is the magnitude of Δ_i, the radius vector from the i^{th} body to the vehicle.

p_j are peturbation accelerations due to drag, oblateness, solar pressure, etc.

The forms of the solar radiation pressure in the p_j term of (3-24) is assumed to be an inverse square repulsive acceleration relative to the sun.

$$p = k_{sp} \frac{R_s}{r_s^3} \qquad (3\text{-}25)$$

where

R_s is the radius vector from the sun to the vehicle.

r_s is the magnitude of R_s.

k_{sp} is a constant including the reflectance of the vehicle, the vehicle's mean sun-directed surface area and the vehicle's mass.

An uncertainty in the constant, k_{sp}, of (3-25) produces an uncertainty in the solar radiation pressure acceleration.

3.1.4 Variational Equation

The statistical analyses for both the solar radiation pressure and planetary mass uncertainties presented in Section 5 make use of the control sensitivity matrix $\Phi_u(t_2, t_1)$. This section presents a description of the variational equations that are integrated to obtain both $\Phi(t_2,t_1)$ and $\Phi_u(t_2,t_1)$.

In order to find the sensitivity of the state at time t_2 to the state deviations and variations in the equation of motion parameters at t_1, the variational equations are integrated.

The acceleration of the vehicle was given in (3-23) as

$$\ddot{R} = F'(R, V, U, t)$$

Any small variation in the V, R, or U result in a first order variation in $\ddot{R}$ given by

$$\Delta\ddot{R} = \frac{\partial F'}{\partial R}\Delta R + \frac{\partial F'}{\partial V}\Delta V + \frac{\partial F'}{\partial u}\Delta U \qquad (3\text{-}26)$$

where $\frac{\partial F'}{\partial A}$ means the gradient of F' with respect to the vector A.

The partial derivative of $\ddot{R}$ with respect to any arbitrary parameter, α, is therefore:

$$\frac{\partial \ddot{R}}{\partial \alpha} = \frac{\partial F'}{\partial R}\frac{\partial R}{\partial \alpha} + \frac{\partial F'}{\partial V}\frac{\partial V}{\partial \alpha} + \frac{\partial F'}{\partial U}\frac{\partial U}{\partial \alpha} \qquad (3\text{-}27)$$

by the chain rule of differentiation. If the order of differentiation in equation (3-27) is interchanged, the following second order linear differential equation results.

$$\frac{d^2}{dt^2}\left(\frac{\partial R}{\partial \alpha}\right) = \frac{\partial F'}{\partial R}\left(\frac{\partial R}{\partial R}\right) + \frac{\partial F'}{\partial V}\frac{d}{dt}\left(\frac{\partial R}{\partial \alpha}\right) + \frac{\partial F'}{\partial U}\frac{\partial U}{\partial \alpha} \qquad (3\text{-}28)$$

Now if α represents the initial state, then $\frac{\partial U}{\partial \alpha} = 0$ and the solution of (3-28) subject to the following initial vehicle state conditions:

$$\begin{pmatrix} \frac{\partial R}{\partial \alpha} \\ \frac{\partial V}{\partial \alpha} \end{pmatrix}_{t=o} = \begin{pmatrix} I_{3x3} & 0_{3x3} \\ 0_{3x3} & I_{3x3} \end{pmatrix} \qquad (3\text{-}29)$$

provides the state transition matrix, $\Phi(t,o) = \frac{\partial x(t)}{\partial x(o)}$. The sensitivity of the state to a control, $\Phi_u(t,o) = \frac{\partial x(t)}{\partial U}$, which is meaningful only if the control vector is constant over the time interval under consideration, is obtained by solving equation (3-28) with $\alpha = U$, subject to the following initial conditions.

$$\begin{pmatrix} \frac{\partial R}{\partial \alpha} \\ \frac{\partial V}{\partial \alpha} \end{pmatrix}_{t=o} = \begin{pmatrix} 0_{3xn} \\ 0_{3xn} \end{pmatrix} \quad (n = \text{dimension of control vector}) \qquad (3\text{-}30)$$

3.2 MEASUREMENT BIASES

The measurement biases considered in the analysis of Section 5 are: (1) onboard clock bias, and (2) an angle bias in the sextant measurements. Section 2 shows that the manner in which these bias errors enter the estimation process is through the gradient of the measurement with respect to the biases, D(t). The following is a derivation of the measurement gradients for the sextant type planet-star observations that are used in the analysis. The measurement sensitivities to the following quantities are derived.

R Position state-radius vector from the central body to the vehicle.

V Velocity state-inertial velocity relative to the central body

τ Time bias-error in onboard clock

δ Angle bias-error in sextant instrument

The sextant star-planet angle measurement is made in the plane defined by the vector from the vehicle to the star and the vector from the vehicle to the body being observed. Figure 3-10 illustrates this measurement. The selection of suitable stars to use in making these measurements is discussed in Reference 27.

From Figure 3-10 the sextant measurement is the following:

$$\alpha = \cos^{-1}(\hat{S} \cdot \hat{P}) = \cos^{-1}(\hat{S}^T \hat{P}) \tag{3-31}$$

where

$$\hat{P} = \frac{\vec{P}}{|P|}$$

The total measurement gradient that is desired is the following:

$$H_z = \left(\frac{\partial \alpha}{\partial R}; \frac{\partial \alpha}{\partial V} ; \frac{\partial \alpha}{\partial \delta} ; \frac{\partial \alpha}{\partial \tau} \right) \tag{3-32}$$

Taking the gradient of (3-31) with respect to R yields

$$-\sin \alpha \frac{\partial \alpha}{\partial R} = \hat{S}^T \frac{\partial \hat{P}}{\partial R} + \hat{P}^T \frac{\partial \hat{S}}{\partial R} \tag{3-33}$$

Since

$$\frac{\partial \hat{P}}{\partial R} = \frac{1}{|P|}[I - \hat{P}\,\hat{P}^T] \qquad \frac{\partial \hat{S}}{\partial R} = 0 \tag{3-34}$$

Equation (3-33) becomes

$$\frac{\partial \alpha}{\partial R} = - \frac{\hat{S}^T}{|P| \sin \alpha} [I - \dot{P} \hat{P}^T] = - \frac{1}{|P|} \left[\frac{\hat{P} \times \hat{S}}{|\hat{P} \times \hat{S}|} \times \hat{P} \right] \qquad (3\text{-}35)$$

The gradient of (3-31) with respect to V yields

$$\frac{\partial \alpha}{\partial V} \equiv 0 \qquad (3\text{-}36)$$

The gradient of (3-31) with respect to the bias angle δ is

$$\frac{\partial \alpha}{\partial \delta} = 1 \qquad (3\text{-}37)$$

The gradient of the measurement with respect to the time bias is

$$\frac{\partial \alpha}{\partial \tau} = \frac{\partial \alpha}{\partial \hat{P}} \frac{\partial \hat{P}}{\partial \tau} \qquad (3\text{-}38)$$

or

$$\frac{\partial \alpha}{\partial \tau} = \left(- \frac{\hat{S}^T}{\sin \alpha}\right) \left(\frac{1}{|P|} [I - \hat{P} \hat{P}^T][\dot{P}_p - V] \right) \qquad (3\text{-}39)$$

Using (3-35) equation (3-39) can be written as

$$\frac{\partial \alpha}{\partial \tau} = \frac{\partial \alpha}{\partial R} (\dot{P}_p - V) \qquad (3\text{-}40)$$

The total measurement gradient with respect to the state and the two biases is shown below.

$$H_z = \left(- \frac{1}{|P|} \left[\frac{\hat{P} x \hat{S}}{|\hat{P} x \hat{S}|} \times \hat{P} \right] \; ; \; 0 \; ; \; 1 \; ; \; - \frac{1}{|P|} \left[\frac{\hat{P} x \hat{S}}{|\hat{P} x \hat{S}|} \times \hat{P} \right] [\dot{P}_p - V] \right) \qquad (3\text{-}41)$$

SECTION 4

DIGITAL COMPUTER PROGRAMS

The analysis of the bias errors described in Section 3 has been performed using three digital computer program simulations. The "Patched Conic A.U. Program" and "Planetary Mass Program" are simulations of the trajectory in two dimensional conic form. The analysis performed using these programs is in the form of deviations or differences from a nominal trajectory due to deviations in the physical constants. The third program used is the "Mark II Error Propagation Program."[28] This program is designed for use in making a statistical error analysis of a navigation system that utilizes a Kalman filter in the data processing.

The following sections will describe the capabilities of these three programs. The Mark II description is limited to those features that are used in the study.

4.1 PATCHED CONIC A.U. PROGRAM

The Patched Conic A.U. Program simulates the effect of a change in the A.U. Conversion to a laboratory unit on the planetary ephemeris and shows the resulting effect on an interplanetary trajectory.

The planet ephemeris model used in the program has the following characteristics. The planets Earth and Mars are on coplanar circular orbits about the Sun at distances of 1 A.U. and 1.53 A.U. respectively. The uncertainty in the A.U. conversion* is included in the model in the following manner. For the Earth on a two body Keplerian orbit, the A.U., mass of the Sun, mass of the Earth, and the period of the Earth about the Sun are related by the following expression.

*The nominal conversion factor used is 149599000 km/A.U.

$$\omega^2 = \frac{G(M_s + M_\epsilon)}{(AU)^3} \qquad (4\text{-}1)$$

where

ω = angular frequency of the Earth
M_s = mass of the Sun
M_ϵ = mass of the Earth
AU = astronomincal unit
G = universal gravitational constant

It is assumed that the Earth's angular frequency is known perfectly and that the earth's mass can be neglected with respect to the Sun's mass. Under these assumptions, the partial derivative of equation (4-1) becomes

$$\left(\frac{\partial GM_s}{\partial AU}\right)_{\omega = CONST} = 3\left(\frac{GM_s}{AU}\right) \qquad (4\text{-}2)$$

The relationship shown in equation (4-2) indicates that a change in the "length" of the A.U. must be accompanied by a change in the mass of the Sun in order to maintain ω constant. In the ephemeris model used, a change in the A.U. is accompanied by changes in the radial distances of the planets and the mass of the Sun. These changes maintain the angular frequencies of the planets constant.

The interplanetary trajectory generation is accomplished as follows. The launch and target planets are positioned with an initial angular separation that will satisfy the planetary geometry required for a specified heliocentric transfer angle and flight time.

The trajectory program obtains an Earth-Mars (Mars-Earth) heliocentric conic trajectory with a specified flight time and transfer angle. The heliocentric conic is then patched to a Mars (Earth) centered conic trajectory at the sphere of influence. The initial heliocentric velocity magnitude is then

varied in a differential correction loop to obtain a specified close approach distance at Mars (Earth). This process establishes a nominal trajectory for the flight time and transfer angle. The initial heliocentric velocity vector is then separated into two parts as shown below.

$$\vec{v} = \vec{v}_{\epsilon} + \vec{v}_{\infty} \qquad (4\text{-}3)$$

where

$\vec{v}$ = initial heliocentric vehicle velocity

$\vec{v}_{\epsilon}$ = heliocentric velocity of Earth

$\vec{v}_{\infty}$ = geocentric hyperbolic excess velocity (velocity relative to Earth at a million km)

The geocentric hyperbolic excess velocity, v_{∞} , represents the Earth departure condition measured in kilometers/sec. This is the initial heliocentric velocity that a mission analysis would show is required for a nominal ephemeris. This velocity is assumed to be known precisely and is not changed. The A.U. conversion factor is then perturbed causing changes in the positions and velocities of Earth and Mars. The gravitational constant is also changed in accordance with equation (4-2). The result of these changes is that the initial vehicle state relative to the Sun deviates from the nominal conditions. The vehicle position is changed with the change in the Earth's position. The vehicle velocity relative to the Sun is changed through the change in the Earth's velocity in equation (4-3). The perturbed heliocentric trajectory is patched to Mars and the approach trajectory differences from the nominal computed. The process is shown pictorially in Figure 4-1.

This program can call the guidance program described in Section 4.4. The velocity required to correct the approach trajectory differences are then computed as a function of time.

4.2 PLANETARY MASS PROGRAM

The Planetary Mass Program is designed to analyze the effect of uncertainties in planetary mass on interplanetary approach trajectories. The characteristics of a planetary approach trajectory are determine by the vehicle velocity state relative to the planet at the "sphere of influence" and the planetary mass.

The trajectory model used in the program is a conic section. During the approach phase of a mission, this is a good approximation to the three dimensional trajectory.

The $\vec{B}$ vector and radius of closest approach (RCA) are used to describe the vehicle passage of the planet. The $\vec{B}$ vector and the associated unit vectors $\hat{R}$, $\hat{S}$, $\hat{T}$ (Figure 4-2) are described in Reference 21. The $\hat{S}$ vector is in the direction of the approach asymptote and the $\hat{R}$, $\hat{T}$ vectors are in the plane normal to the $\hat{S}$ vector and containing the $\vec{B}$ vector.

The magnitude of the vehicle velocity state at the sphere of influence, v_∞, is a program input used to simulate approach trajectories of different energies. The flight path angle of the approach velocity vector is used as a control by the program to obtain a trajectory with a specified distance of closest approach.

After the generation of the desired nominal approach trajectory, the program perturbes the planetary mass and computes the differences between the perturbed approach trajectory and the nominal. The program can call the guidance program which will compute the velocity required to correct the differences.

4.3 MARK II ERROR PROPAGATION PROGRAM

The Mark II Error Propagation Program is used in the statistical analyses of the effects of the bias errors on the navigation system performance. The capabilities of the program that are used in the analysis and the program modifications added during the study are described below.

The program has the capability of simulating an onboard navigation system with the following types of measurements:

a. Range (Radar)
b. Range Rate
c. Theodolite (Right Ascension and Declination)
d. Sextant (Star-Planet Angle)
e. Range (Subtended Angle)

The sextant measurement is the only one used in the study. The star-planet angles used in the analysis are measured in two specific directions relative to the trajectory plane. The angles being measured are assumed to lie in the trajectory plane or normal to it. Figure 4-3 illustrates the orientation of the two angles and shows the stars required for such measurements.[27]

The standard deviation, σ, of the instrument random error is input to the program. The instrument noise is the quantity, q, in the expression for a measurement, y, shown below.

$$y = Hx + q \qquad (4\text{-}4)$$

where

y measurement
H measurement gradient
x Deviation state
q random noise

The program is capable of analyzing the effects of the following bias errors.

a. Sextant Bias (Modification added during study)
b. Onboard Clock Bias
c. Earth Planetary Mass Uncertainty
d. Mars Planetary Mass Uncertainty
e. Solar Radiation Pressure Uncertainty

The standard deviation on the estimate of each of these quantities is input to the program.

The Mark II program, with modifications incorporated during the study, is capable of analyzing the effects of the bias errors for each of the three techniques described in Section 2.2; (1) Neglecting, (2) Including, and (3) Considering. The parametric analysis techniques described in Section 2.3 have also been added to the program capability.

The error analysis quantities computed by the program and used in Section 5, are defined below with a summary of the equations used in the Kalman trajectory estimation and end point prediction processes. A basic assumption in the theory is that linearity is satisfied in the neighborhood of a nominal trajectory.

Between the onboard observations, the deviation state estimate and the error covariance matrix are propagated in time along the nominal trajectory as follows.

$$\hat{x}(t_2) = \varphi(t_2;t_1)\ \hat{x}(t_1) \tag{4-5}$$

$$P(t_2) = \varphi(t_2;t_1)P(t_1)\varphi^T(t_2;t_1) \tag{4-6}$$

At the time of an observation, the measurement information is included in the state estimate and a new covariance matrix obtained in the following manner.

$$\hat{x}_n = \hat{x}_o + K(y-\hat{y}) \tag{4-7}$$

$$P_n = P_o - KHP_o \tag{4-8}$$

where

$K = P_o H^T (HP_o H^T + Q)^{-1}$ (Kalman Filter Gain)

H = measurement gradient

y = actual measurement

$\hat{y}$ = estimate of measurement

Q = convariance matrix of random measurement noise

The equations shown above are for the case in which all the bias errors are neglected. The sequence of program operations described by equations (4-5) through (4-8) is the same when using the different types of treating bias errors but the form of each equation is different (see Section 2).

The Mark II program computes the statistical quantities at any requested time point along the nominal trajectory. The program also computes the statistical characteristics of the estimate of the trajectory end point constraints. The estimated deviation state and covariance matrix of the error in estimate are propagated to the end point. The propagation to the end time, T, appropriately includes the effects of bias errors in the equations of motion if they are being analyzed in the simulation.

$$\hat{x}(T) = \varphi(T,t)\ \hat{x}(t) \tag{4-9}$$

$$P(T) = \varphi(T,t)\ P(t)\ \varphi^T(T,t) \tag{4-10}$$

where

T = End point time

The estimated end point deviation, $\hat{x}(T)$, and the covariance matrix of the error in estimate, P(T), are then transformed into an estimate of the constraint deviations and the associated error in estimate respectively. The constraints used to describe the end deviations in the program are $\vec{B} \cdot \hat{T}$ and $\vec{B} \cdot \hat{R}$.[21] The constraint data are obtained by means of a point transformation as follows.

$$\begin{pmatrix} \delta \vec{B} \cdot \hat{T} \\ \delta \vec{B} \cdot \hat{R} \end{pmatrix} = G(T)\ \hat{x}(T) \tag{4-11}$$

$$\begin{pmatrix} \sigma^2_{B\cdot T} & \rho\sigma_1\sigma_2 \\ \rho\sigma_1\sigma_2 & \sigma^2_{B\cdot R} \end{pmatrix} = G(T)\ P(T)\ G^T(T) \tag{4-12}$$

where

$$G(T) = \begin{pmatrix} \frac{\partial\ B\cdot T}{\partial\ x(T)} \\ \\ \frac{\partial\ B\cdot R}{\partial\ x(T)} \end{pmatrix} \quad \text{point transformation}$$

Equations (4-5) through (4-12) describe the processes by which the statistical navigation data shown in Section 5 are obtained.

4.4 GUIDANCE PROGRAM

The guidance program is used by the A.U. Program and the Planetary Mars Program to compute the velocity required to correct specified trajectory deviations. The program is capable of using two guidance laws; (1) fixed time of arrival (FTA), and (2) variable time of arrival (VTA). The three end point constraints used with each guidance law are shown below:

$$FTA = \begin{pmatrix} X(T) \\ Y(T) \\ Z(T) \end{pmatrix}_T \qquad VTA = \begin{pmatrix} B\cdot T \\ B\cdot R \\ V_\infty \end{pmatrix}_{T+\Delta T}$$

where

T = nominal arrival time

$\vec{B}\cdot\hat{T}, \vec{B}\cdot\hat{R}$ = orthogonal components of the $\vec{B}$ vector

V_∞ = hyperbolic excess velocity

X,Y,Z = nominal vehicle position state at time, T

The guidance velocity correction required at time, t, is computed in the following manner. The vehicle deviation state is propagated along a nominal trajectory to the end point (equation 4-13) and transformed into appropriate constraint deviations (equation 4-14).

$$\vec{x}(T) = \varphi(T,t)\ \vec{x}(t) \tag{4-13}$$

$$\vec{D}(T) = C(T)\ \vec{x}(T) = C(T)\ \varphi(T,t)\ \vec{x}(t) \tag{4-14}$$

where

$\vec{x}$ = deviation state vector

$\vec{D}$ = constraint deviation vector

$C(T)$ = point transformation from the state to either FTA or VTA constraints

The sensitivity of the end constraints to a velocity correction at time, t, is obtained from the partioned transition matrix.

$$A(T,t) = (A_1 \mid A_2) = C(T)\ \varphi(T,t) \tag{4-15}$$

3x6 3x3 3x3 3x6 6x6

where

A_1 = sensitivity of end constraints to a position change at time, t.

A_2 = sensitivity of end constraints to velocity change at time, t.

The velocity correction required to null the constraint deviation vector, $\vec{D}(T)$, in equation (4-14) is the following.

$$A_2 \dot{\vec{x}}_g(t) + \vec{D}(T) = 0$$

or

$$\dot{\vec{x}}_g(t) = A_2^{-1} \vec{D}(T) = -(A_2^{-1} A_1 \; I) \vec{x}(t) \qquad (4\text{-}16)$$

where $\dot{\vec{x}}_g$ = the guidance velocity correction.

The deviation state, $\vec{x}(t)$, used in the guidance program is input by the parent program. It is obtained by taking the difference between a nominal approach trajectory and a perturbed trajectory. The trajectory is perturbed due to an uncertainty in the planetary mass or an uncertainty in the astronomincal unit conversion.

SECTION 5

MIDCOURSE NAVIGATION STUDY

The results presented in this section show the effects of bias errors on the performance of an onboard navigation system. These results are an evaluation of the navigation system requirements generated in the original study[1] with the constraint that only random errors were considered in the analysis. The analysis is performed for the midcourse phases of both the outbound Earth to Mars trajectories and the return Mars to Earth trajectories.

The navigation analysis is limited to the use on onboard sextant measuring device with a random error of 10 arc seconds. The initial study showed that an instrument of approximately this accuracy was capable of performing the Earth Mars round trip navigation such that ±3.5 km entry corridors were achieved at both Mars and Earth. The onboard measurement schedules used for the outbound and return trajectories are shown in Tables 5-1 and 5-2 respectively. The analysis of the schedule selection is in Reference 1.

There are several trajectories utilized in the following analyses. The statistical analyses with the Mark II program uses the same round trip nominal trajectory used in the original study. This nominal trajectory, a 235 day outboard and 296 day return with a 40 day stay at Mars, is shown and described in Appendix B. The trajectory was selected from the study results described in Reference 29. The Patched Conic A.U. Program and Planetary Mars program are used to analyze equation of motion error effects on a large number of trajectories. The trajectories analyzed include many transfer and approach trajectories of practical interest.

The initial covariance matrices of the error in estimate used in the statistical analyses on the outbound and return trajectories are shown in Tables 5-3 and 5-4 respectively.

5.1 EARTH-MARS TRANSFER

The results of two forms of analysis are presented below for the outbound trajectories. The first type of analysis evaluates the trajectory deviations or differences from a nominal trajectory that are introduced by deviations in the equation of motion parameters. These analyses are performed with the Patched Conic A.U. Program and the Planetary Mass Program.

The second type of analysis is a statistical evaluation of the effect of bias errors on the navigation system performance. These results are obtained with the Mark II Error Propagation Program.

5.1.1 Equation of Motion Errors

The equation of motion bias errors analyzed are uncertainties in the following: (1) A.U. conversion, (2) Earth and Mars planetary masses, and (3) solar radiation pressure.

5.1.1.1 A.U. Conversion. The data and results presented in this section were generated using an uncertainty in the conversion of the A.U. to kilometers of ±1000 km. This is slightly larger than the uncertainty shown in Table 3-1 for the 1963 adopted value.

The approach phase of a number of Earth-Mars trajectories is analyzed to determine the navigation and guidance requirements due to the uncertainty in the A.U. conversion. Five heliocentric transfer angles are used with flight times for each from 100 to 500 days. Three trajectories of interest listed in Table 5-5, are included in the analysis. They are: (1) Hohmann transfer 180 degrees, 260 days, (2) Mariner IV trajectory 160 degrees, 228 days, and (3) High energy outbound leg of round-trip trajectory[29] 270 degrees, 235 days.

The trajectory data and corresponding target approach deviations are shown in Figures 5-1A through 5-5B. Part A of each figure shows the flight time, launch velocity, and target approach velocity as a function of the direction

of the hyperbolic approach asymptote, $\hat{S}$. Part B shows the deviation in close approach distance for a 1000 km change in the A.U. conversion to kilometers. The 160, 180, and 200 degree transfers each show two deviation minimums. The 225 and 270 degree transfers each has a single minimum. The minimum deviations are near zero for the 180 degree transfer and increase with transfer angles away from 180. The minimum deviations for the 225 and 270 degree transfers are 125 km and 550 km respectively. These data show the possibility of selecting trajectories that minimize the effect of the uncertainty in the A.U. conversion on the close approach distance. The Mariner IV trajectory is one that is near a minimum. The 228 day 160 degree transfer has a deviation of 175 km uncertainty in the conversion.

The position deviation state at the sphere of influence (patch point) for all the trajectories is approximately 1000 km. The close approach deviation minimums are the result of these errors at the patch point being in directions that result in cancellation or partial concellation of the deviation in the periaries distance.

The trajectories marked with an asterisk on the 160, 180, and 270 degree transfers are analyzed to determine the approach guidance velocity required to correct the deviations. The results of this analysis are shown in Figures 5-6, 5-7, and 5-8. The solid lines indicate the Δv required for a fixed time of arrival (FTA) and the dotted lines the requirements for a variable time of arrival (VTA). The curves show that the requirements for FTA are nearly the same for all the trajectories shown. A correction at the sphere of influence requires about 10 meters/second and grows to approximately 200 meters/second as periaries is approached. The Δv requirements for the VTA guidance law show a wide variation depending on the specific trajectory selected.

The trajectories that have small close approach deviations, curve 1 in Figure 5-6 and curves 1 and 3 in Figure 5-7, have velocity requirements that range from less than 1 meter/second at the sphere of influence to 8, 4 and 2 meters/second respectively at periaries. The remaining VTA curves in

Figures 5-6 and 5-7 show larger Δv requirements that range from 2 meters/second to 40 meters/second for the trajectories with larger deviations. These requirements are considerably smaller than those required with a FTA guidance law. Figure 5-8 shows the Δv requirements on a 270 degree transfer. Figure 5-5B shows the minimum deviation for the 270 degree transfer is 550 km, which is much larger than other transfer minimums and the velocity requirements are correspondingly higher. The VTA velocity requirements are only slightly smaller than those required for a FTA guidance law.

The time at which a reasonable guidance correction can be made is determined by the navigation system. The error in estimate of the end constraints must be below a predetermined level before the guidance maneuver can be executed. The selection of an entry mission at Mars with a ±10 km entry corridor defines tolerable limits on the end constraint deviations. If it is required that the confidence in hitting the entry corridor is to be 99 percent (3 sigma), then the one sigma error in estimate of the close approach distance must be reduced to ±3.3 km. The guidance correction can then be made with a 99 percent confidence (neglecting execution errors) of hitting the ±10 km corridor.

Figure 5-9 shows the error in estimate of the end constraints for three approach trajectories of different energies. The navigation measurements are made with a 10 arc second sextant. Measurements are taken every 15 min minutes. The initial error in estimate of state is assumed to be 1000 km in each of the inplane position coordinates and 0.2 meters/second in the velocity coordinates. These errors correspond to the actual deviations that occur at the time of patch to the target due to a 1000 km uncertainty in the A.U. conversion. Due to the onboard observations, the error in estimate of the constraints is quickly reduced to less than 100 km. It then remains relatively constant until the last few hours of the approach. The error in estimate is sufficiently small for an entry mission (3.3 km) approximately 3 or 4 hours prior to periaries on each trajectory.

Figures 5-6 through 5-8 indicate that this time corresponds to corrections of 50 to 70 meters/second for a FTA guidance law. The VTA guidance requirements at this time are less than 10 meters/second except for the 270 degree transfer where they are about 30 meters/second. A FTA guidance policy allowing for two approach corrections could reduce the total Δv required considerably from the 50-70 meters/second required for a single correction.

A factor that has been neglected in the guidance analysis is the execution errors. A correction of 70 meters/second with proportional errors of 1 percent would produce a 0.7 meter/second execution error. Three or four hours before periaries the close approach sensitivity to a velocity change is such that 0.7 meter/second error will cause deviations that are the same order of magnitude as the entry corridor. This factor also favors the guidance policy of two smaller approach corrections for an accurate planet passage.

5.1.1.2 Mars' Planetary Mass. The results presented in this section show the navigation and guidance requirements for controlling the approach trajectory under the influence of an uncertainty in the planetary mass. The results assume that the midcourse guidance system has controlled the vehicle to the sphere of influence perfectly. The only equation of motion uncertainty considered is the planetary mass.

The time history of the growth in the predicted deviations in close approach distance and $\vec{B}$ magnitude (equations 4-9 and 4-11) based on the state deviation is shown in Figure 5-10. These data were obtained using a planetary mass uncertainty of 130 km^3/sec^2 and a close approach distance of 5000 km. The curves all display the characteristic of having very small deviations until 4 to 8 hours before periaries. The deviations then grow rapidly to values from 2 to 15 kilometers. The approach guidance Δv required to correct these deviations is shown in Figure 5-11 as a function of time along the trajectory. The requirements are shown for both FTA and VTA guidance laws. The Δv required on these trajectories for each guidance law is between 1 and 10 meters/second during the last few hours. The VTA velocity requirements are smaller in all cases.

The time at which a guidance correction can be made is determined by the capability of the navigation system to estimate the end point deviations to a satisfactory accuracy. The capability of an onboard navigation system using a 10 arc second sextant to estimate the end constraints is shown in Figure 5-12. The results are shown for three nominal trajectories with different energies. The parameters being estimated include the vehicle state and the planetary mass. The initial vehicle state uncertainty is assumed to be zero and the uncertainty in the planetary mass is 130 $km^3/sec.^2$ The tolerable error in estimate for an entry mission is shown on Figure 5-11 as ±3.3 km. The times on these trajectories that this level is reached are 2 days 19 hours for the trajectory with v_∞ = 2.0 km/sec and 1 day 12 hours for the v_∞ = 4.0 km/sec trajectory. Using these correction times in Figure 5-11 shows the guidance velocity requirements are approximately 1 meter/sec for a VTA guidance law and 3 meters/sec for FTA guidance law. The significance of these approach corrections in terms of the total mission is discussed in Section 6.

5.1.1.3 Statistical Analysis. The statistical analysis of the navigation system is performed with the Mark II Error Propagation Program. The measurement instrument is a 10 arc second accuracy sextant. The results presented in this section are obtained while using the initial state covariance matrix shown in Table 5-3 and the measurement schedule shown in Table 5-1. The sequence of measurements used within the schedule is the following. Three inplane measurements are made followed by a single out of plane measurement. This sequence is continually repeated. The nominal trajectory used is described in Appendix B.

The results presented in Figures 5-13A and B show the effects of neglecting the equation of motion bias errors on the error in estimate of the end point constraints $\vec{B}\cdot\hat{T}$ and $\vec{B}\cdot\hat{T}$ respectively. The $\hat{T}$ vector is in the trajectory plane and the $\hat{R}$ vector is normal to the trajectory plane. The theory for the error analysis being used is presented in Section 2.2.1.

The number 4 curve in each figure shows the expected error in estimate of the end constraint under the assumption of a perfect physical model. These

uncertainties shown are due to injection errors and random errors in the measurements. These results correspond to those obtained in the original study.[1] The three remaining curves in each figure show the additional error in estimate due to the neglected uncertainties in the planetary masses of Earth and Mars and the solar radiation pressure. The planetary mass uncertainties used are 15 km^3/sec^2 for the Earth and 150 Km^3/sec^2 for Mars. These are approximately the uncertainties shown in Tables 3-2 and 3-3 for the 1961 adopted values. The assumed form of the solar radiation pressure acceleration from equation (3-25) is

$$p = k_{sp} \frac{R_s}{r_s^3} \qquad (5\text{-}1)$$

The solar radiation constant, k_{sp}, is a function of the vehicle mass, vehicle area projected normal to the vehicle-sun line, and the surface reflectance. For a hypothetical vehicle with a reflectance of one, a constant normal area of 100 square feet, and a weight of 200 pounds, the constant, k_{sp}, is approximately 10^7 km^3/sec^2. The results shown in Figures 5-13A and B are for an uncertainty in the solar radiation pressure constant of 10^6 km^3/sec^2 or 10%.

The characteristics of the three curves in Figures 5-13A and B showing the error due to neglecting the uncertainties in the planetary masses and solar radiation pressure are due to the following effects. The initial uncertainties show the error each would introduce if no navigation measurements were taken. At different points in time, each of the errors begins decreasing due to the measurements that are being taken. The decrease in error begins to occur at a time when the equation of motion error source has had some influence on the trajectory and the navigation system is estimating the perturbed trajectory. For example, the planetary mass of Earth has an immediate strong effect on the trajectory. A large portion of the effect of this error is quickly removed by the navigation system. In contrast, the mass of Mars has essentially no effect on the trajectory until the sphere of influence is reached (234 days). Therefore, the errors in the end constraint estimates due to neglecting this error remains constant

(number 2 curves) until the last day. At this time the mass of Mars does influence the trajectory and the effects of its uncertainties can be removed.

The total error in estimate of the end constraints due to neglecting the three equation of motion parameters is shown in Figures 5-14A and B by the number 1 curves. These curves are obtained by taking the root sum square of the errors due to the individual error sources. Curve number 2 in Figures 5-14A and B is the error in estimate when the bias errors are neglected. Curve Number 3 in these Figures is the total error in estimate of the constraint. This curve is the root sum square of curves 1 and 2. The difference between curves 2 and 3 shows the degree to which the results of the original study concerning the navigation system performance were optimistic due to neglecting the bias errors.

The $\vec{B}\cdot\hat{T}$ constraint estimate is the more critical of the two because it indicates the accuracy to which the entry altitude is known. As indicated earlier, for an entry mission at Mars the altitude corridor is ±3.5 km. Figures 5-13A and 5-14A show that the error in $\vec{B}\cdot\hat{T}$ due to neglecting the uncertainty in Mars planetary mass is 4 to 5 km. The effect of an error of this magnitude must be evaluated in terms of mission requirements. While this error makes an entry mission at Mars marginal, it would have only a minor effect on a flyby or orbiter mission.

During the approach phase of the mission, Figures 5-13A and B indicate that the effects of neglecting uncertainties in the planetary mass of Earth and the solar radiation pressure are negligible compared to the effect of Mars' mass uncertainty. This result indicates that these two error sources can be neglected without affecting the end point estimation performance.

Bias Error Included. The equation of motion bias errors instead of being neglected can be included in an expanded state vector and estimated in addition to the vehicle state. The theory describing this estimation process is presented in Section 2.2.2. The results obtained with this type of processing are shown in Figure 5-15A and B and 5-16A and B. Figures 5-15A and B show the effects of an uncertainty in the solar radiation pressure when it is being estimated as part of the state. Parametric curves are shown for uncertainties in the solar radiation constant ranging from 0 to 10^6 km^3/sec^2. The curve for a zero uncertainty in the constant is equivalent to neglecting the bias error. The differences between this zero uncertainty curve and the curves for the solved for bias error show the extent ot which the end point estimate is optimistic when neglecting the radiation pressure uncertainty. These differences approach zero at approximately 230 days. At this time, the error in estimate of the end constraint for the zero uncertainty case is no longer optimistic. Essentially the same conclusion can be reached from the data shown in Figures 5-13A and B.

The error in estimate in Figures 5-13A and B due to neglecting the solar pressure uncertainty completely is of significant magnitude for a slightly longer time (234 days) and then becomes negligible. This is due to the fact the uncertainty is not being estimated as is the case for the results shown in Figures 5-15A and B.

The effects of uncertainties in the planetary masses of Earth and Mars are shown in Figures 5-16A and B. These results were obtained while including the mass uncertainties in the state vector and solving for them. The conclusions that can be drawn from these results are in general agreement with those shown in Figure 5-13A and B for the neglected mass uncertainties. The effect of uncertainties in the Earth's mass is negligible after approximately 200 days. At this time, the curves for the zero uncertainty and the maximum uncertainty form a single curve (Figures 5-16A and B). The second half of the curves in Figures 5-16A and B show the effect of Mars planetary mass uncertainty. The error in estimate of $\vec{B}\cdot\hat{T}$ in Figure 5-16A

shows that uncertainties from 0 and 450 km^3/sec^2 in the planetary mass cause the error in estimate to increase from 3 km to approximately 20 km. An error as large as ±20 km in the $\vec{B}\cdot\hat{T}$ estimate would be unsatisfactory for an entry mission at Mars.

5.1.2 Measurement Bias Errors

The analysis of the effects of the measurement biases is performed with the Mark II Error Propagation Program. The bias errors are analyzed by two techniques. One technique is that of including them as part of the state and estimating them. This analysis technique is described in Section 2.2.2. The second technique used is that of considering the effect of a bias error. This process is described in Section 2.2.3. The Mark II program is not capable of analyzing the error due to completely neglecting measurement biases as was done for the equation of motion errors.

The results shown in Figures 5-17A and B are for the two methods of treating the bias error in the sextant measurement. Curve one shows the error in estimate of the end constraint for an instrument with a 10 arc second random error and no bias error. Curve two shows the error in estimate for the addition of a 10 arc second bias that is included in the state and estimate. The third curve is for the case in which the 10 arc second bias is considered in the estimation process but is not estimated (variance is held constant) as part of the state. Curves one and two in Figures 5-17A and B show that the increase in the error due to an instrument bias error that is solved for is negligibly small (less than 1 km at the end time).

Figure 18 shows the manner in which the standard deviation of the measurement bias is reduced as it is estimated along with the state. The figure shows the reduction for initial uncertainties of 10 and 20 arc seconds. In both cases, the initial uncertainty is quickly reduced to two arc seconds and finally to one arc second.

Curve three shows that there is a considerable increase in the error in estimate when the bias error is considered but not estimated. The end point estimate error in $\vec{B}\cdot\hat{T}$ is increased from 7 km to 14 km. This result indicates that if the error source were neglected completely, the error due to neglecting it would be larger than the 7 km difference shown above.

Figure 5-19 shows the effect of a 60 second onboard clock bias on the error in estimate. The clock bias is included in the state and estimate. These results indicate that the clock bias can be estimated rapidly and its effect removed from the estimation process. The effect of completely neglecting this error source is not presented. The high correlation between the clock and the estimate, as shown by the ability to solve for the bias, indicates it would be a significant error if present and neglected.

5.2 MARS-EARTH TRANSFER

The results obtained on the effects of bias errors on the Mars-Earth trajectories are presented in this section. The data presentation is restricted because the results and conclusions that can be reached are in general the same as obtained for the outbound portion of the mission.

The analysis of the measurement bias errors is omitted. The analysis in Section 5.1.2 indicates that these are error sources that can not be neglected without introducing significant errors. This conclusion applies to the return trajectories equally well.

5.2.1 Equation of Motion Errors

The equation of motion bias errors analyzed are uncertainties in the following: (1) A.U. Conversion, (2) Earth and Mars planetary masses, and (3) solar radiation pressure.

5.2.1.1 A.U. Conversion. The data presented in this section were computed using a conversion uncertainty in the A.U. to kilometer of ±1000 km. This is slightly larger than the uncertainty shown in Table 3-1 for the 1963 adopted value. These data were generated with the Patched Conic A.U. Program.

Five heliocentric transfer angles are used with flight times for each from 100 to 500 days. One trajectory of interest included in the analysis is the Mars-Earth nominal trajectory (296 days 270 degrees) used in the original study. The trajectory data and corresponding target approach deviations are shown in Figure 5-20A through 5-24B. Part A of each figure shows the flight time, launch velocity, and target approach velocity as a function of the direction of the hyperbolic approach asymptote, $\hat{S}$. Part B shows the deviation in close approach distance for a 1000 km change in the A.U. Conversion to kilometers. The 160 and 180 degree transfers each show two deviation minimums. The remainder of the curves have a single minimum. These are essentially the same type of characteristics that where exhibited on the outbound trajectories shown in Figures 5-1A through 5-5B.

The 270 degree transfers show a very narrow deviation minimum around the point of a 470 day flight time. The 296 day nominal trajectory from the first study has a close approach deviation of over 2000 km for the 1000 km conversion deviation.

The conversion of these trajectory deviations into velocity requirements was not performed. The velocity requirements, as in the cases for the outbound trajectory, would vary from near zero at the minimum points to extremely large values away from the minimums.

5.2.1.2 Statistical Analysis. The statistical analysis of the navigation system is performed with the Mark II Error Propagation Program. The measurement instrument is a 10 arc second sextant. The results presented in this section are obtained while using the initial state covariance matrix shown in Table 5-4 and the measurement schedule shown in Table 5-2. The

sequence of measurement within the schedule is three inplane measurements followed by a single out-of-plane measurement. The nominal trajectory used is described in Appendix B.

The results presented in Figures 5-25A and B show the effect of neglecting the equation of motion bias errors on the estimate of the end constraints $\vec{B}\cdot\hat{T}$ and $\vec{B}\cdot\hat{R}$ respectively. The theory of the error analysis being used is presented in Section 2.2.1.

The number 4 curve in each figure shows the expected error in estimate of the constraint under the assumption of a perfect physical model. These uncertainties are due to the injection errors and random errors in the measurements. These results correspond to those obtained in the original study.(1) The three remaining curves in each figure show the additional error in estimate due to the neglected uncertainties in planetary masses of Earth and Mars and the solar radiation pressure. The planetary mass uncertainties used are 15 km^3/sec^2 for the Earth and 150 km^3/sec^2 for Mars. These are approximately the uncertainties shown in Tables 3-2 and 3-3 for the 1961 adopted values. The uncertainty in the solar radiation constant, k_{sp}, is taken as 10^6 km^3/sec^2.

The curves in Figures 5-25A and B have the same character as those shown in 5-13A and B for the outbound trajectory with the roles of Earth and Mars planetary masses interchanged. In the return case, the uncertainty in the mass of Earth is so small that it has negligible effect on the terminal accuracy. The mass of Mars and the solar radiation pressure exhibit an effect until late in the flight. During the final day, their effects become quite small.

The total error in estimate of the end constraints due to neglecting the three equation of motion parameters is shown in Figures 5-26A and B by the number 1 curves. These curves are obtained by taking the root sum square of the errors due to the individual error sources. Curve number 2 in Figures 5-26A and B is the error in estimate when the bias errors are

neglected. Curve number 3 in these figures is the total error in estimate of the constraint. This is the root sum square of curves 1 and 2. The difference between curves 2 and 3 shows the degree to which the results of the original study were optimistic concerning the navigation system performance when neglecting the bias errors. The curve differences indicate that neglecting the equation of motion biases would not adversely effect an entry mission requiring a ±3.5 km terminal accuracy.

SECTION 6

SUMMARY AND CONCLUSIONS

The theoretical analysis in Section 2 presents some new developments in the analysis of the effects of bias errors on an orbit estimation process. These developments concern three areas of interest. They are the following: (1) the effect of neglecting bias errors in the modeling of the physical process, (2) the separable properties of the effects due to random errors and those due to bias errors, and (3) techniques for efficient parametric analysis by means of matrix manipulations.

The data results obtained on the effects of equation of motion bias error sources on the navigation system performance indicated the following. The uncertainty in Mars planetary mass produces deviations in close approach of 10 to 20 km for practical Mars approach trajectories. The error in the state estimate due to neglecting this uncertainty is on the order of 4 to 5 km at the end point. This is a significant error when considering an entry mission with a 3.5 km corridor requirement. The effect of Mars mass uncertainty on the return trajectory is negligible following the navigation measurements that are used.

The uncertainty in the planetary mass of Earth causes approach deviations of less than 1 km on the practical approach trajectories. On the Earth-Mars outbound trajectory, the effects of this mass uncertainty is removed by the navigation measurements.

The effects of a solar radiation pressure uncertainty of 10 percent can be removed on both the outbound and return trajectories by means of the navigation measurements.

The effect of an uncertainty in the A.U. conversion to laboratory units is

a strong function of the particular heliocentric trajectory being used. The analysis of 5 heliocentric transfer angles for various flight times for both the outbound and return trajectories shows one or two minimums in the close approach deviations for each transfer angle. The deviation minimums vary from near zero to 550 km for a 1000 km uncertainty in the A.U. The minimum deviations are near zero for a 180 degree transfer and increase for larger and smaller transfer angles. The deviations can be estimated by the navigation system to a satisfactory accuracy for an entry mission.

The guidance analysis is restricted to the determinations of the velocity required to correct the deviations caused by the Mars planetary mass uncertainty and the A.U. conversion uncertainty. The ΔV required is a function of the time at which the correction is applied. The ΔV required to control the deviations due to Mars mass uncertainty for a FTA guidance law vary from 5 to 10 meters/second and from 1 to 5 meters/second with a VTA guidance law. The velocity requirements for an uncertainty in the A.U. are quite trajectory dependent. The guidance velocity corrections for a FTA guidance law are from 50 to 70 meters/second when using only one correction. The corrections for a VTA law vary considerably. The trajectories with small deviations (less than 100 km) require corrections from 1 to 10 meters/second. The trajectories with the larger deviations require corrections of 10 to 30 meters/second.

The guidance requirements for an Earth-Mars mission obtained in the original study while neglecting the two uncertainties that have been described above are shown in Table 6-1. The results in Table 6-1 for a VTA guidance law include the effects of errors in an onboard navigation system and guidance system execution errors. The approach trajectory deviations due to a planetary mass uncertainty cannot be estimated until the last few hours of the approach trajectory. It would therefore be necessary to control these deviations with the final correction. The 1 meter/second final correction shown in Table 6-1 would increase to a

maximum of approximately 5 meters/second with a mass uncertainty of 150 km^3/sec^2. The trajectory deviations due to the uncertainty in the A.U. conversion can be estimated with an error of 30 to 40 km one day prior to periaries with a 10 arc second instrument. This allows the possibility of making a correction at this time that will correct the deviations to an accuracy consistent with the estimate. The deviations remaining after the correction could then be removed with the final maneuver. On the trajectories with large deviations due to the A.U. conversion, this would increase the third correction of Table 6-1 by approximately 10 meters/second. The final correction would be increased by 2 to 3 meters/second.

The discussion of guidance Δv requirements above is summarized in Table 6-2. These results were obtained by algebraically adding the velocity requirements caused by the two uncertainties in the equation of motion to those due to injection errors, navigation errors, and guidance system execution errors. This very pessimistic analysis of adding these independent effects algebraically increases the total velocity requirements from 23 meters/second to 41 meters/second.

The sextant angle measurement bias and onboard clock bias both have a significant influence on the navigation system accuracy. If these errors are neglected, the results imply a degradation in the end point estimate accuracy of greater than 7 km. This is not satisfactory for an entry mission. If the bias error sources are included as part of the state being estimated their effect can be eliminated by the "calibration" of the sextant instrument and clock.

SECTION 7

RECOMMENDATIONS

Additional study areas that would extend the scope of the present study and are considered important for defining the navigation and guidance requirements of an interplanetary mission are the following:

a. Guidance Analysis. The guidance analysis performed with trajectory deviations in this study should be extended to a statistical analysis that includes the effects of equation of motion bias errors.

b. Measurement Biases. The effect of neglecting the measurement bias errors should be analyzed. The theory is described in section 2.0 but the digital simulation program is not available at present.

c. A. U. Conversion. The theory required for a statistical analysis of the effect of the uncertainty in the A. U. conversion should be developed. The theory should account for the changing of the reference body centers.

d. Filtering Techniques. The study has assumed the use of a Kalman filter in the data processing. The use of other filtering techniques should be evaluated and, in particular, consideration should be given to their onboard implementation. The performance of some non-optimum data processing filters used with an imperfect physical model should be investigated.

e. Onboard Computers. The design of the onboard computer should be studied to determine means of trading off speed for reliability

(500 - 600 day missions). Also techniques for simplifying calculations for estimating and predicting the state should be investigated. This investigation should include the effects of truncation errors in the computer.

f. Beacons. The importance of having beacons on Mars should be evaluated for the approach phase of the mission, terminal maneuvering phase and orbital phase.

g. Powered Flight. The guidance system inertial equipment requirements should be determined for the retro maneuver (powered and/or atmospheric) and the powered flight out of Mars orbit. A retro analysis is also required at perigee on the return.

h. Mars Orbit. The navigation requirements in orbit should be determined in terms of specific mission objectives. The influence of the oblateness of Mars on these requirements should be evaluated.

SECTION 8

REFERENCES

1. Interplanetary Navigation and Guidance Study, 3 Volumes, Philco-Ford WDL-TR2629, Palo Alto, California, 30 October 1965.

2. Kalman, R. E., "A New Approach to Linear Filtering and Prediction Theory," ASME, Journal of Basic Eng., March 1960, pp. 35-45.

3. Schmidt, S. F., "State Space Techniques Applied to the Design of a Space Navigation System," JACC Conference paper, 1962.

4. Smith, G. L., Schmidt, S. F., and McGee, J. A., Application of Statistical Filter-Theory to the Optimal Estimation of Position and Velocity Onboard a Circumlunar Vehicle, NASA Technical Report R-135, Ames Research Center, 1962.

5. McLean, J. D., Schmidt, S. F., and McGee, J. A., Optimal Filtering and Linear Predictions Applied to a Midcourse Navigation System for the Circumlunar Mission, Technical Report D-1208, NASA Ames Research Center, March 1962.

6. Schmidt, S. F., The Application of State Space Methods to Navigation Problems, WDL-TR4, Philco-Ford WDL Guidance and Control Systems Engineering Department, Palo Alto, California, July 1964.

7. Gunckel, T. L., "Parametric Analyses of Optimal Estimation," Unnumbered Memo, Autonetics Division of North American Aviation, Inc., December 1965.

8. Sorenson, H. W., "Kalman Filtering Techniques," Advances in Control Systems, Volume 3, Leondes, C. T., Editor, Academic Press, New York, 1966.

9. Tyler, J. S., "Methods for Treating Bias Error Sources in the Statistical Error Analyses of Space Systems," WDL-TR2892, Philco-Ford WDL, Palo Alto, California, May 1966.

10. Rohde, P. J., "Influence of Uncertainties in the Astronomincal Unit Conversion and Mars Planetary Mass on Earth-Mars Trajectories," WDL-TR3040, Philco-Ford WDL, Palo Alto, California, September 1966.

11. Makemson, M. W., Baker, R. M. L., Jr., Westrom, G. B., "Analysis and Standardization of Astrodynamic Constants," The Journal of Astronautical Sciences, Volume VIII, Number 1, Spring 1961.

12. Brouwer, D., "System of Constants," Progress in Astronautics and Aeronautics, Volume 14, Academic Press, New York, 1964.

13. Muhleman, D. O., "Relationship Between the System of Astronomincal Constants and the Radar Determinations of the Astronomincal Unit," California Institute of Technology, Jet Propulsion Laboratory, TR-32-477, January 15, 1964.

14. Marsden, B. G., "An Attempt to Reconcile the Dynamical and Radar Determinations of the Astronomical Unit" Symposium #21, I.A.U., on Fundamental Constants of Astronomy, Paris, June 1963.

15. Anderson, J. D., Null, G. W., Thorton, C. T., "The Evaluation of Certain Astronomical Constants from the Radio Tracking of Mariner II," Academic Press, New York, 1964.

16. "Astrodynamic Constants Analysis," LR 17571 Lockheed California Compnay, Burbank, California, June 1963.

17. Herrick, S., Westrom, G. B., Makemson, M. W., "The Astronomical Unit and the Solar Parallax," U.C.L.A. Astrodynamical Report No. 5, 1959.

18. Herrick, S., Baker, R. M. L., Jr., and Hilton, G. G., "Gravitational and Related Constants for Accurate Space Navigation," Proceedings of The Eighth International Astronautical Congress, Barcelona 1957, pages 147-235.

19. Battin, R. H., "Astronautical Guidance, McGraw-Hill Book Company, 1964, Pages 12-14.

20. Baker, R. M. L., Jr. "Influence of Planetary Mass Uncertainty on Interplanetary Orbits," ARS Journal, December 1962, page 1919.

21. Kizner, W., "A Method of Describing Miss Distance for Lunar Interplanetary Trajectories," JPL Publication Number 674, 1 August 1959.

22. Swenson, B. L., Carlson, R. W., Tindle, E. L., "Some Requirements on Lifting Vehicles for Manned Mars Operation," AIAA/AAS Stepping Stones to Mars Meeting, Baltimore, Maryland, March 28-30, 1966.

23. Manned Mars Mission Study, Report for NASA Ames, Contract No. NAS 2-1409 by TRW, STL Redondo Beach, California, 28 March 1964.

24. Tsu, T. C., "Interplanetary Travel by Solar Sail," ARS J. 29, 422-427 (1959).

25. Fimple, William R., "Generalized Three Dimensional Trajectory of Planetary Escape by Solar Sail," ARS J. 32, 883-887 (1962)

26. Wiggins, L. E., "Theory and Application of Radiation Forces," LMSC/A372407, Lockheed Missles and Space Company, Sunnyvale, California, 22 February 1963.

27. Rohde, P. J., "The Scheduling of Measurements for Analysis of An Onboard Navigation System," WDL-TR2600, Philco Corporation, Palo Alto, California, October 1965.

28. Mark II Error Propagation Program, WDL-TR2757, Philco Corporation, Palo Alto, California, 15 February 1966.

29. "A Study of Manned Mars Exploration in the Unfavorable Time Period (1975-1985)," F2M-4039-4, General Dynamics, Fort Worth, 15 February 1964.

APPENDIX A

EQUIVALENT FORM FOR THE COVARIANCE MATRIX

The state covariance matrix following an observation that is weighted with the optimum gain, K(t) is the following.

$$P_n = P - PH^T(HPH^T + Q)^{-1} HP \qquad \text{(A-1)}$$

This can be written as

$$P_n = P - PH^TQ^{-1}(I + HPH^TQ^{-1})^{-1} HP \qquad \text{(A-2)}$$

Using the matrix identity

$$(I + M)^{-1} = I - M + M^2 - M^3 + \cdots\cdots \qquad \text{(A-3)}$$

Equation (A-2) can be expanded

$$P_n = P - PH^TQ^{-1}\left\{ I - HPH^TQ^{-1} + [HPH^TQ^{-1}]^2 - [HPH^TQ^{-1}]^3 + \cdots\cdots \right\} HP \qquad \text{(A-4)}$$

$$P_n = P\left\{ I - H^TQ^{-1}HP + H^TQ^{-1}HPH^TQ^{-1}HP - (H^TQ^{-1}HP)^3 + \cdots \right\} \qquad \text{(A-5)}$$

Again using the identity of (A-3)

$$P_n = P[I + H^TQ^{-1}HP]^{-1} \qquad \text{(A-6)}$$

or

$$P_n = [\, P^{-1} + H^TQ^{-1}H]^{-1} \qquad \text{(A-7)}$$

Equation (A-7) shows the equivalence between the Kalman filter and the weighted least sequences.

APPENDIX B

INTERPLANETARY TRAJECTORIES

This appendix presents a description of the two nominal interplanetary trajectories which have been used in this study. The trajectories are: (1) Nominal high-energy Earth-Mars, (2) Direct-return Mars-Earth. The data which are shown are in Earth equator and equinox of 1950 coordinates. Ecliptic projections of the trajectories are shown in Figures B-1 and B-2.

B.1 NOMINAL HIGH-ENERGY EARTH-MARS TRAJECTORY

This trajectory (Figure B-1) has a launch date of 10 February 1975, 1 hours, 32 minutes, 28.629 seconds, with a park orbit length of 1736.518 seconds.

	Earth-Centered Conic (Injection)	Sun-Centered Conic (Patch)	Mars-Centered Conic (Patch)
Date	10 February 1975	10 February 1975	10 October 1975
Fractional Date	$2^h1^m25.147^s$	$23^h43.^m24.812^s$	$21^h35^m48.596^s$
x (km)	-0.51940523+04	-0.11441701+09	-0.44850600+06
y	-0.33714096+04	0.84261958+08	0.27226599+06
z	-0.21758862+04	0.36545250+08	0.20978100+06
$\dot{x}$ (km/sec)	0.97623321+01	-0.95000336+01	0.43146753+01
$\dot{y}$	-0.11540529+02	-0.27582250+02	-0.26728354+01
$\dot{z}$	-0.5422576+01	-0.1185094+02	-0.20487671+01

The trajectory has a radius of closest approach at Mars of 3860 km (500 km altitude). It passes Mars on the Sun light side near the ecliptic plane. The flight time is 235 days.

B.2 DIRECT-RETURN MARS-EARTH TRAJECTORY

This trajectory (Figure B-2) is the return trajectory which leaves Mars 40 days after the arrival of the nominal high-energy trajectory.

	Mars-Centered Conic (Injection)	Sun-Centered Conic (Patch)	Earth-Centered Conic (Patch)
Date	12 November 1975	13 November 1975	3 September 1976
Fractional Date	$10^h47^m26.241^s$	$19^h41^m18.707^s$	$5^h4^m57.839^s$
x (km)	-0.34075300+04	0.91568038+08	-0.88066700+06
y	-0.18867350+04	0.18887866+09	0.27005599+06
z	-0.66730232+03	0.84164875+08	0.84061749+05
$\dot{x}$ (km/sec)	0.32159301+01	-0.17725844+02	0.99308927+01
$\dot{z}$	-0.48195511+01	0.80037536+01	-0.30949005+01
$\dot{z}$	-0.32001703+01	0.3498172+01	-0.10445975+01

The trajectory has a perigee radius of 6442 km (76 km altitude). Perigee is at a latitude of -59.98 degrees and longtitude of 223.06 degrees. The flight time is 296 days 18 hours.

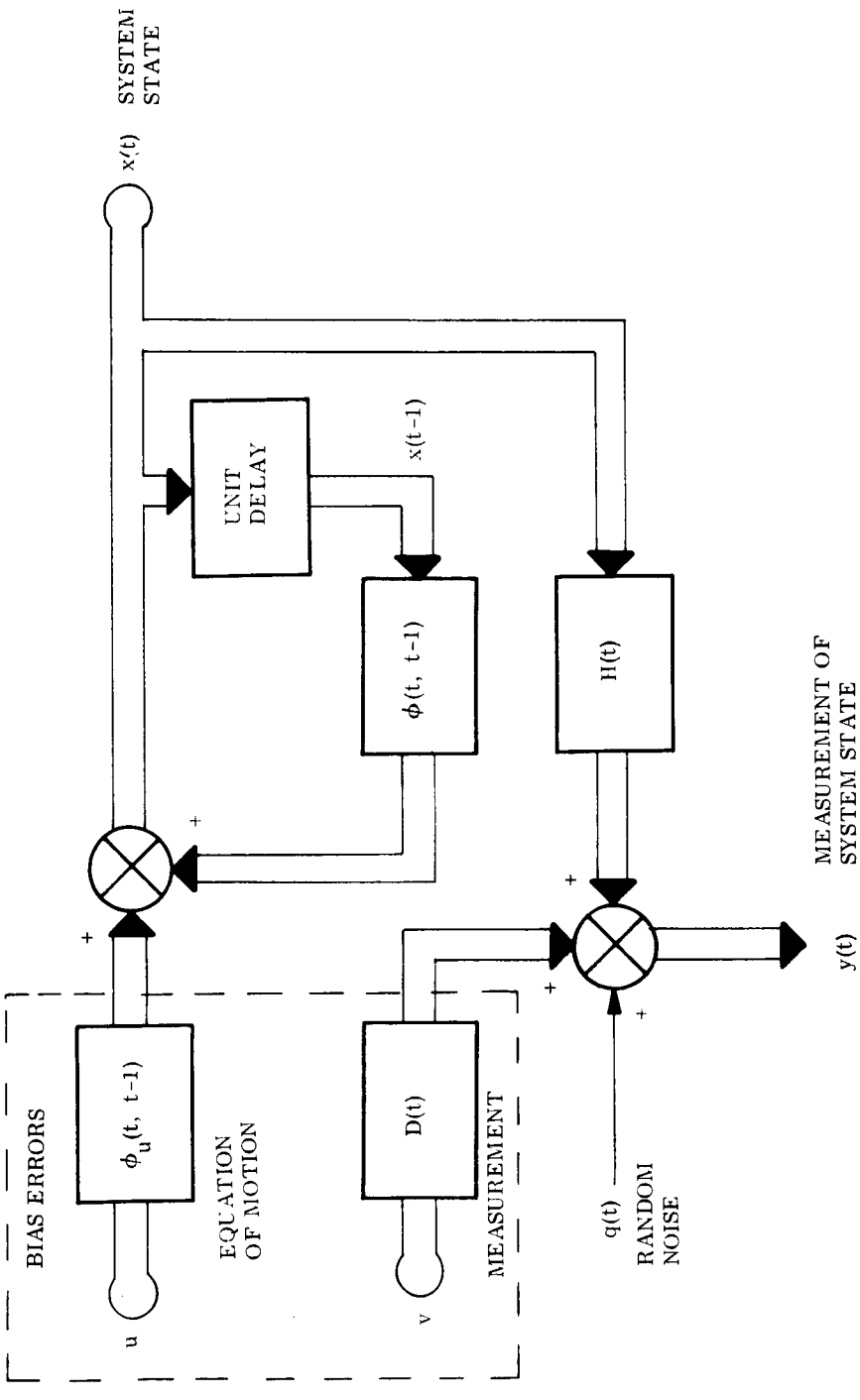

FIGURE 2-1 PHYSICAL PROCESS

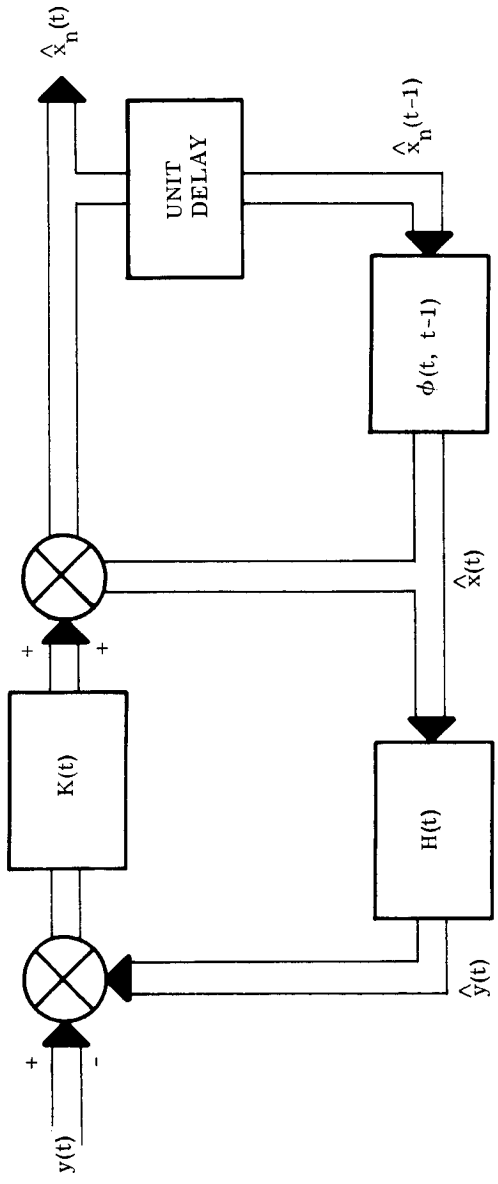

FIGURE 2-2 LINEAR FILTER

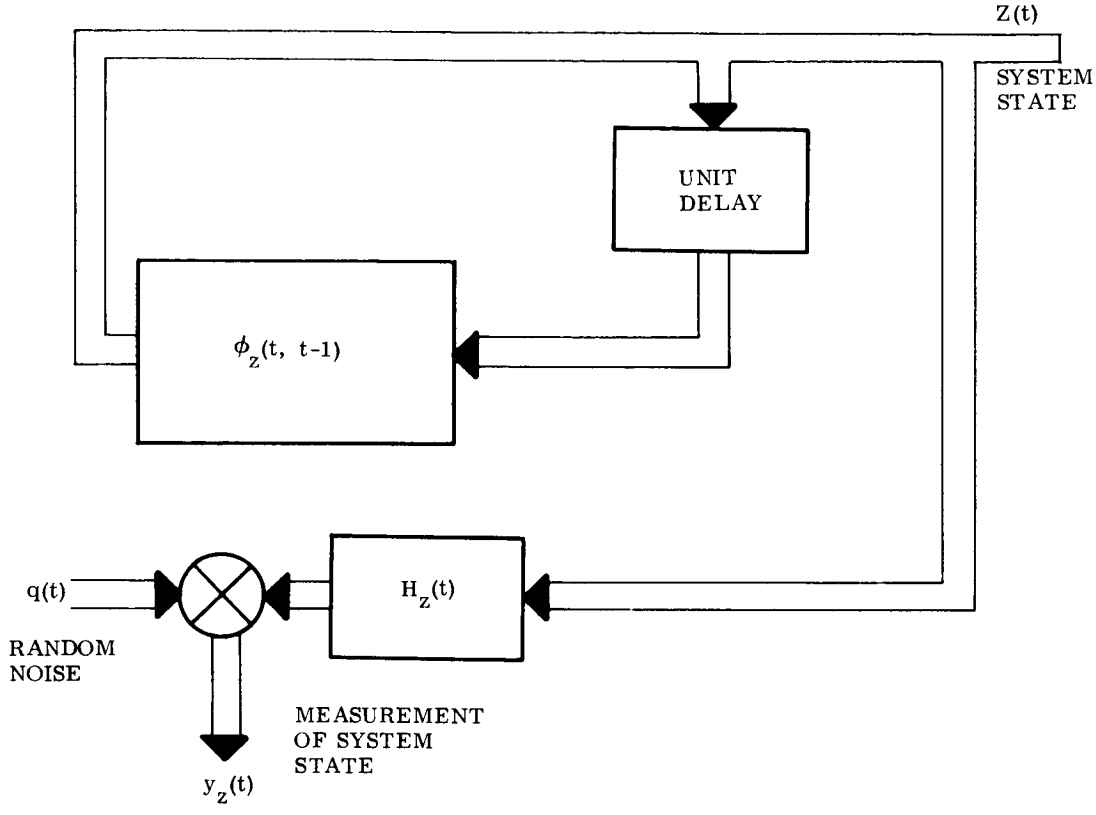

$$z(t) \equiv \begin{pmatrix} x(t) \\ u \\ v \end{pmatrix} \qquad \phi_z(t,\ t-1) = \begin{pmatrix} \phi(t,\ t-1) & \phi_u(t,\ t-1) & 0 \\ 0 & I & 0 \\ 0 & 0 & I \end{pmatrix}$$

$$H_z(t) \equiv \begin{pmatrix} H(t) & 0 & D(t) \end{pmatrix}$$

FIGURE 2-3 PHYSICAL PROCESS

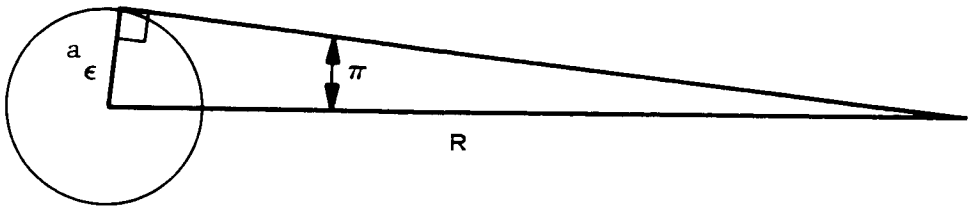

WHERE a_ϵ — EARTH EQUATORIAL RADIUS (KM)

R — EARTH SUN MEAN DISTANCE (KM)

π — SOLAR PARALLAX

FIGURE 3-1 - SOLAR PARALLAX

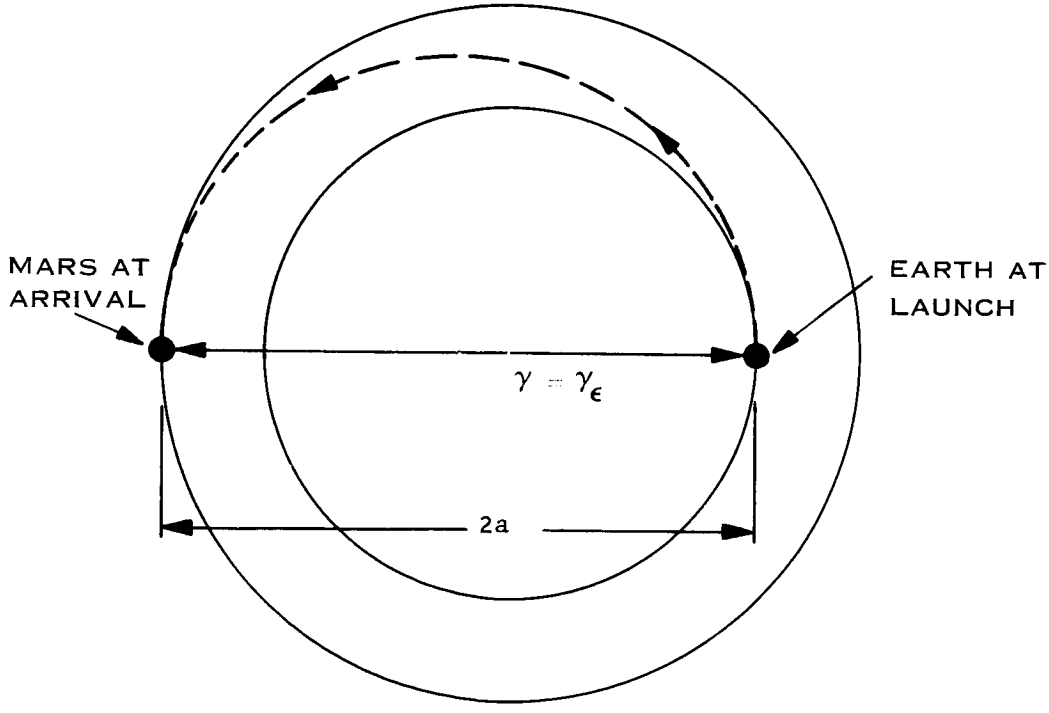

FIGURE 3-2 HOHMANN TRANSFER

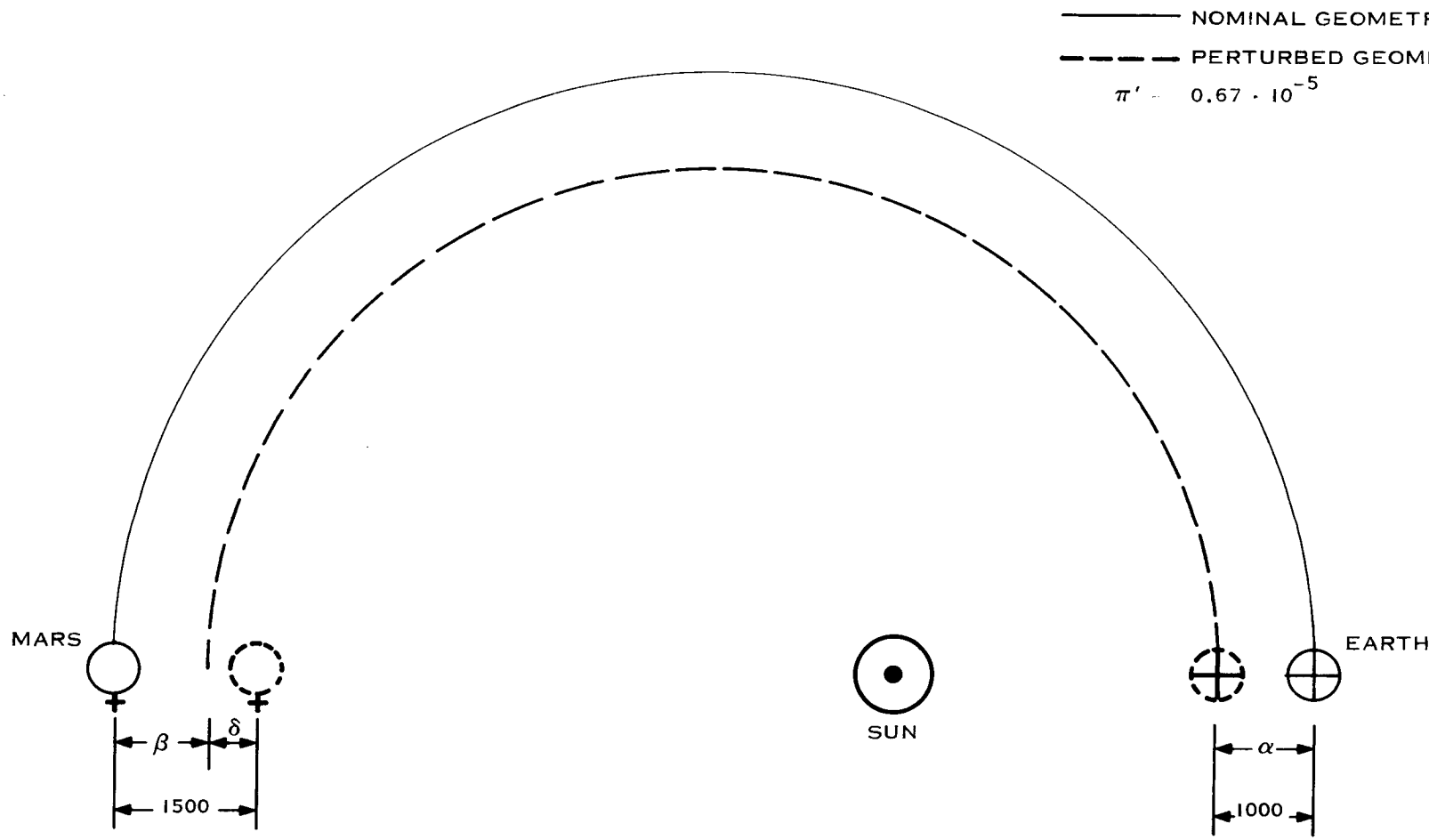

$\alpha = 1000$ KM $\alpha + \beta = 1940$ KM $\delta = 560$ KM

$\alpha + \beta = \Delta a$ TREATING MARS POSITION AS UNCERTAIN (EQ. 3-12)

$\delta = \Delta a$ TREATING MARS POSITION AS KNOWN (EQ. 3-11)

FIGURE 3-3 EFFECT OF ERROR IN SOLAR PARALLAX

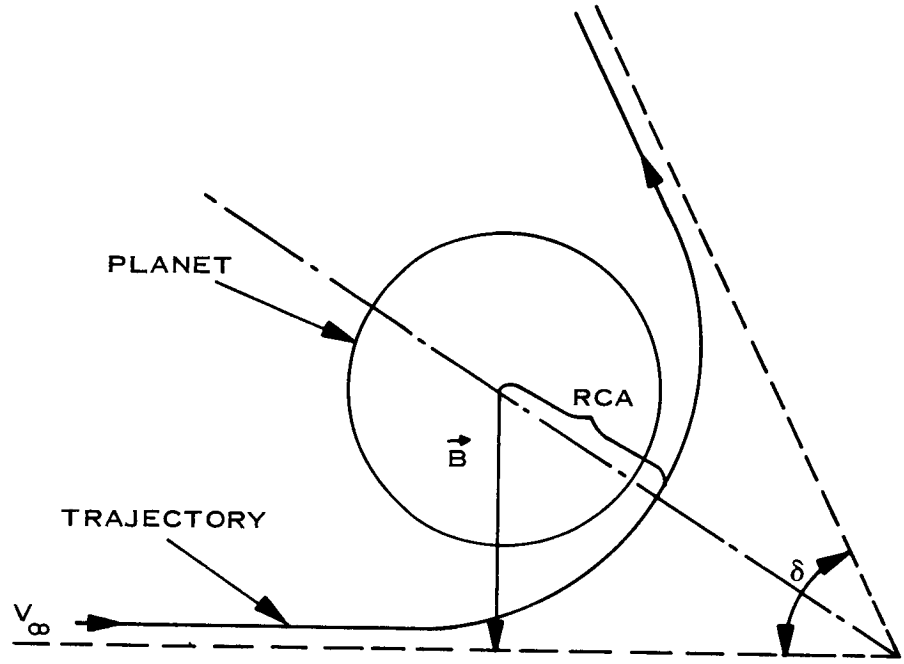

RCA = RADIUS CLOSEST APPROACH

δ = SCATTERING ANGLE

$\vec{B}$ = B VECTOR

V_∞ = VELOCITY AT INFINITY

--- = ASYMPTOTES

FIGURE 3-4 APPROACH TRAJECTORY GEOMETRY

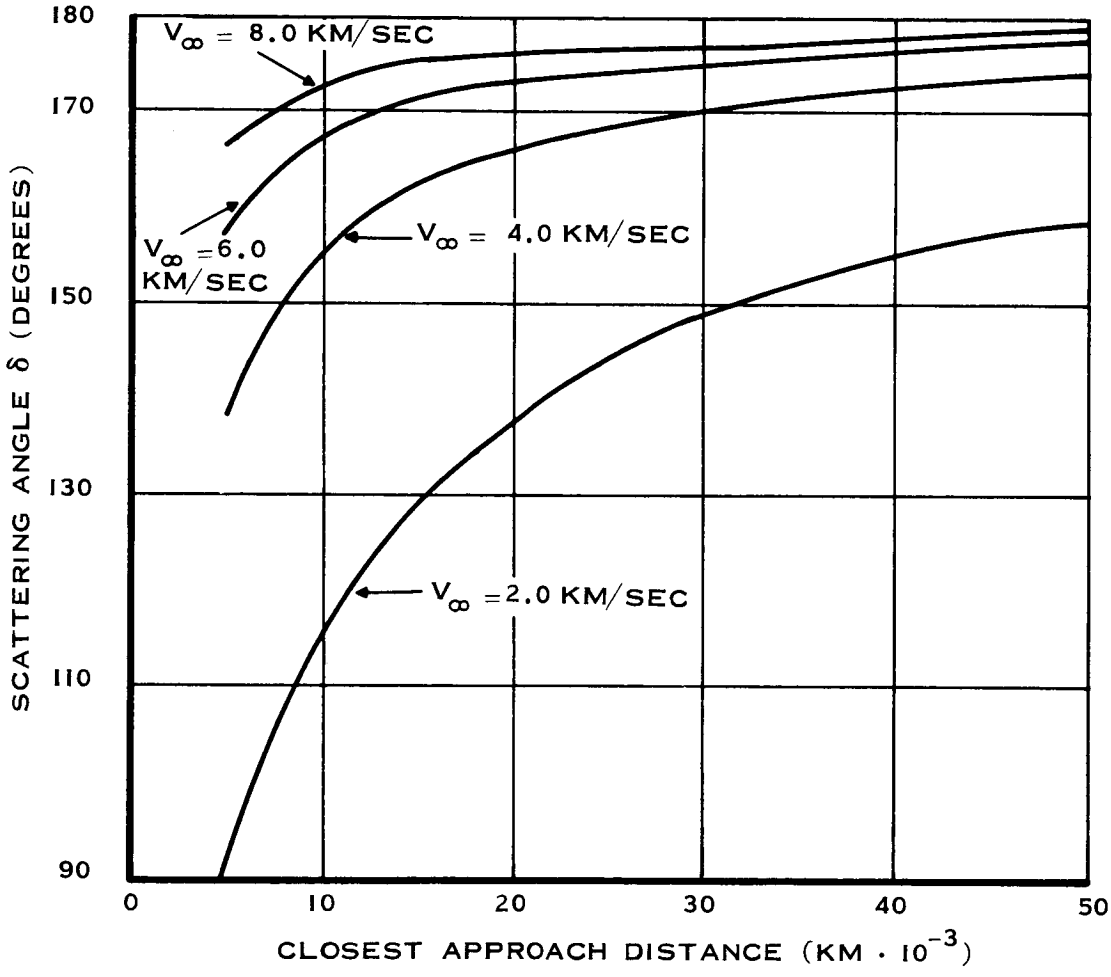

FIGURE 3-5 MARS APPROACH TRAJECTORY SCATTERING ANGLE

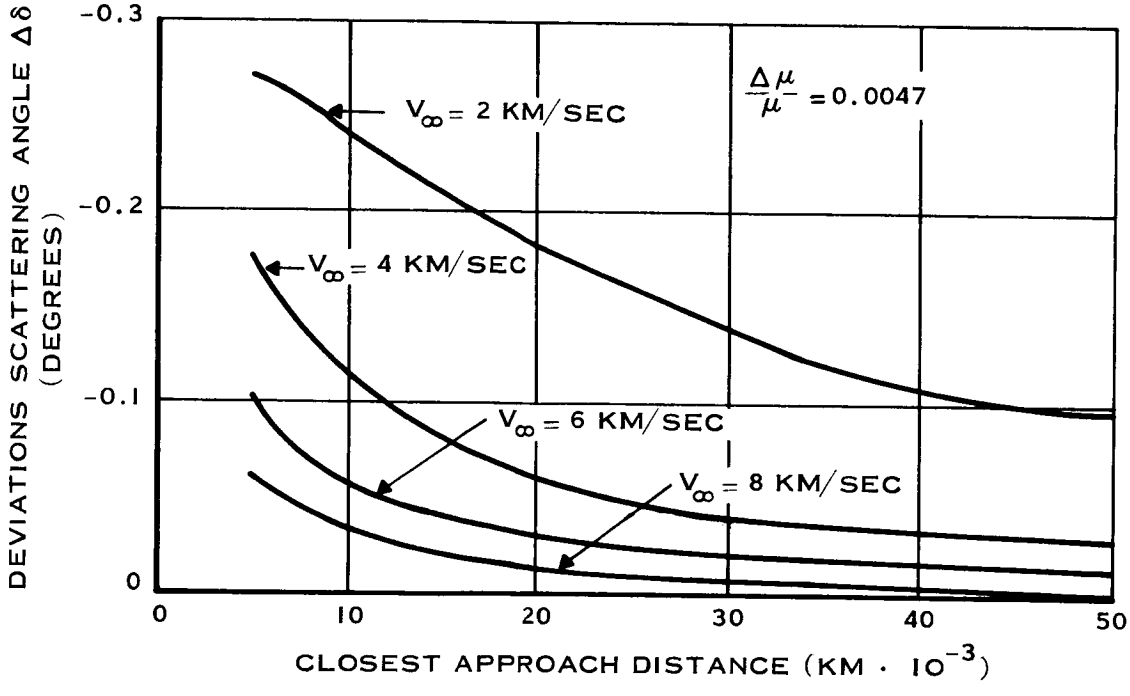

FIGURE 3-6 MARS' SCATTERING ANGLE DEVIATION

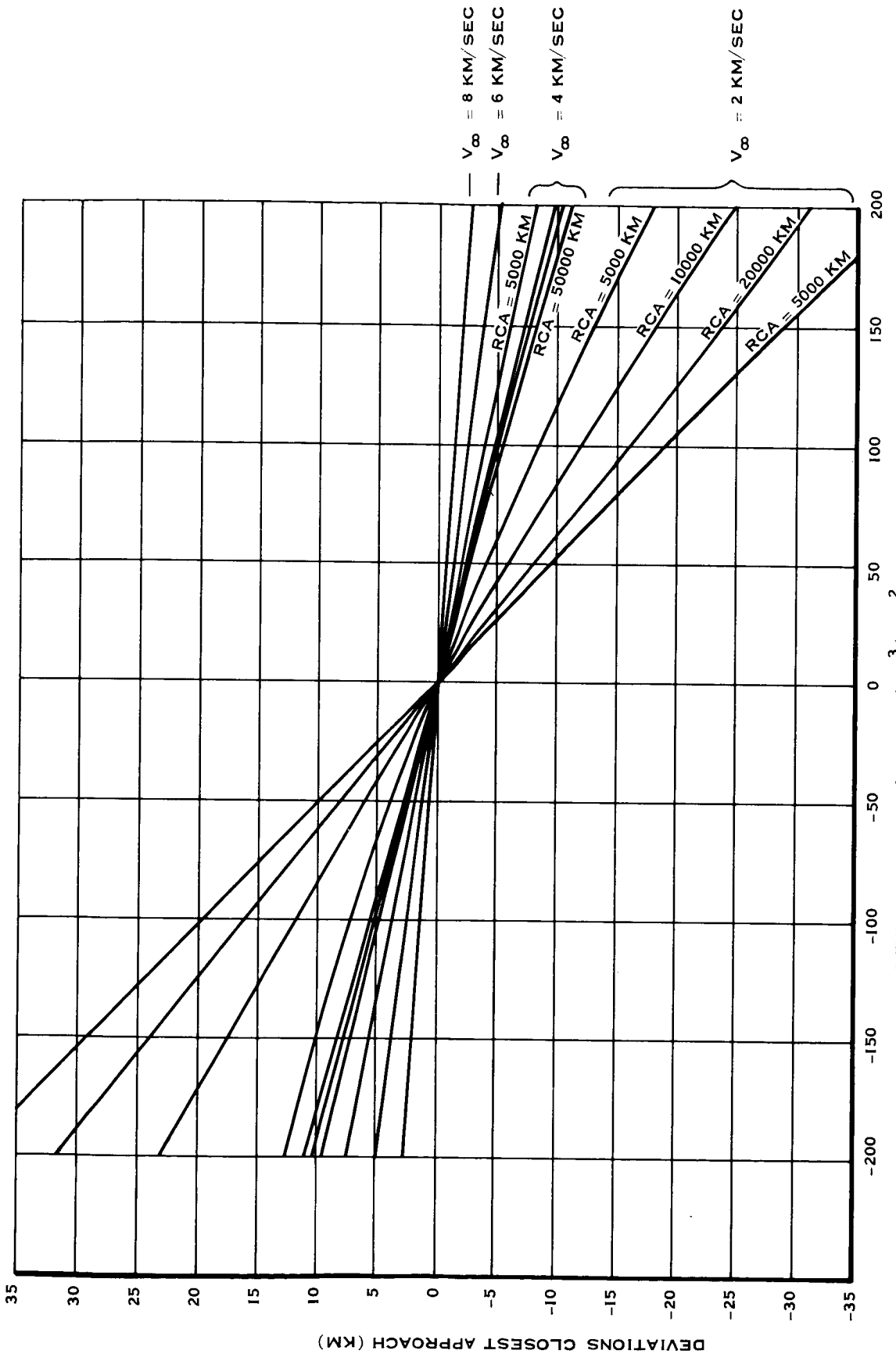

FIGURE 3-7 DEVIATIONS IN CLOSEST APPROACH DISTANCE

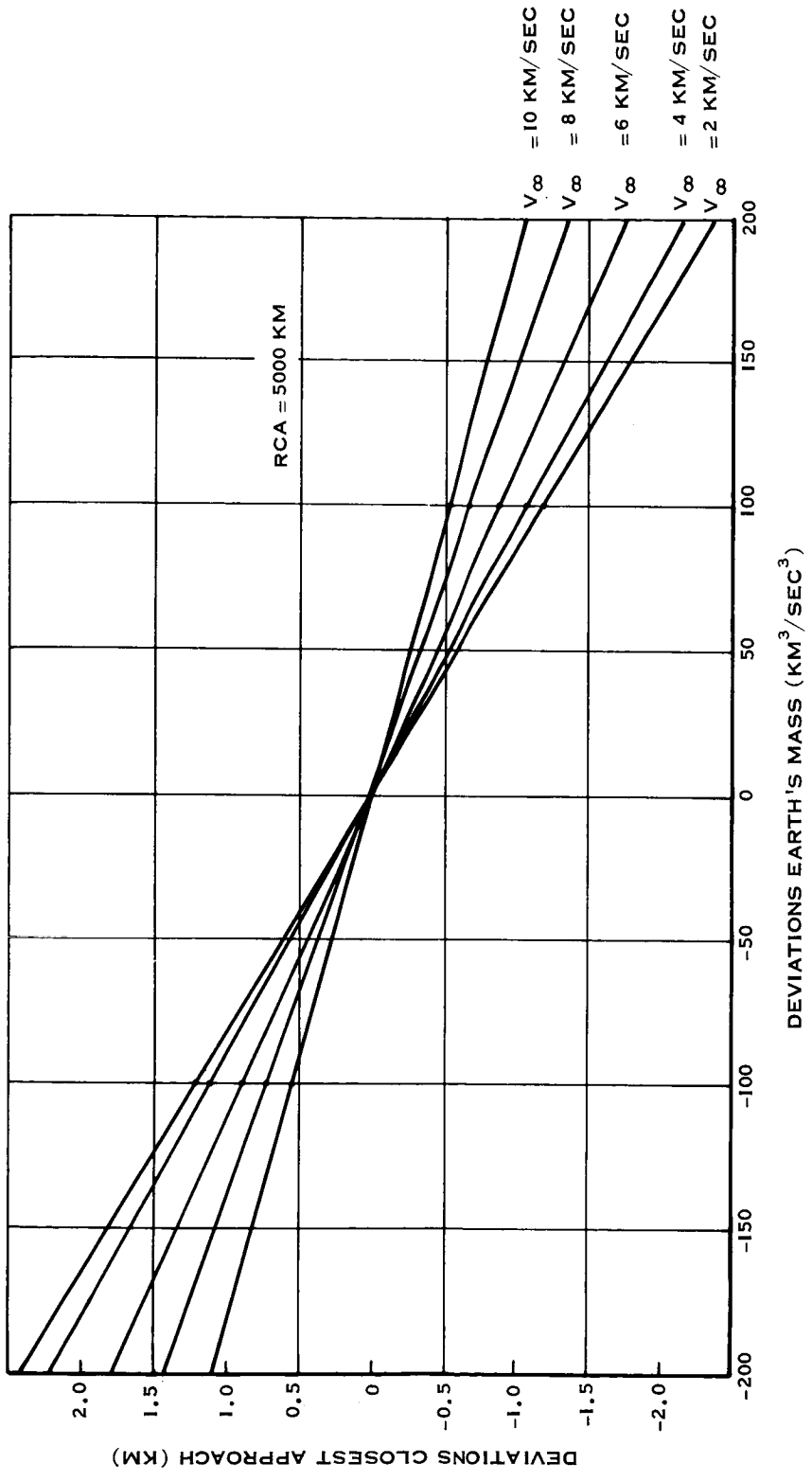

FIGURE 3-8 DEVIATIONS IN CLOSEST APPROACH DISTANCE

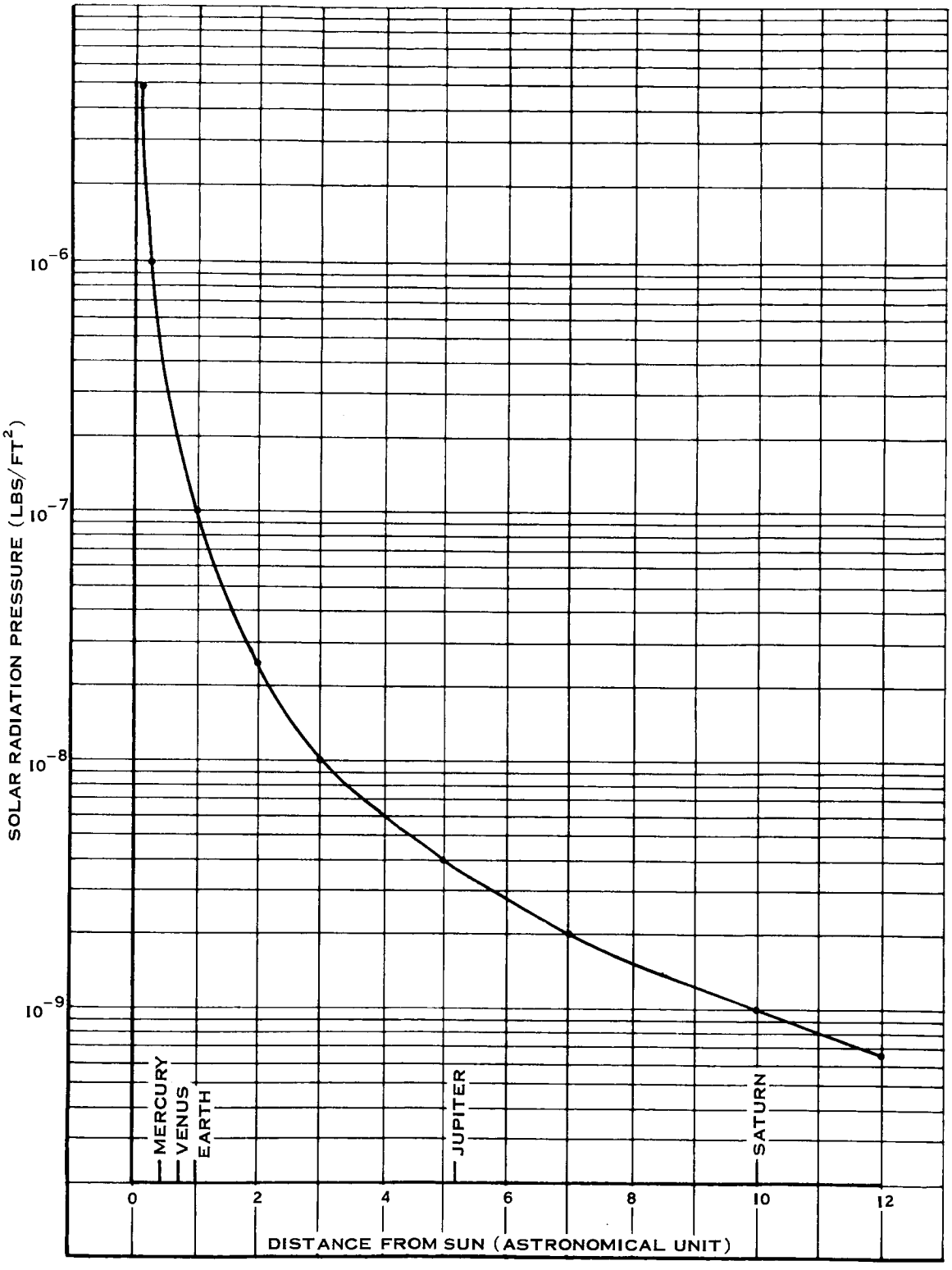

FIGURE 3-9 SOLAR RADIATION PRESSURE VARIATION WITH DISTANCE FROM THE SUN

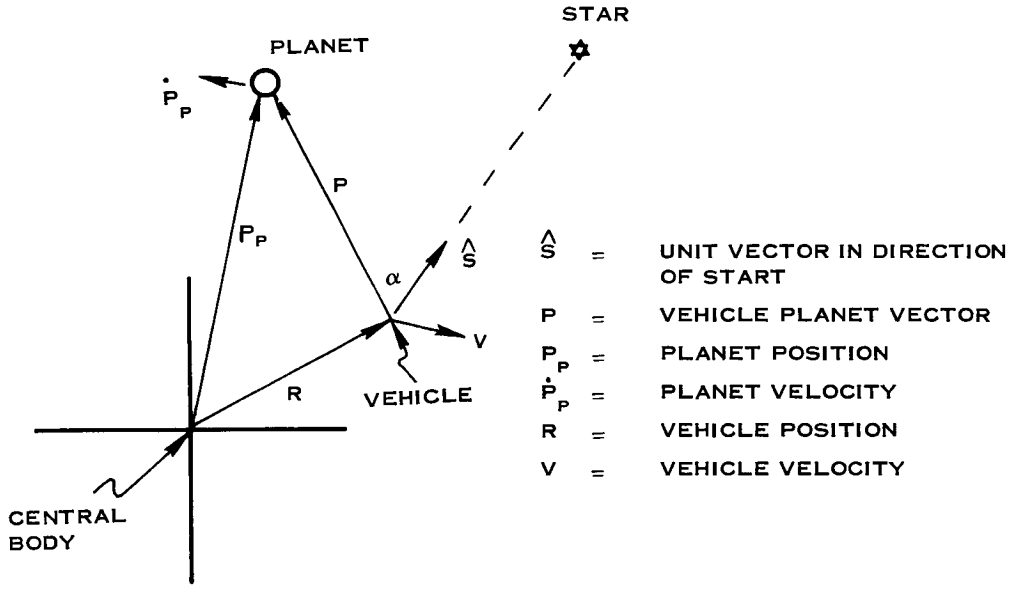

FIGURE 3-10 SEXTANT MEASUREMENT GEOMETRY

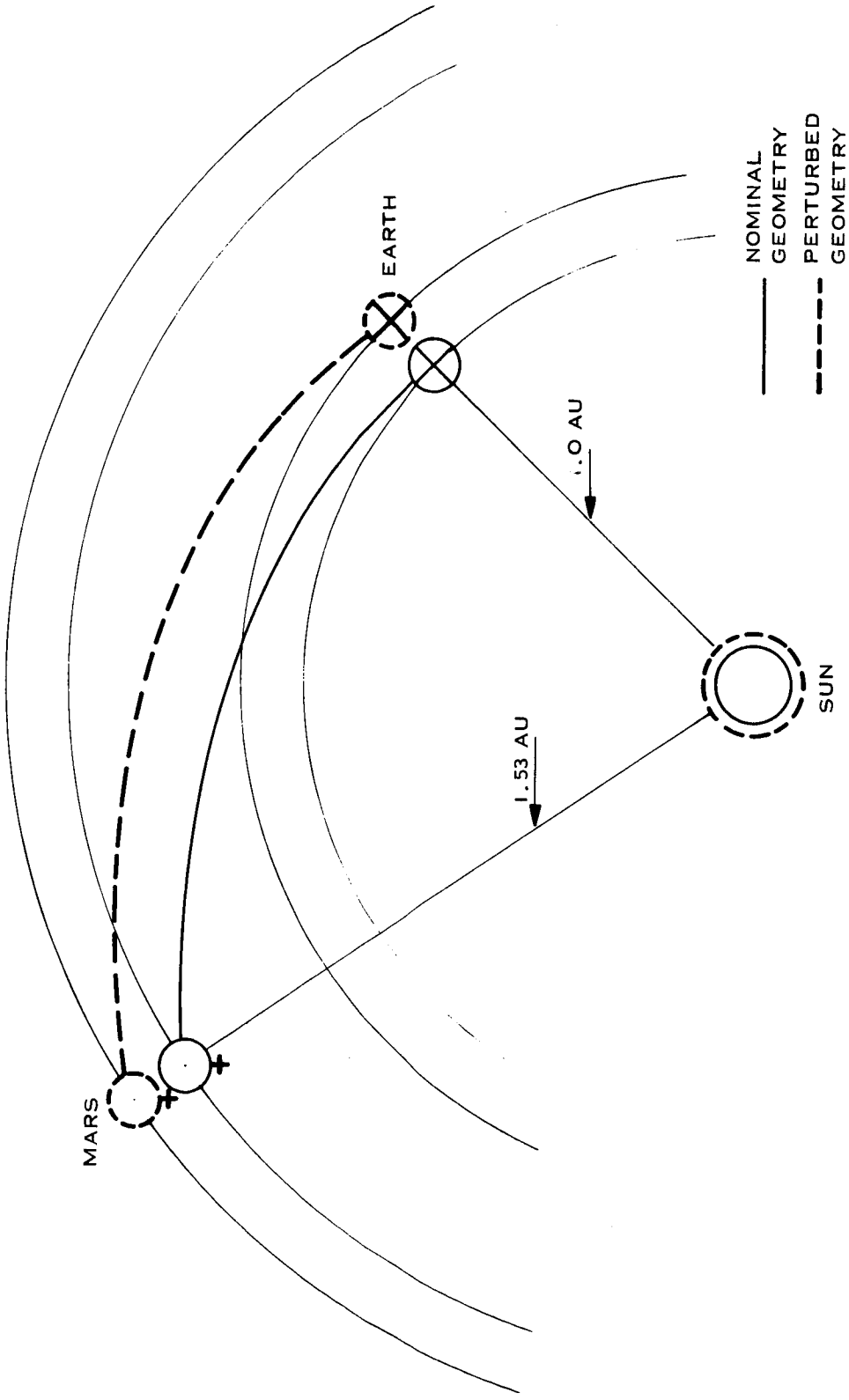

FIGURE 4-1 EPHEMERIS GEOMETRY CHANGE WITH A.U. CHANGE

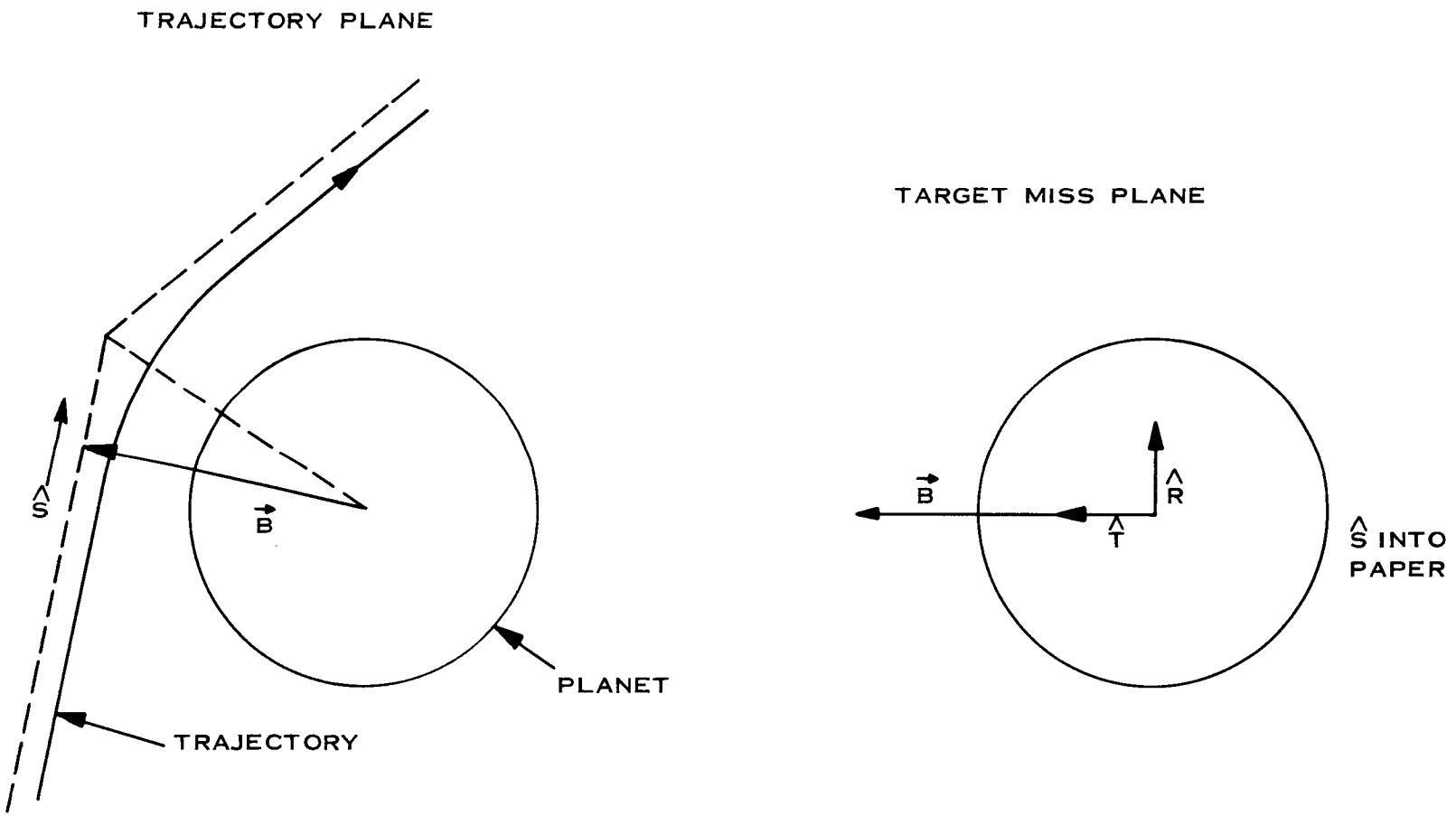

FIGURE 4-2 TRAJECTORY MISS COORDINATES

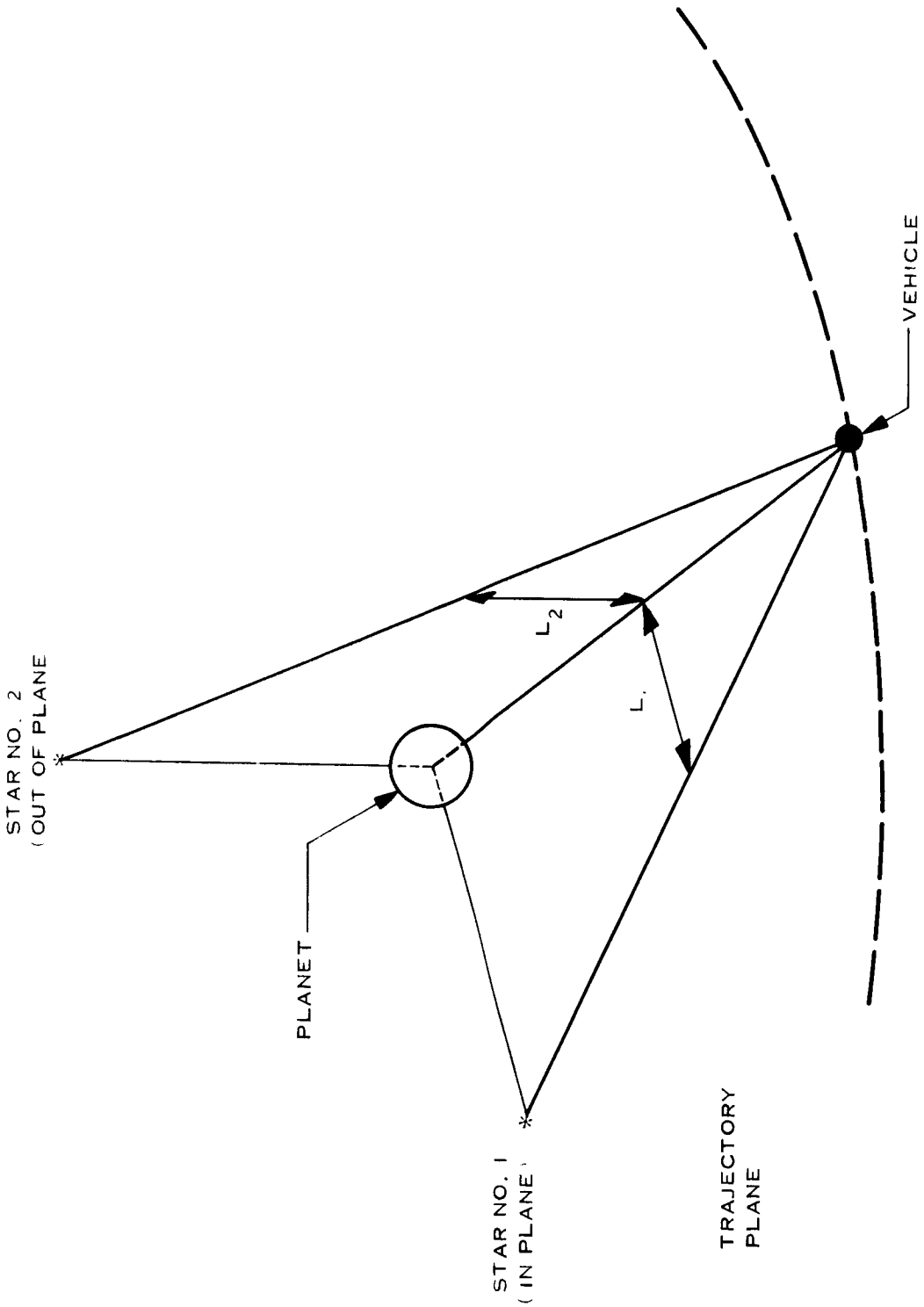

FIGURE 4-3 SEXTANT IN PLANE AND OUT OF PLANE STARS

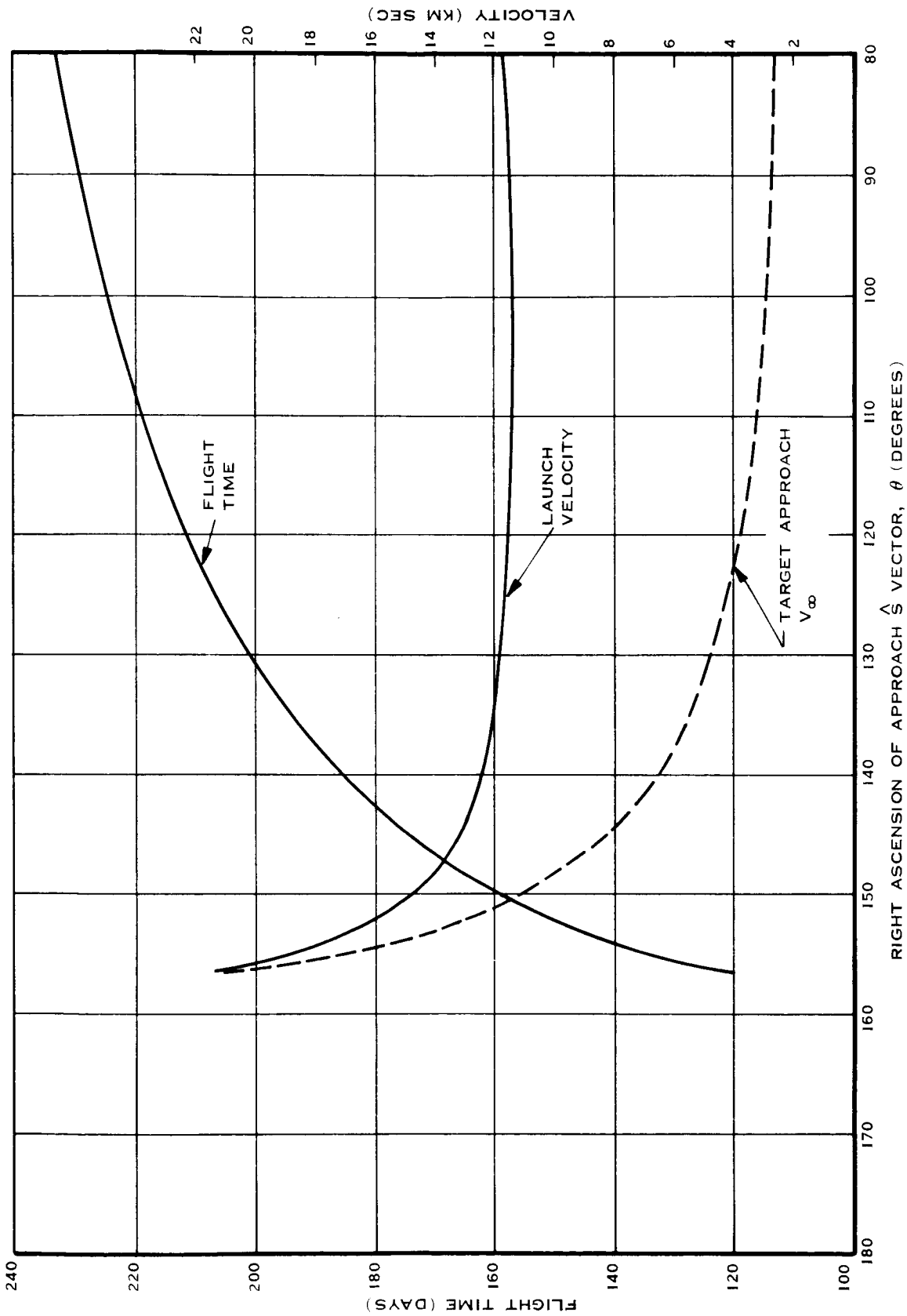

FIGURE 5-1A TRAJECTORY CHARACTERISTICS - 160° TRANSFER, EARTH-MARS

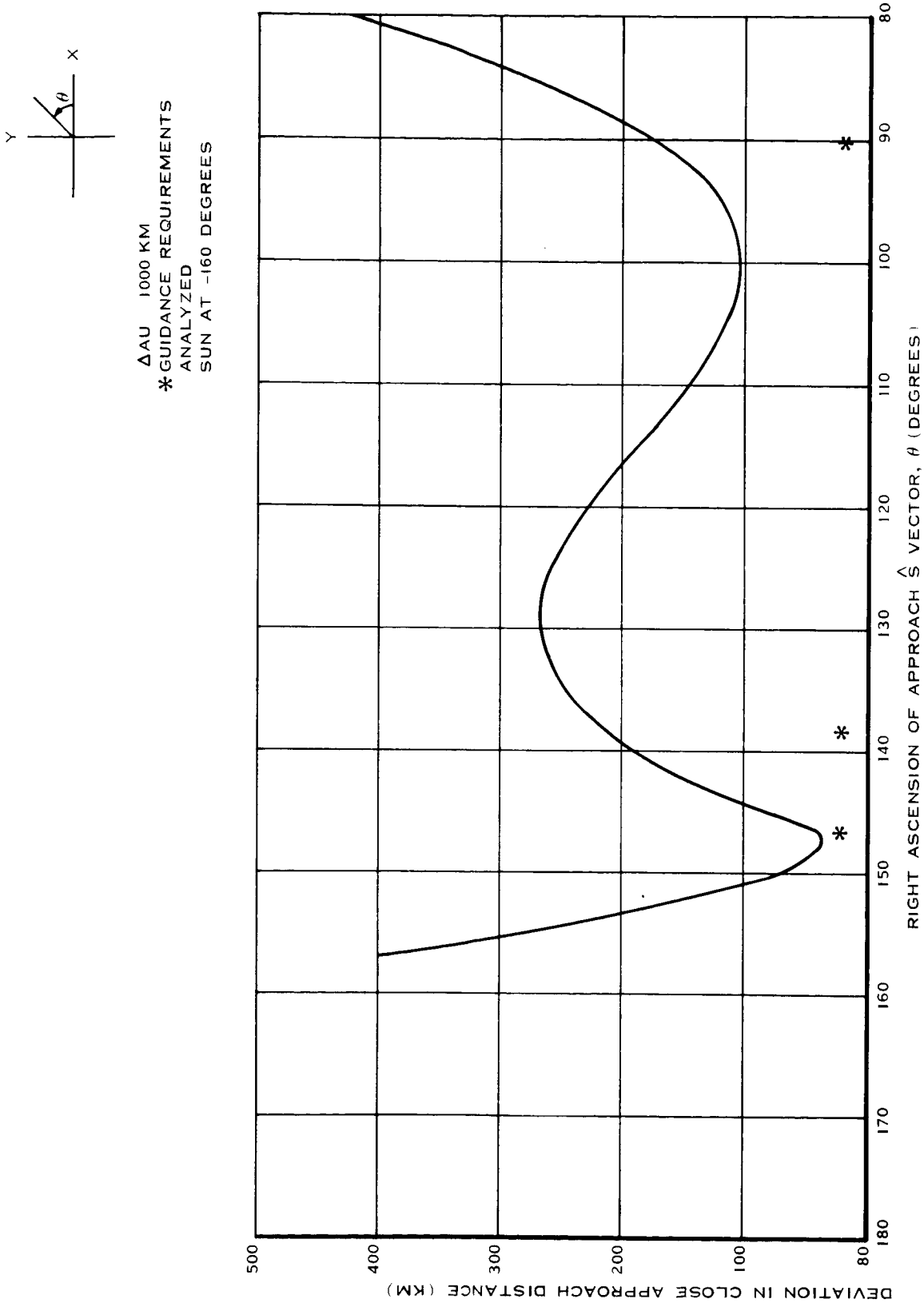

FIGURE 5-1B DEVIATION IN CLOSE APPROACH - 160° TRANSFER, EARTH-MARS

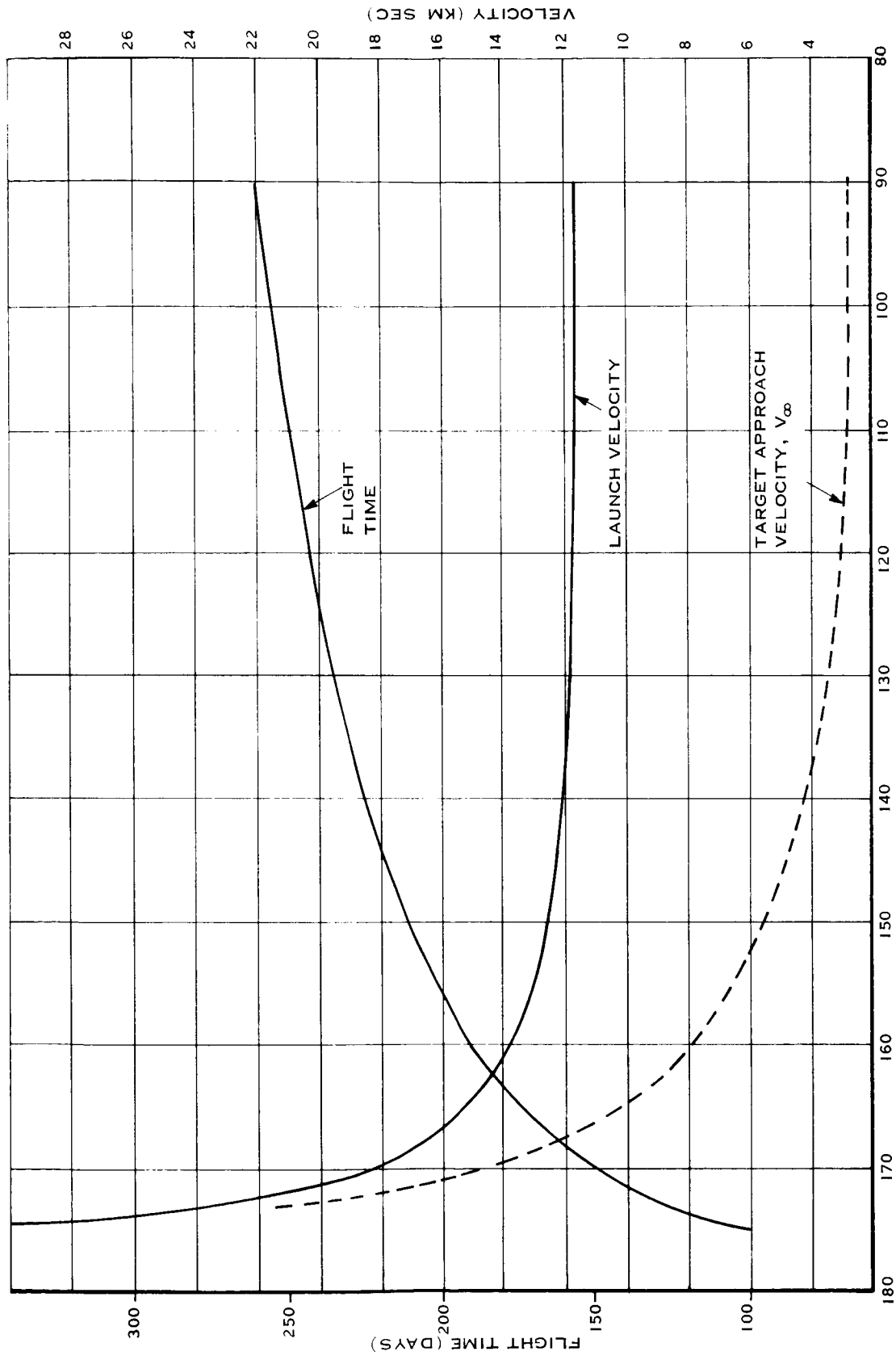

FIGURE 5-2A TRAJECTORY CHARACTERISTICS - 180° TRANSFER, EARTH-MARS

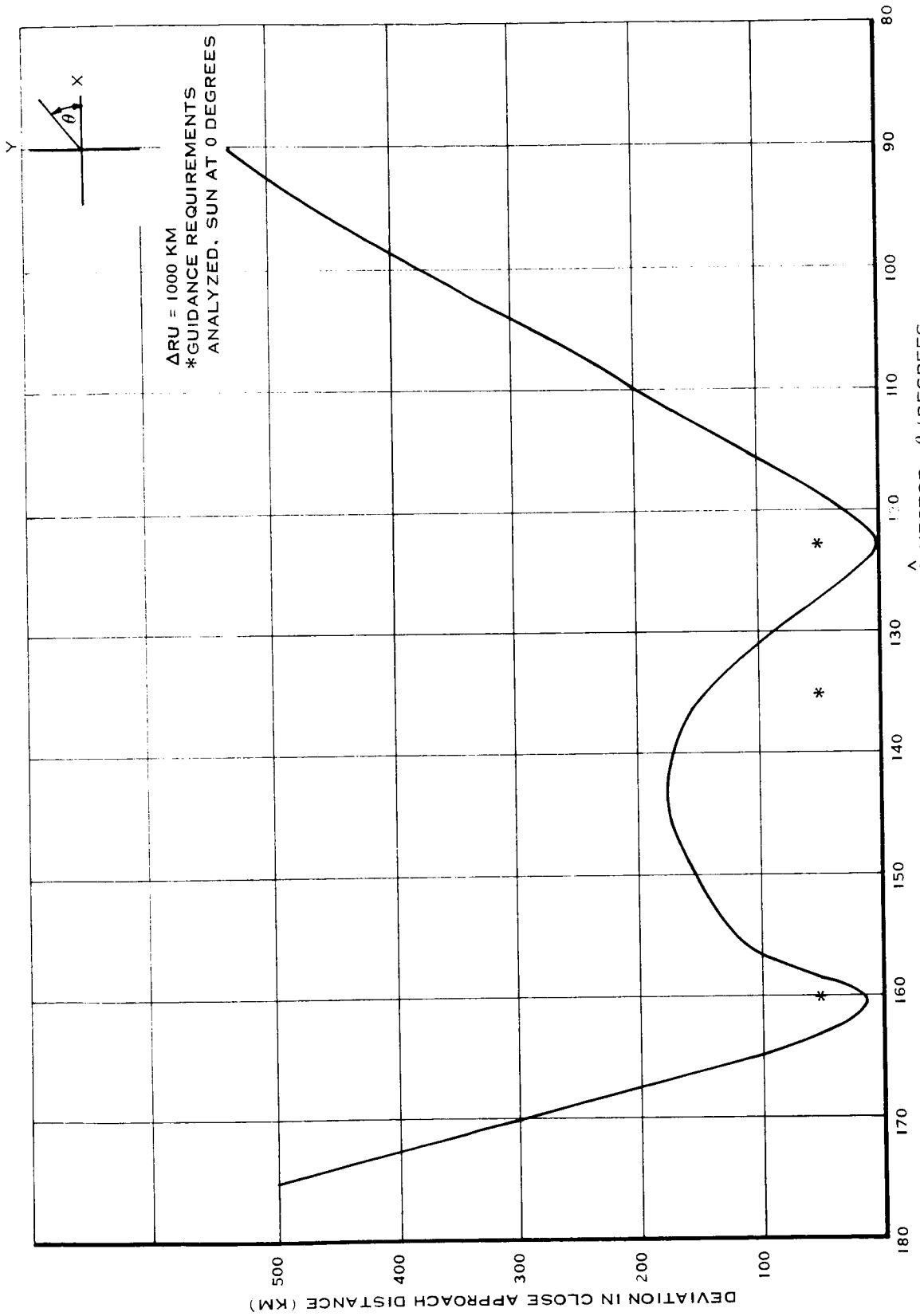

FIGURE 5-2B DEVIATION IN CLOSE APPROACH - 180° TRANSFER, EARTH-MARS

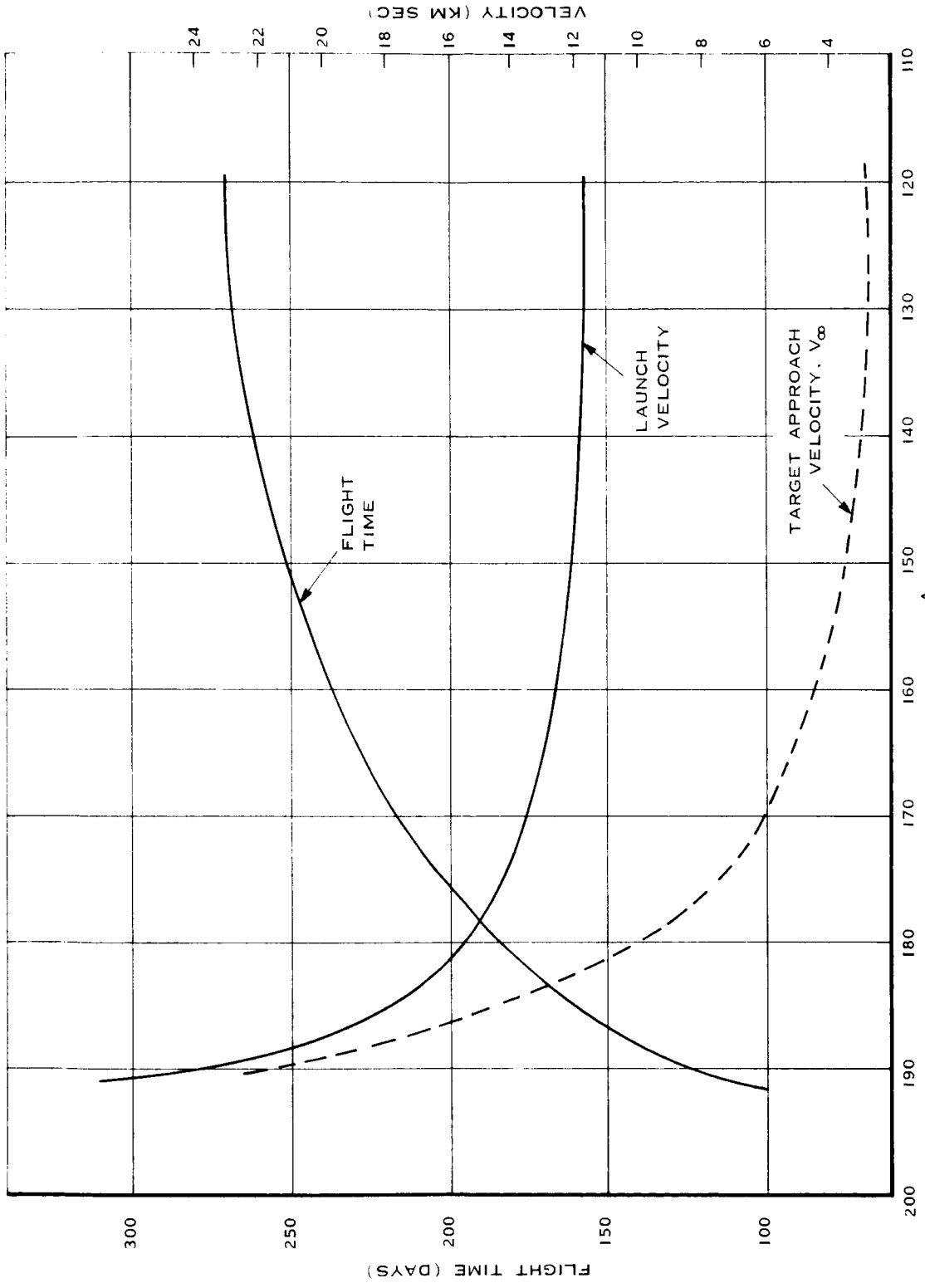

FIGURE 5-3A TRAJECTORY CHARACTERISTICS - 200° TRANSFER, EARTH-MARS

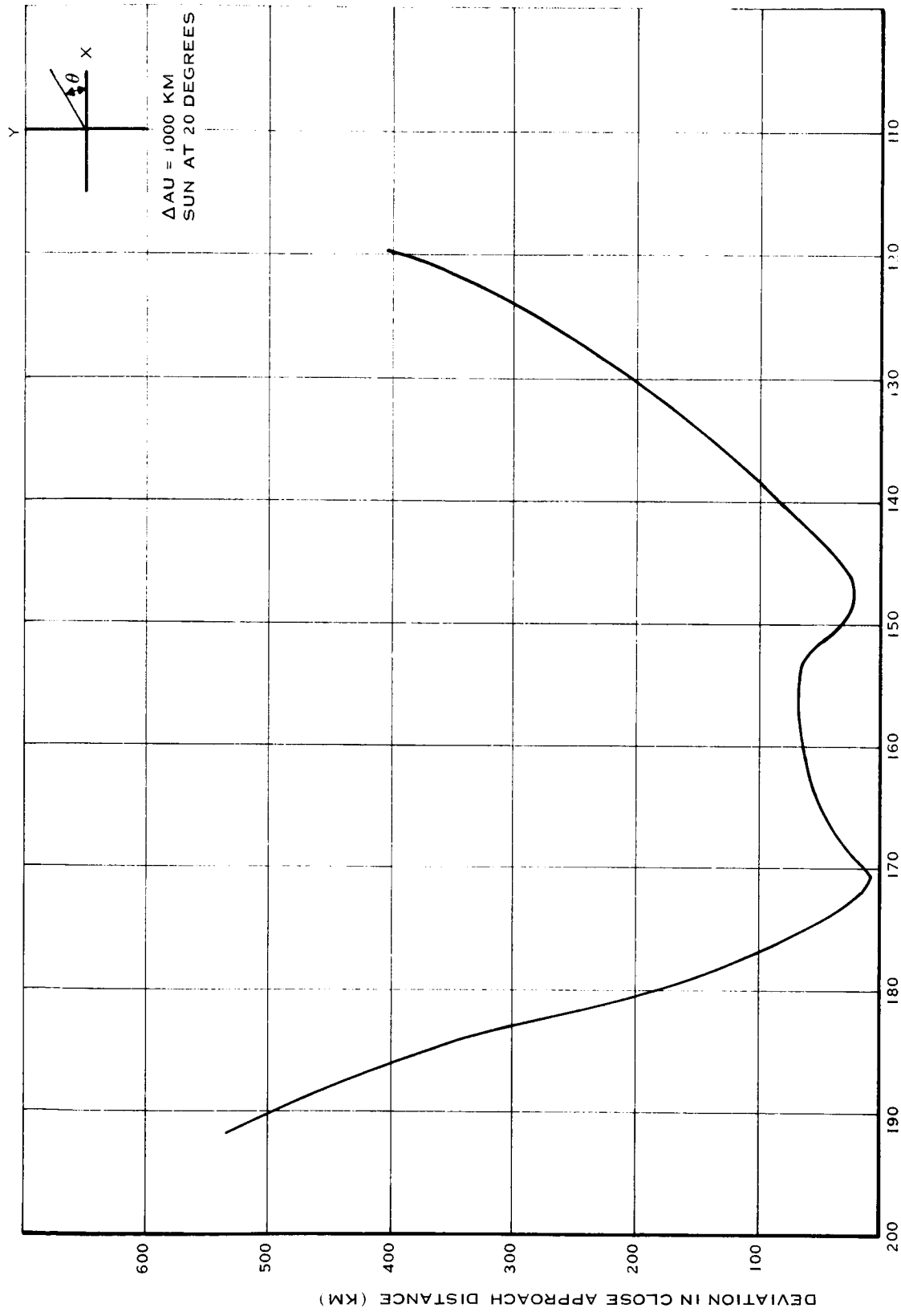

FIGURE 5-3B DEVIATION IN CLOSE APPROACH - 200° TRANSFER, EARTH-MARS

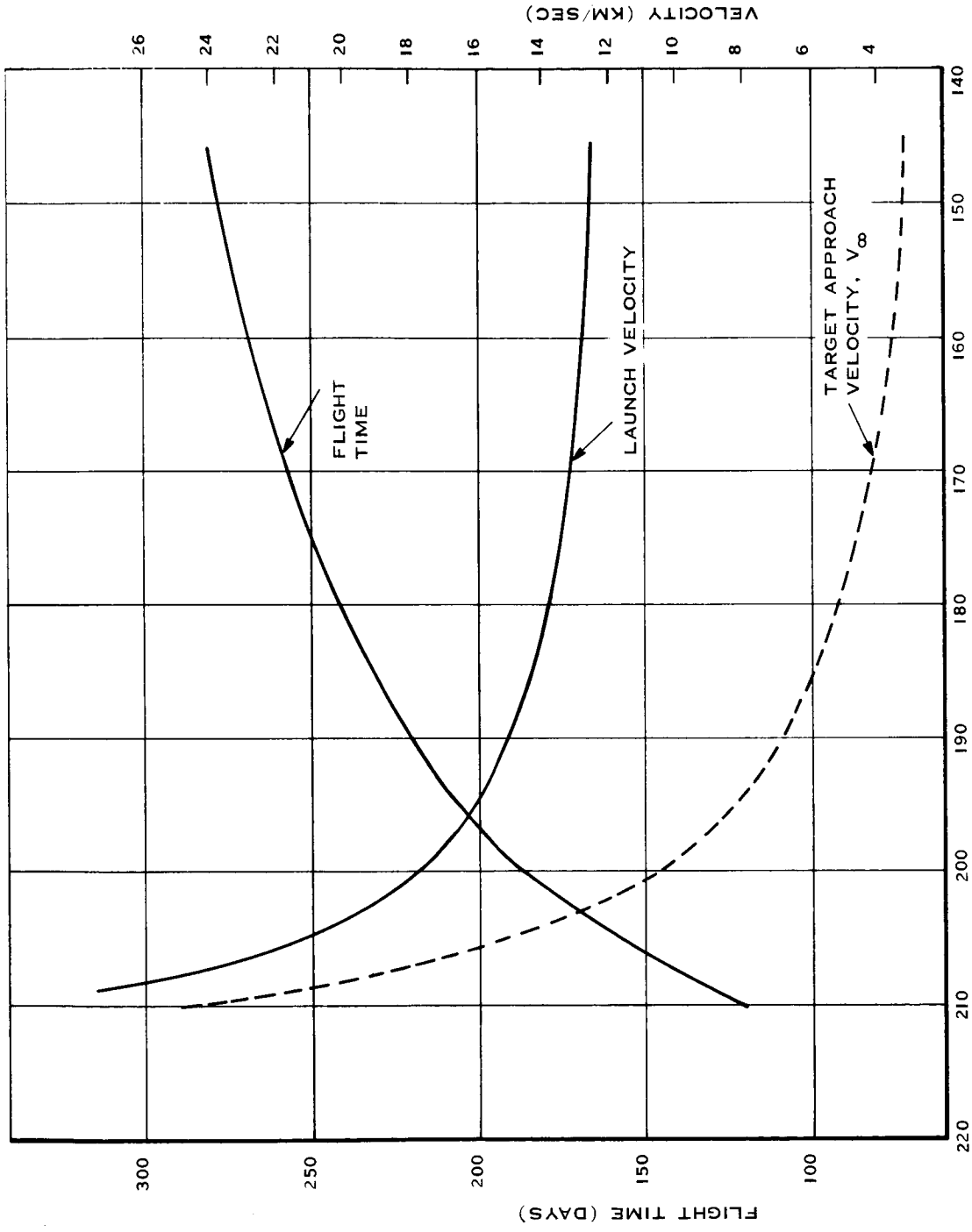

FIGURE 5-4A TRAJECTORY CHARACTERISTICS - 225^{0} TRANSFER, EARTH-MARS

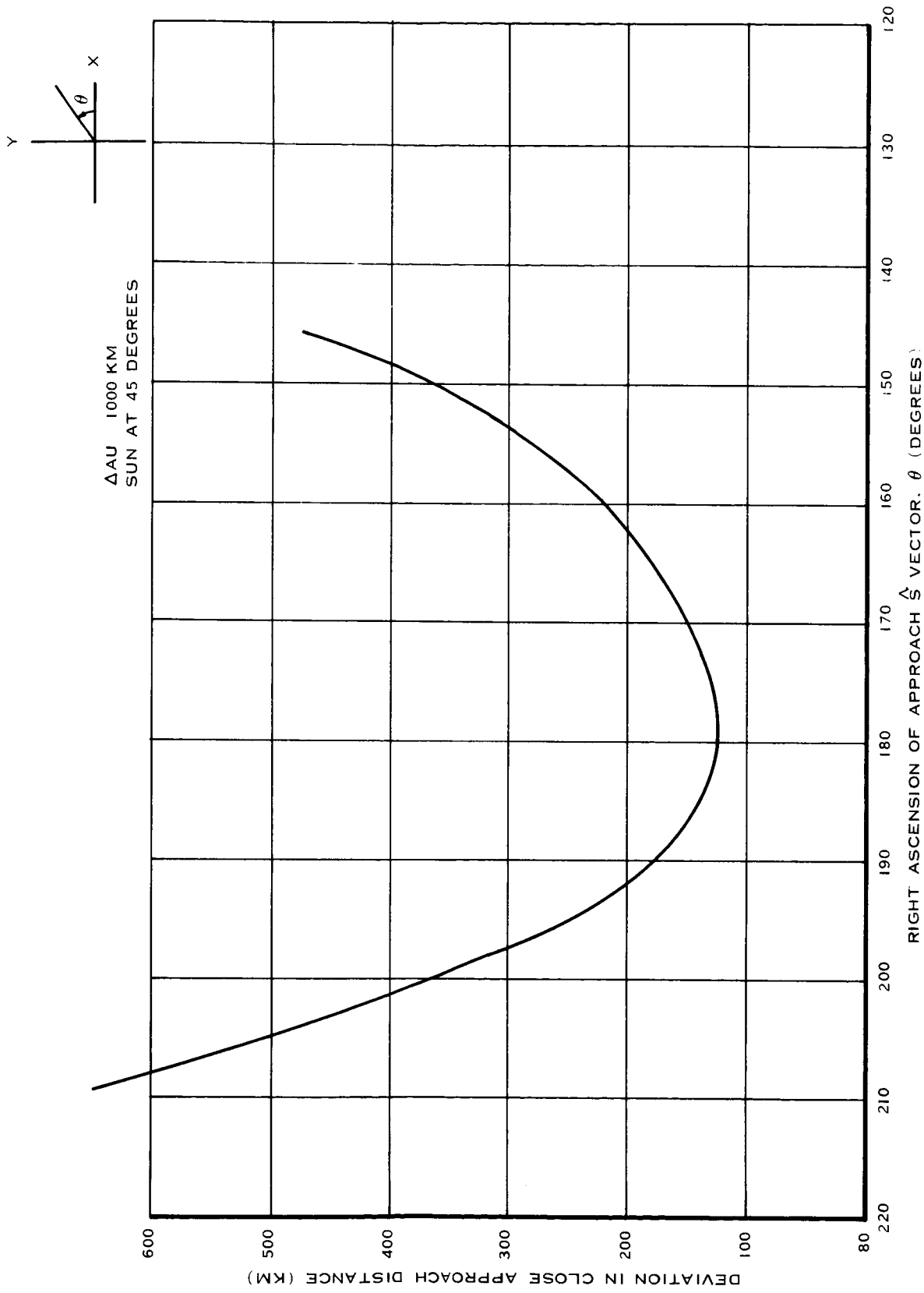

FIGURE 5-4B DEVIATION IN CLOSE APPROACH - 225° TRANSFER, EARTH-MARS

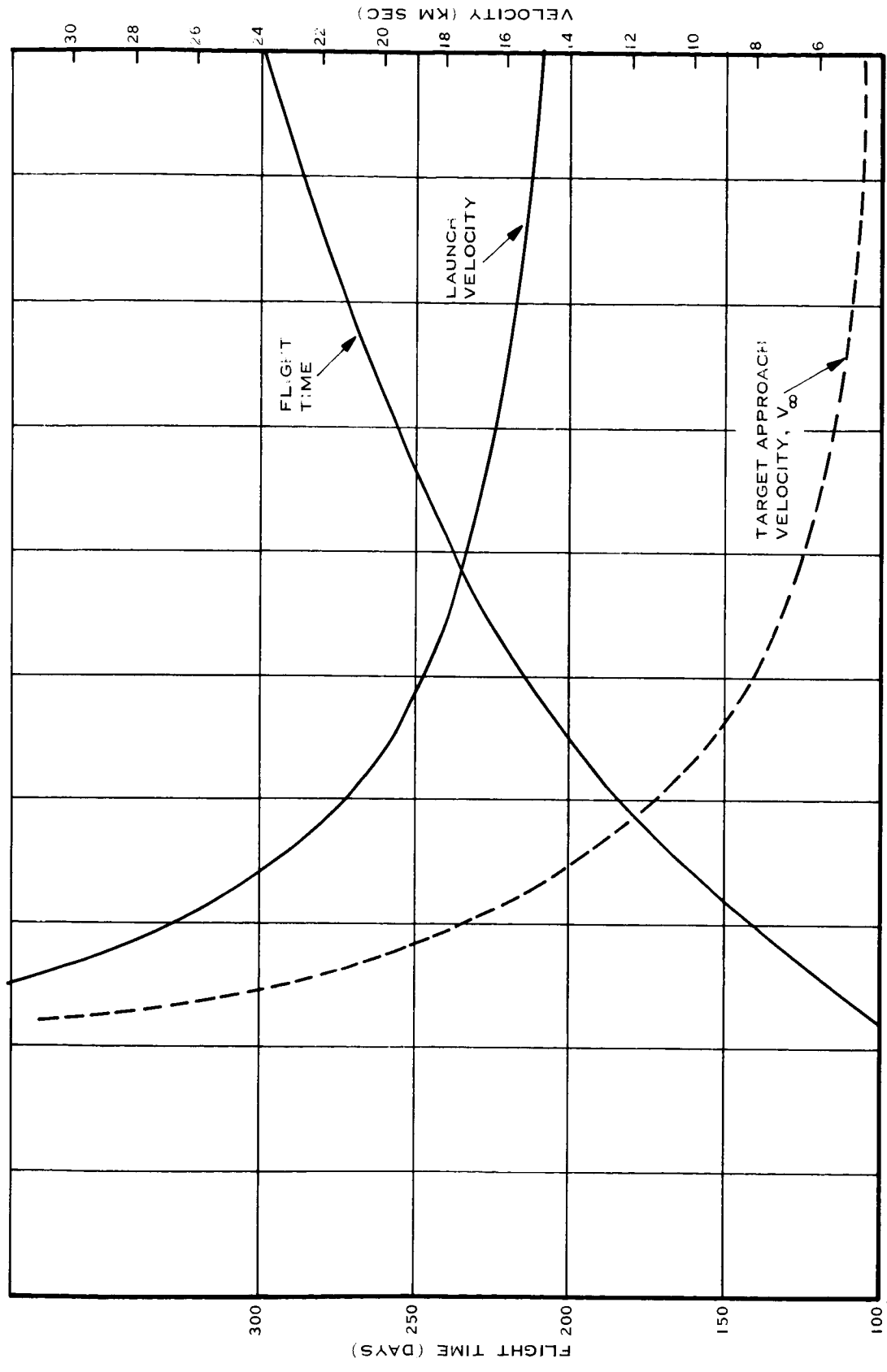

FIGURE 5-5A TRAJECTORY CHARACTERISTICS – 270^0 TRANSFER, EARTH-MARS

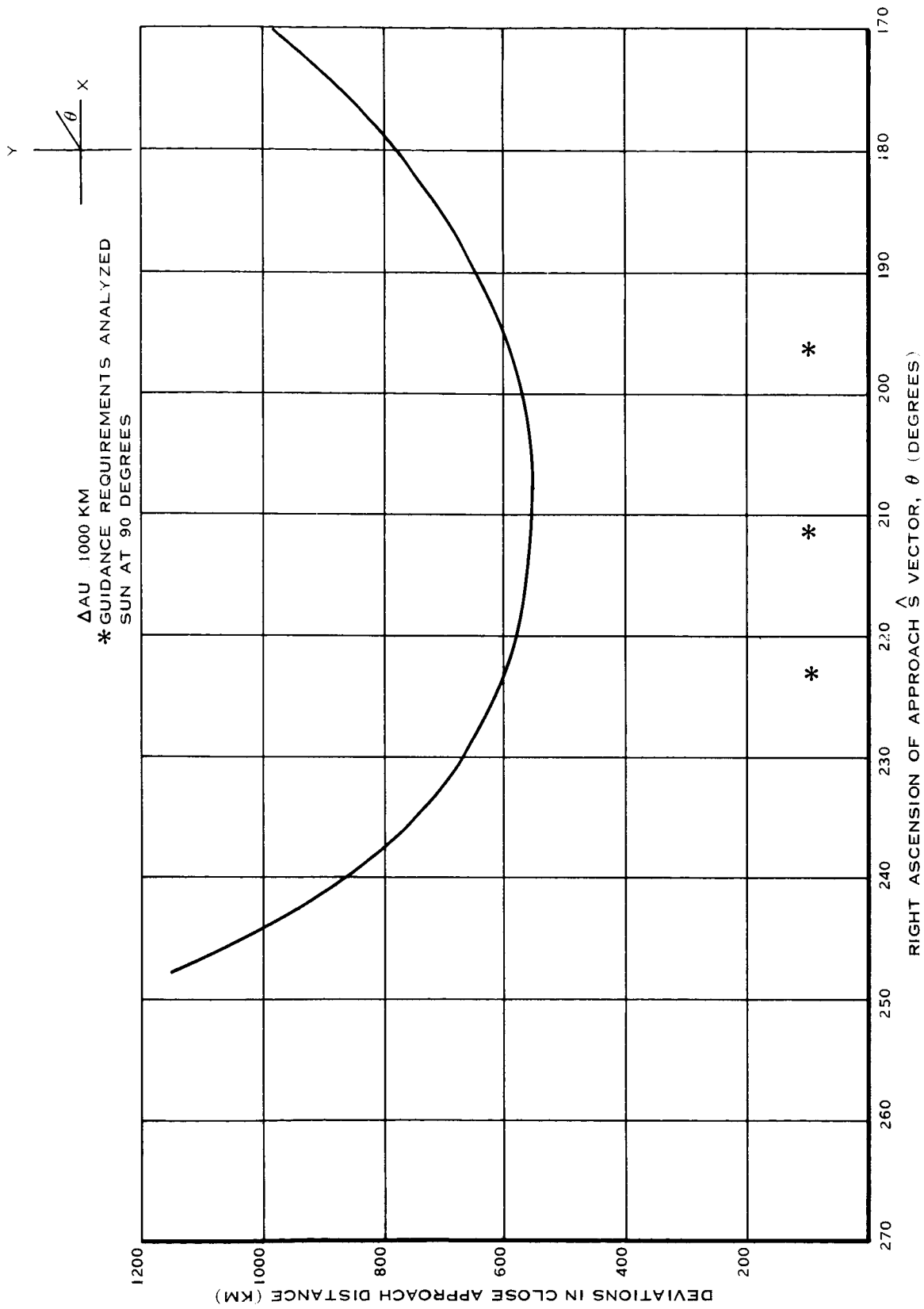

FIGURE 5-5B DEVIATIONS IN CLOSE APPROACH - 270° TRANSFER, EARTH-MARS

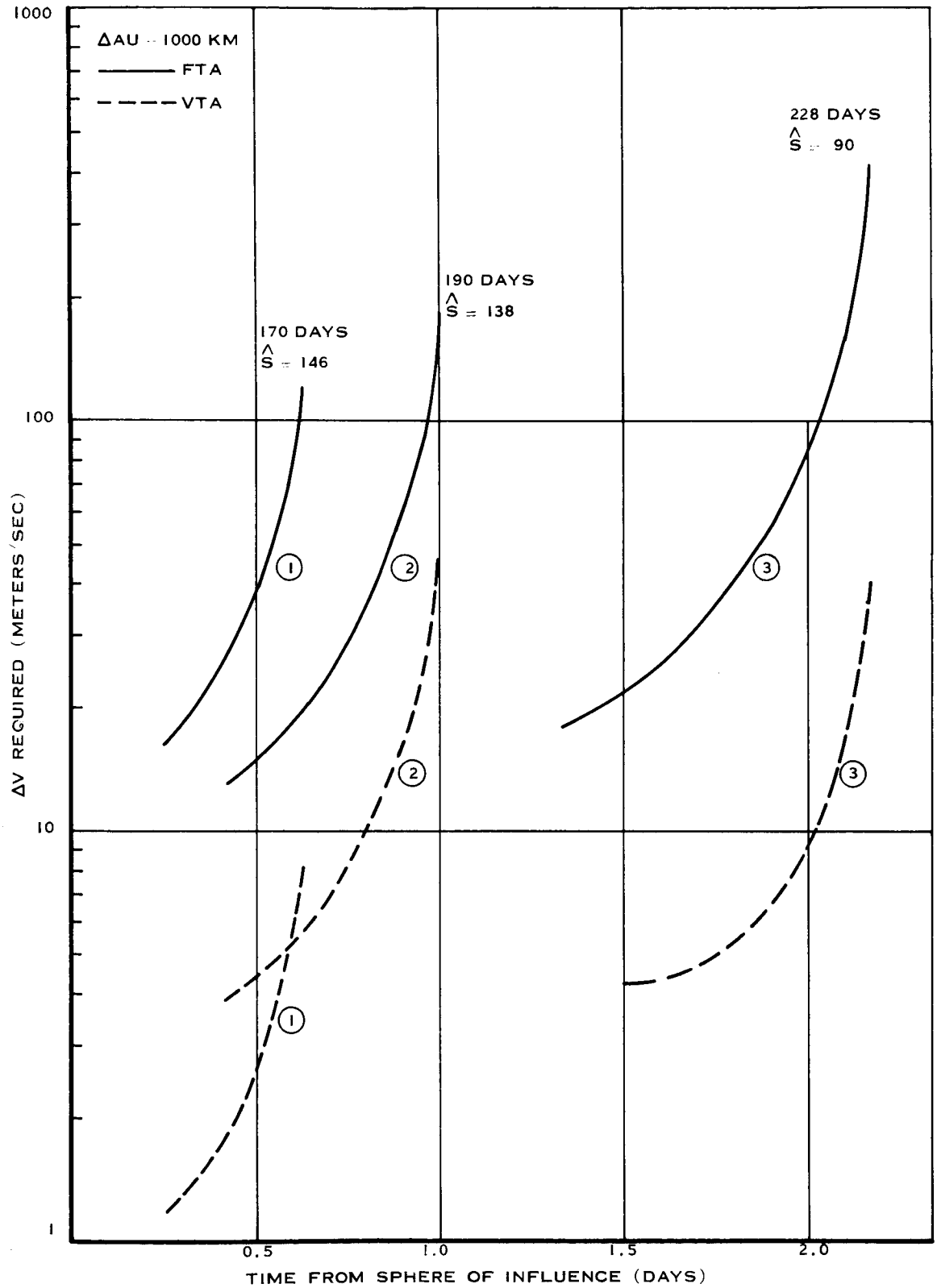

FIGURE 5-6 APPROACH ΔV REQUIRED FOR 160° TRANSFER

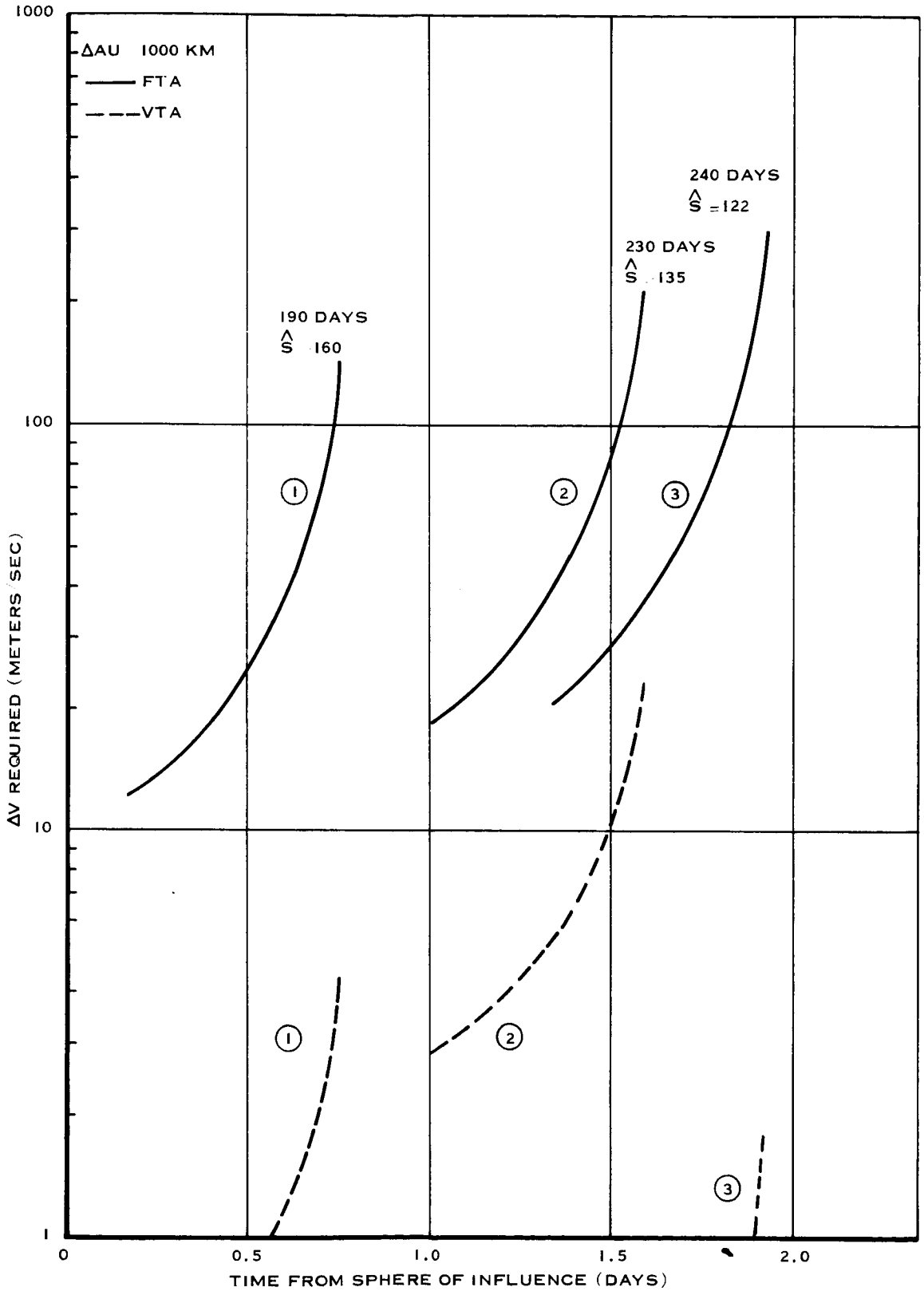

FIGURE 5-7 APPROACH ΔV REQUIRED FOR 180° TRANSFER

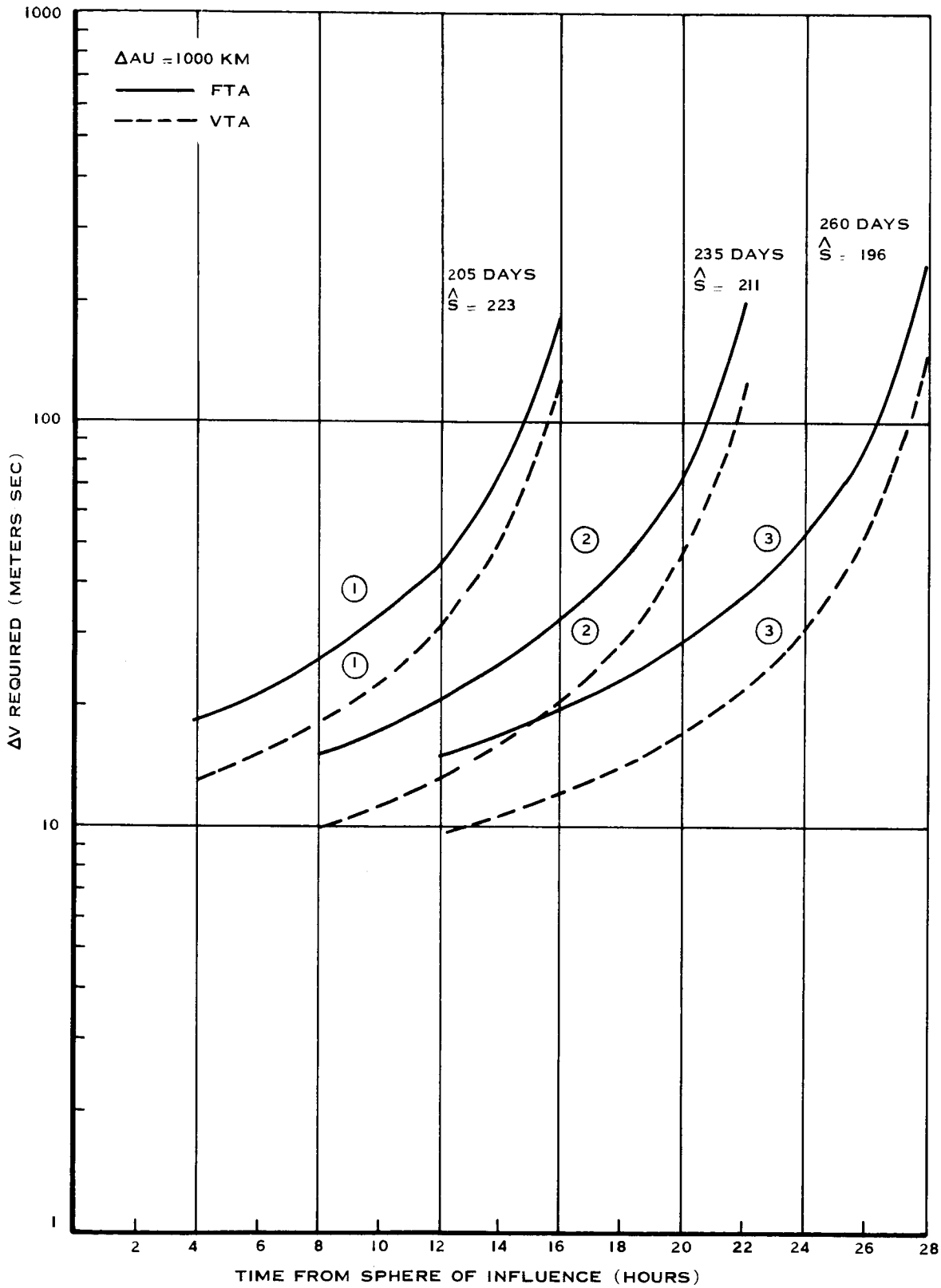

FIGURE 5-8 APPROACH ΔV REQUIRED FOR 270° TRANSFER

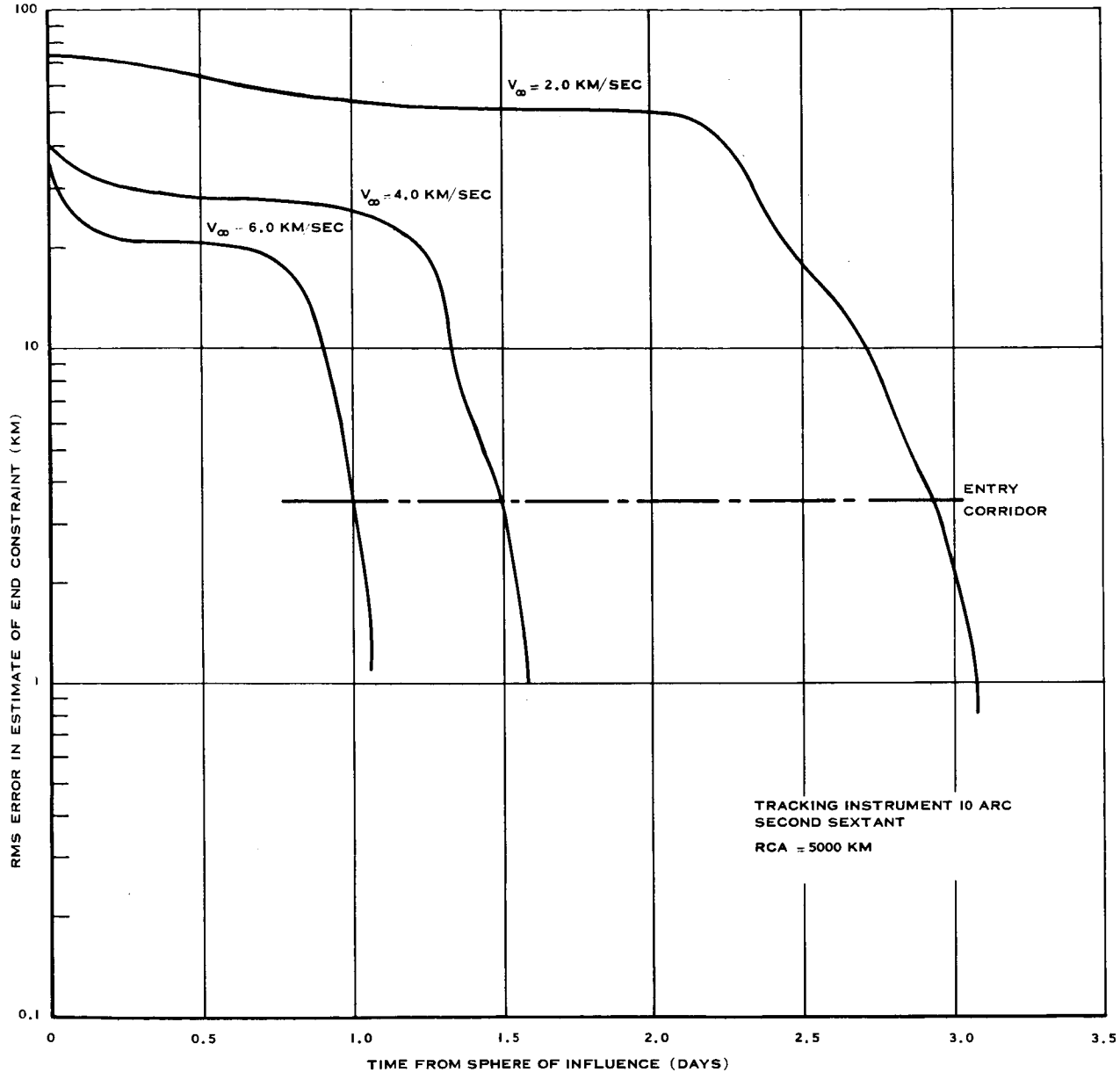

FIGURE 5-9 ERROR IN ESTIMATE OF $\vec{B}$ MAGNITUDE

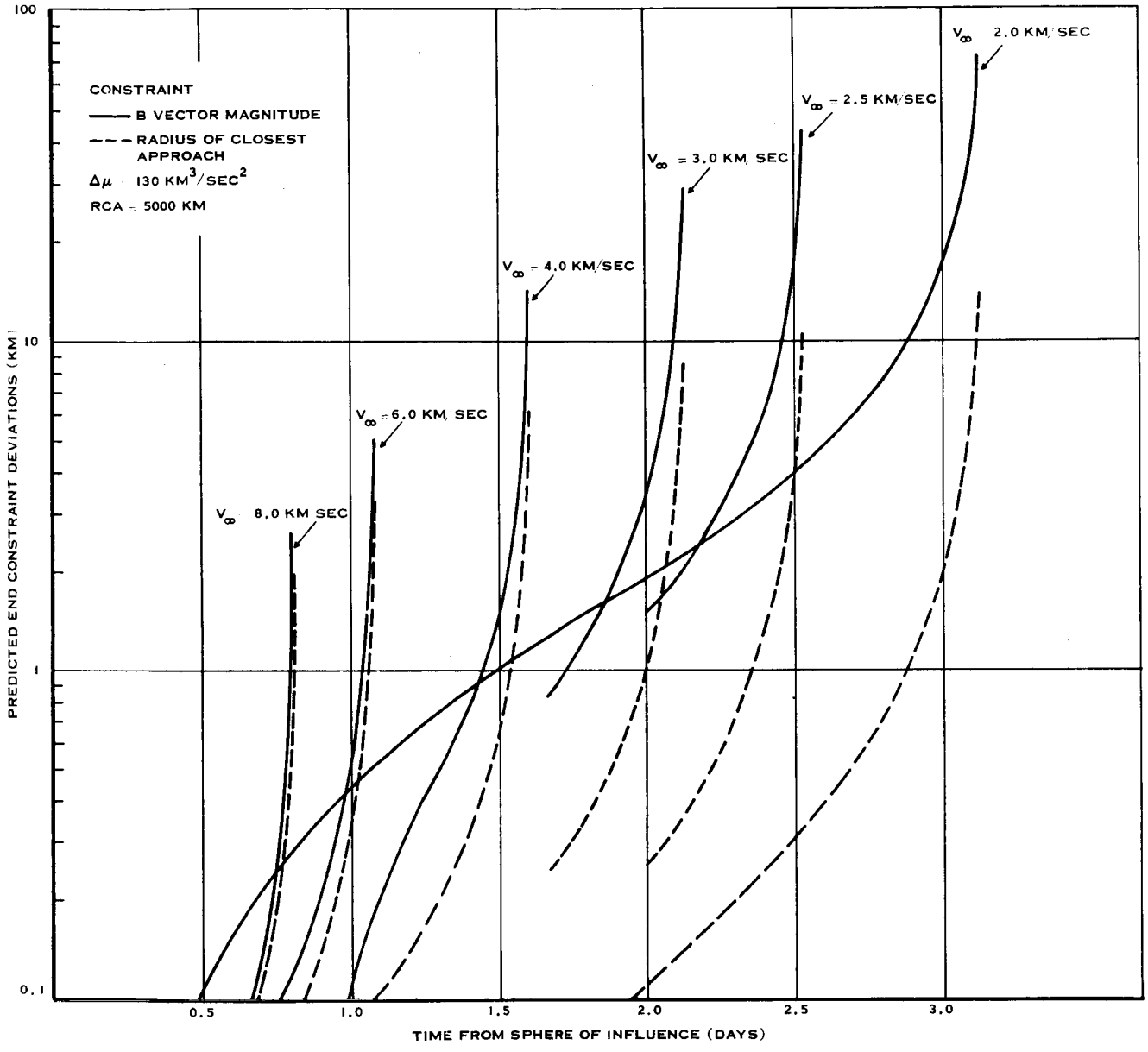

FIGURE 5-10 TIME HISTORY OF PREDICTED END CONSTRAINT DEVIATIONS

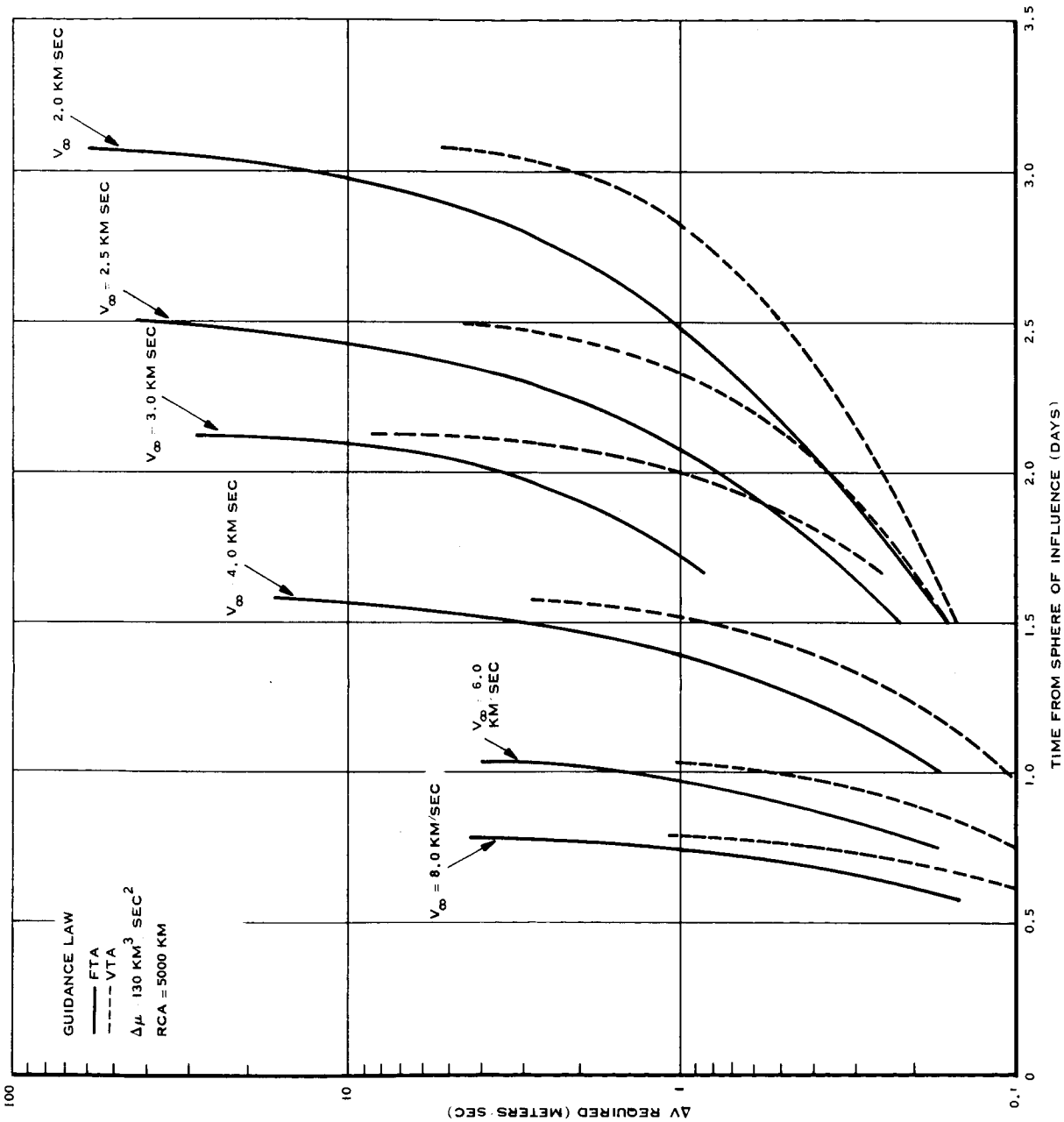

FIGURE 5-11 ΔV REQUIRED FOR APPROACH GUIDANCE

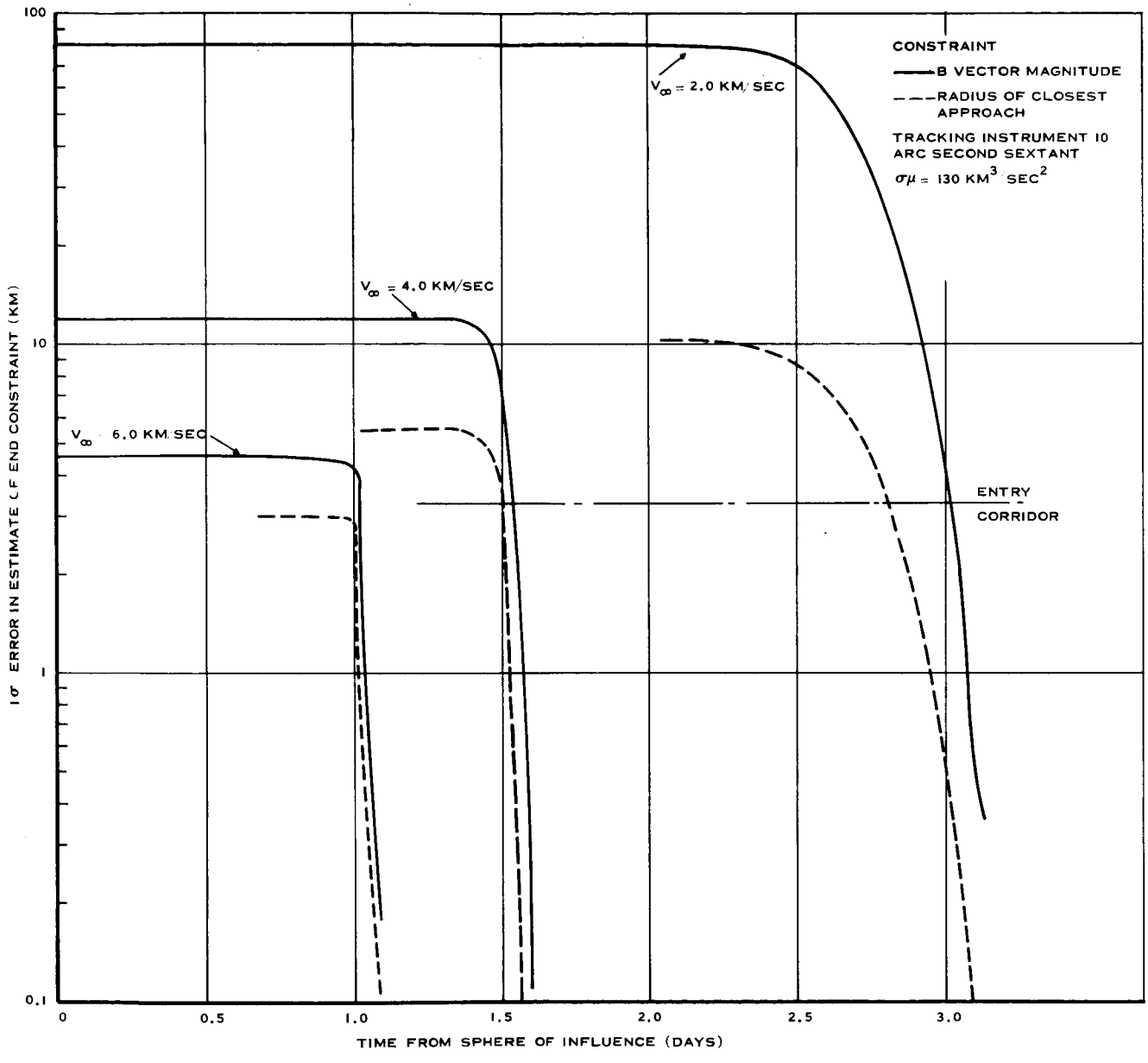

FIGURE 5-12 ERROR IN ESTIMATE OF END CONSTRAINTS

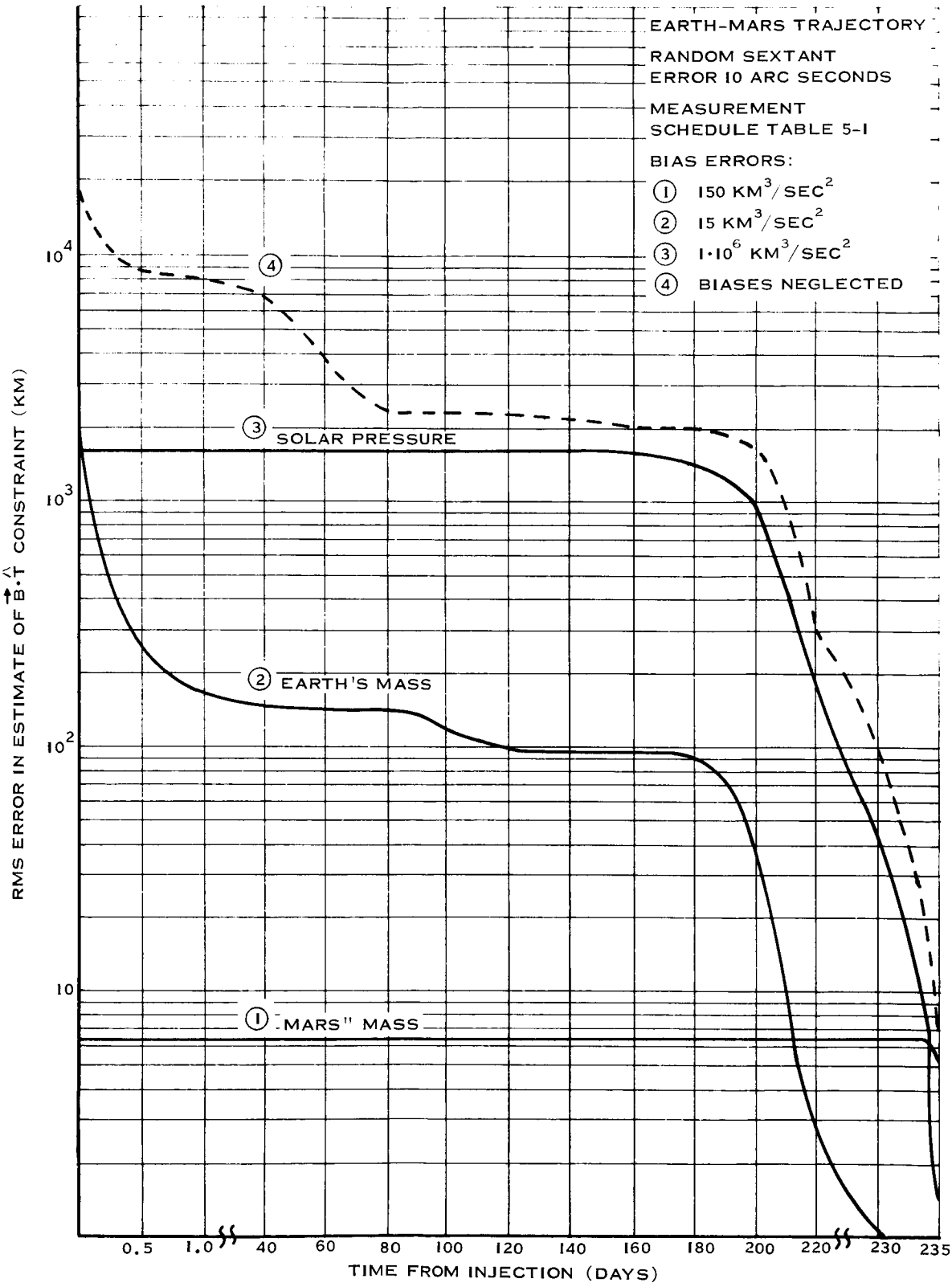

FIGURE 5-13A ERROR IN ESTIMATE OF B·T DUE TO NEGLECTING BIAS ERRORS

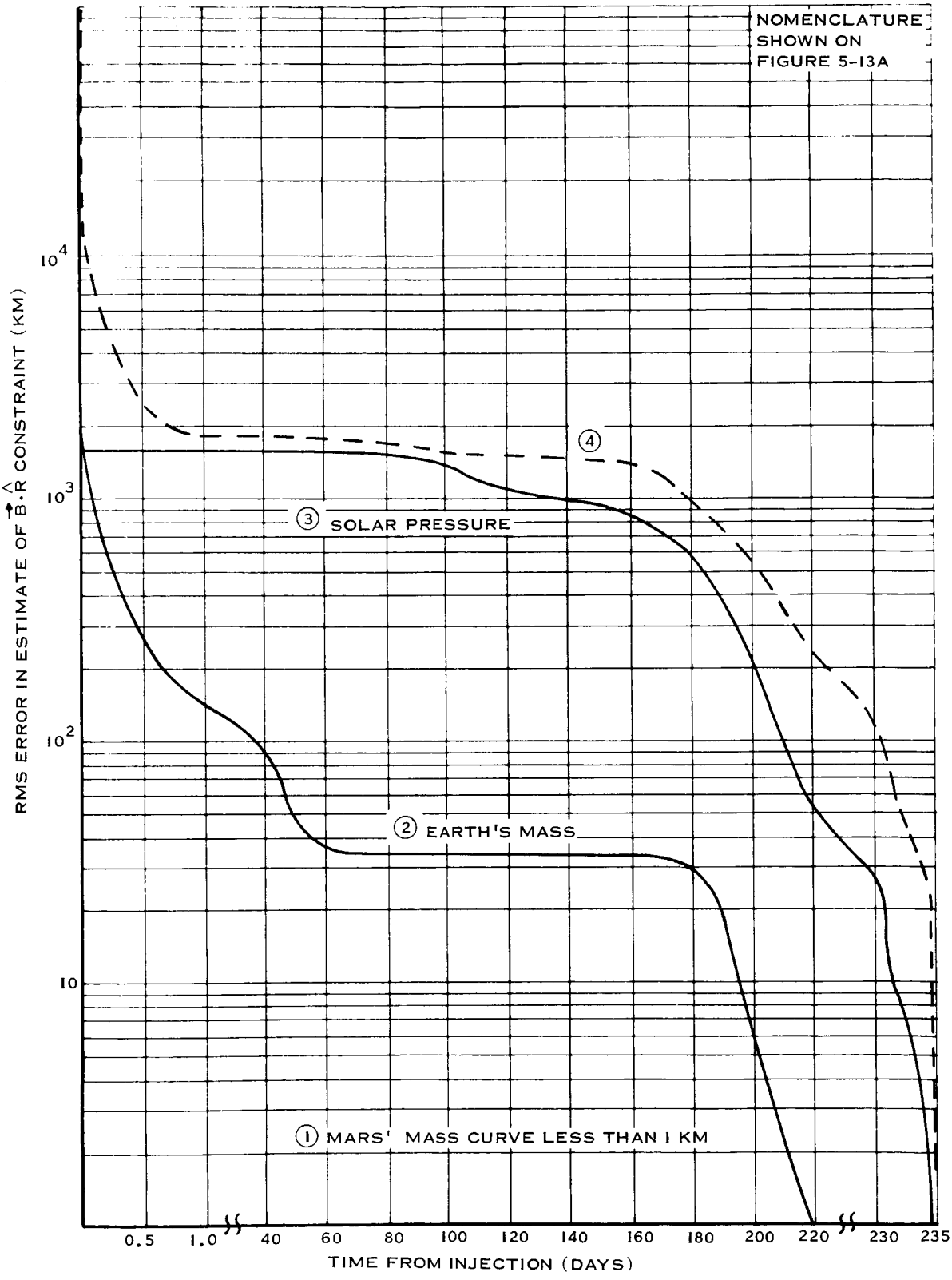

FIGURE 5-13B ERROR IN ESTIMATE OF $\vec{B}\cdot\hat{R}$ DUE TO NEGLECTING BIAS ERRORS

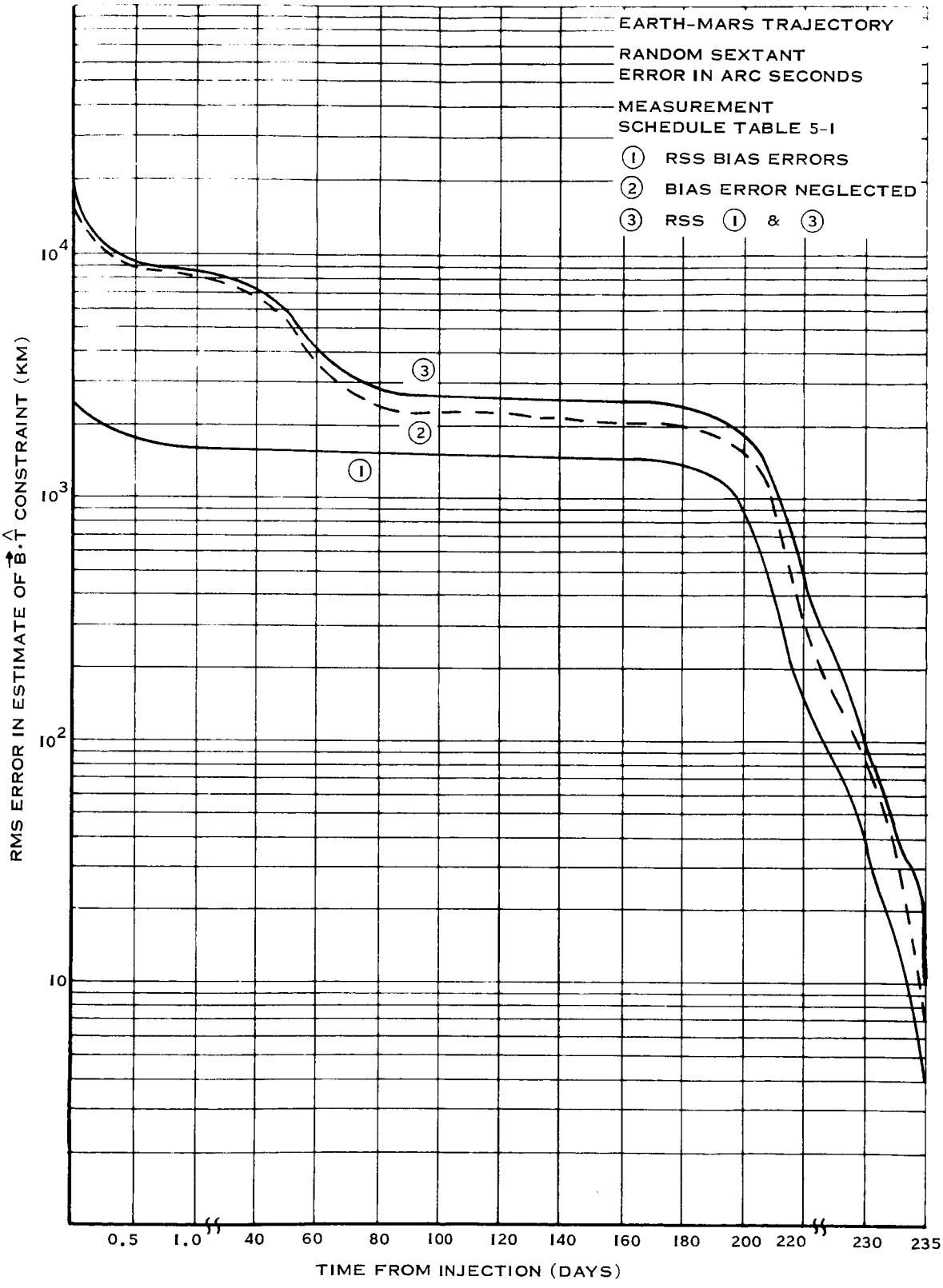

FIGURE 5-14A COMPOSITE EFFECT OF BIAS ERROR ON $\hat{B}\cdot\hat{T}$ ESTIMATE

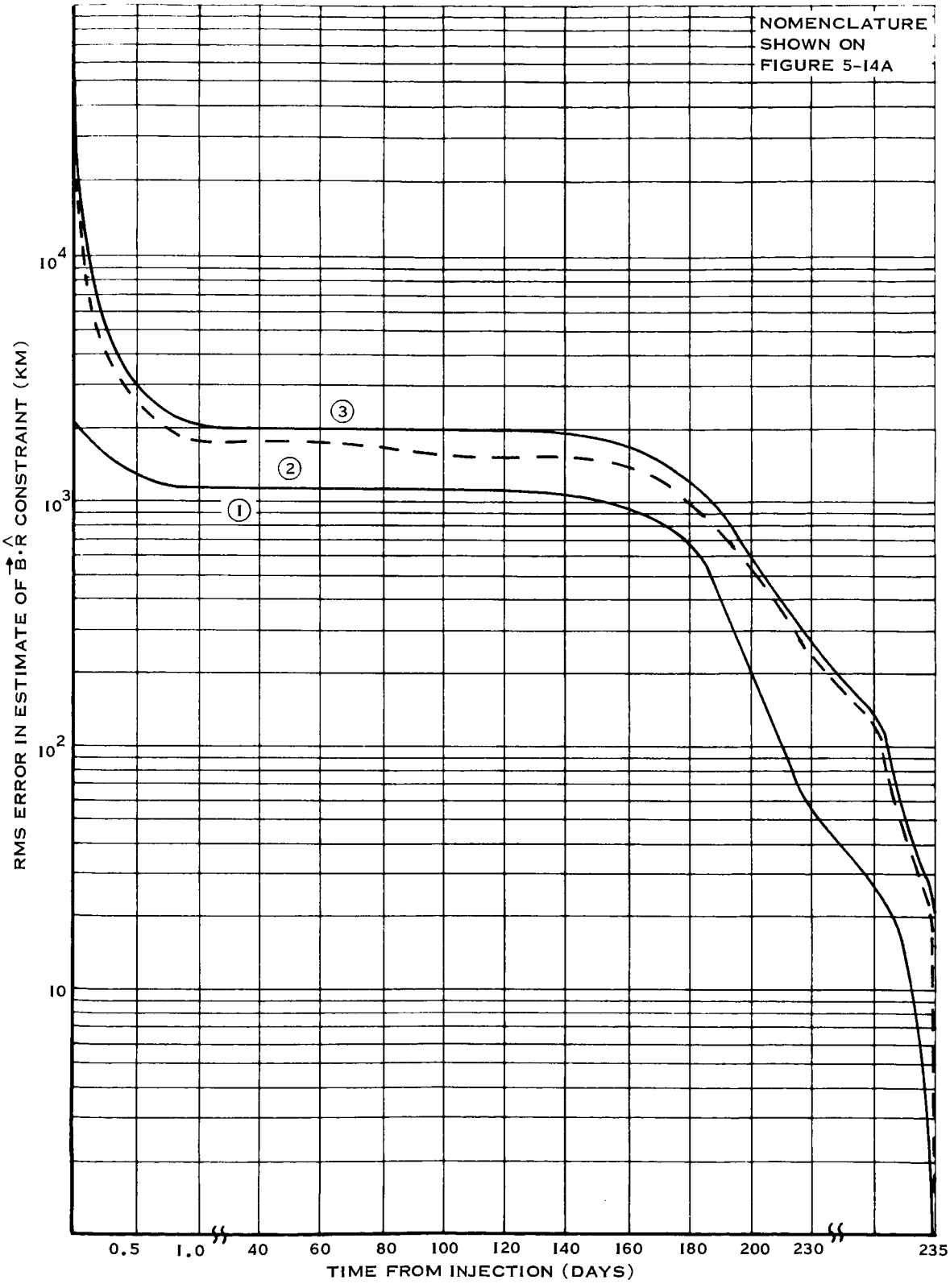

FIGURE 5-14B COMPOSITE EFFECT OF BIAS ERROR ON $\vec{B}\cdot\hat{R}$ ESTIMATE

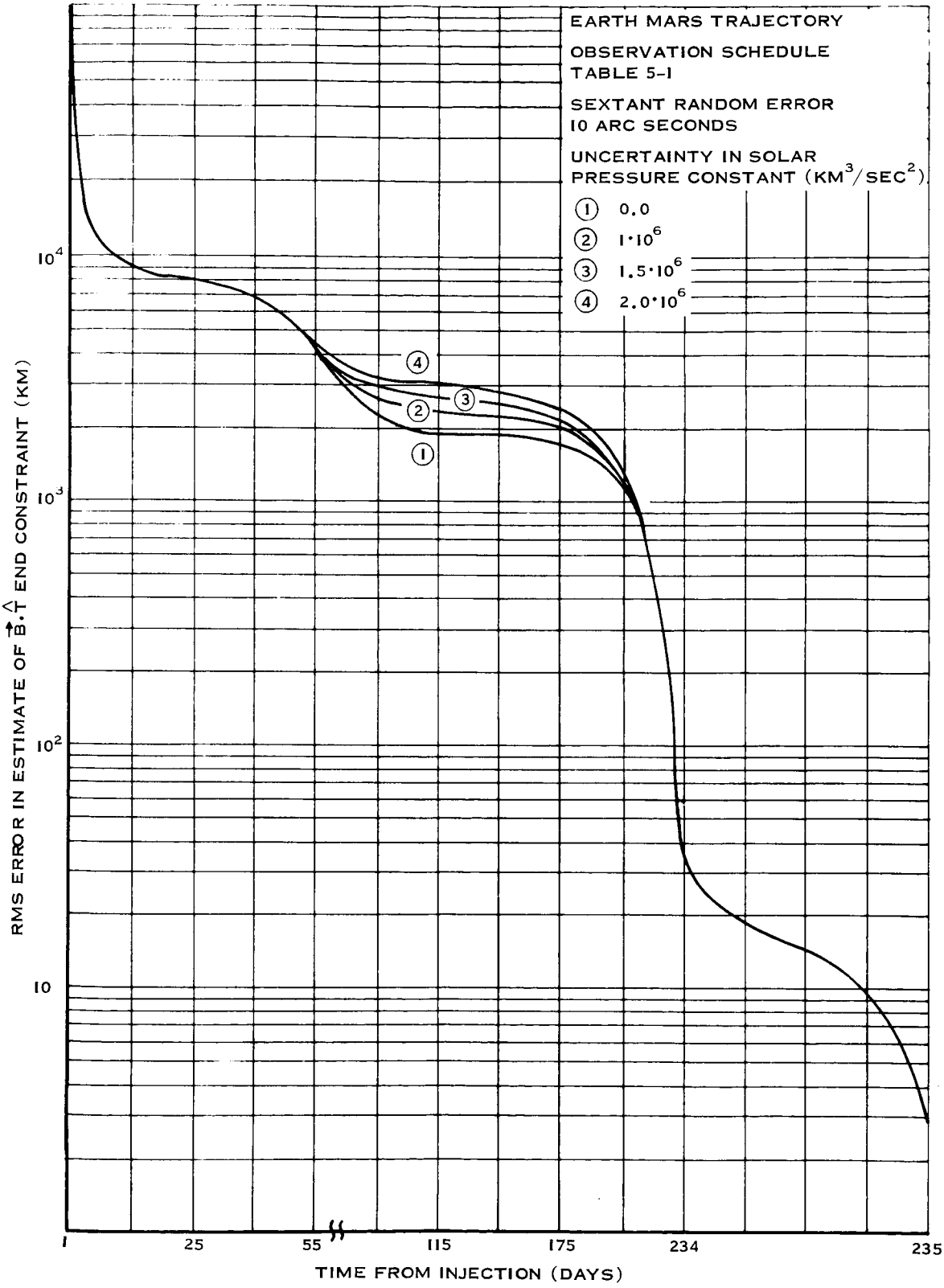

FIGURE 5-15A EFFECT OF SOLAR PRESSURE ON $\vec{B}\cdot\hat{T}$ ESTIMATE

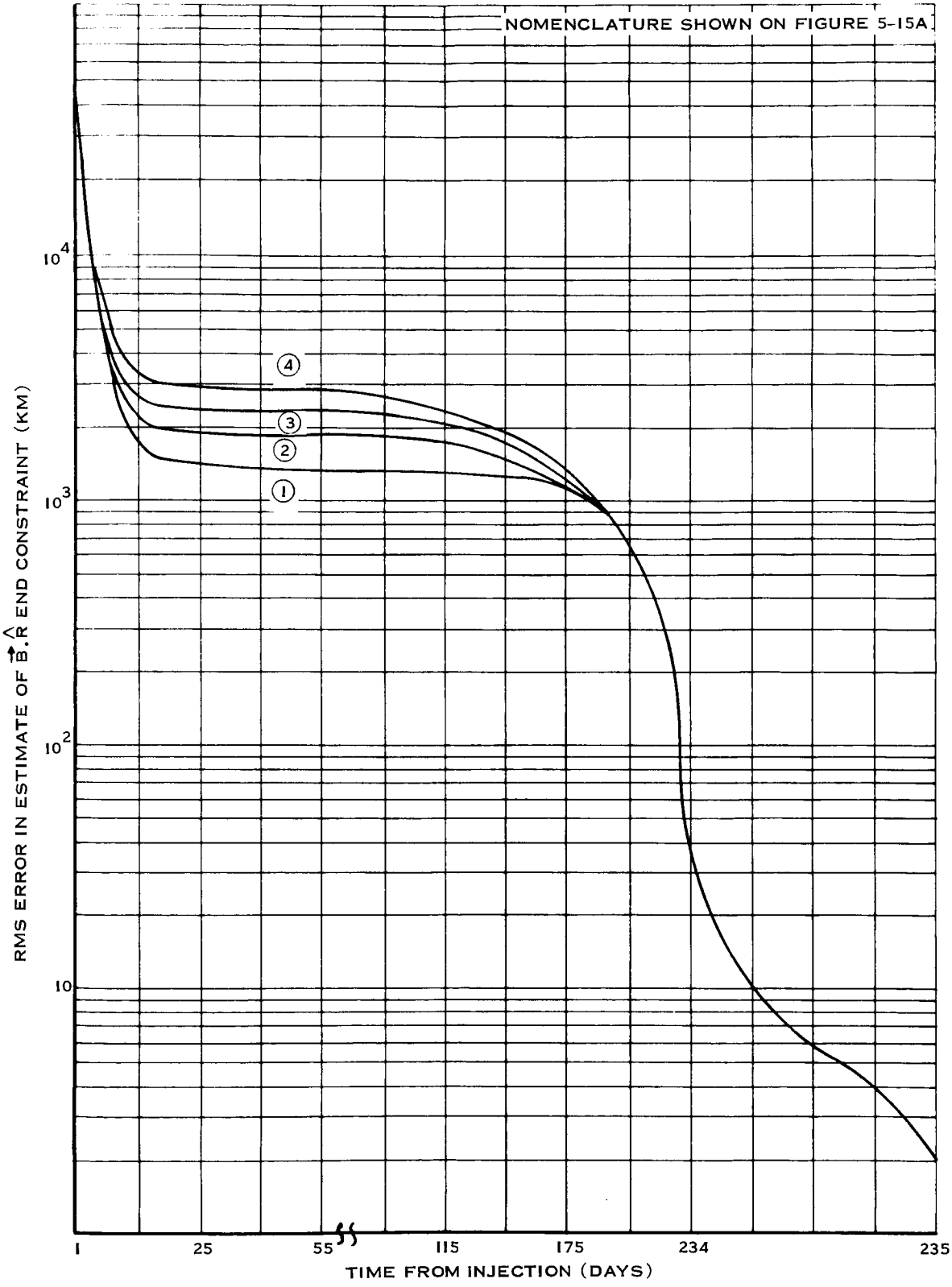

FIGURE 5-15B EFFECT OF SOLAR PRESSURE ON $\vec{B}\cdot\hat{R}$ ESTIMATE

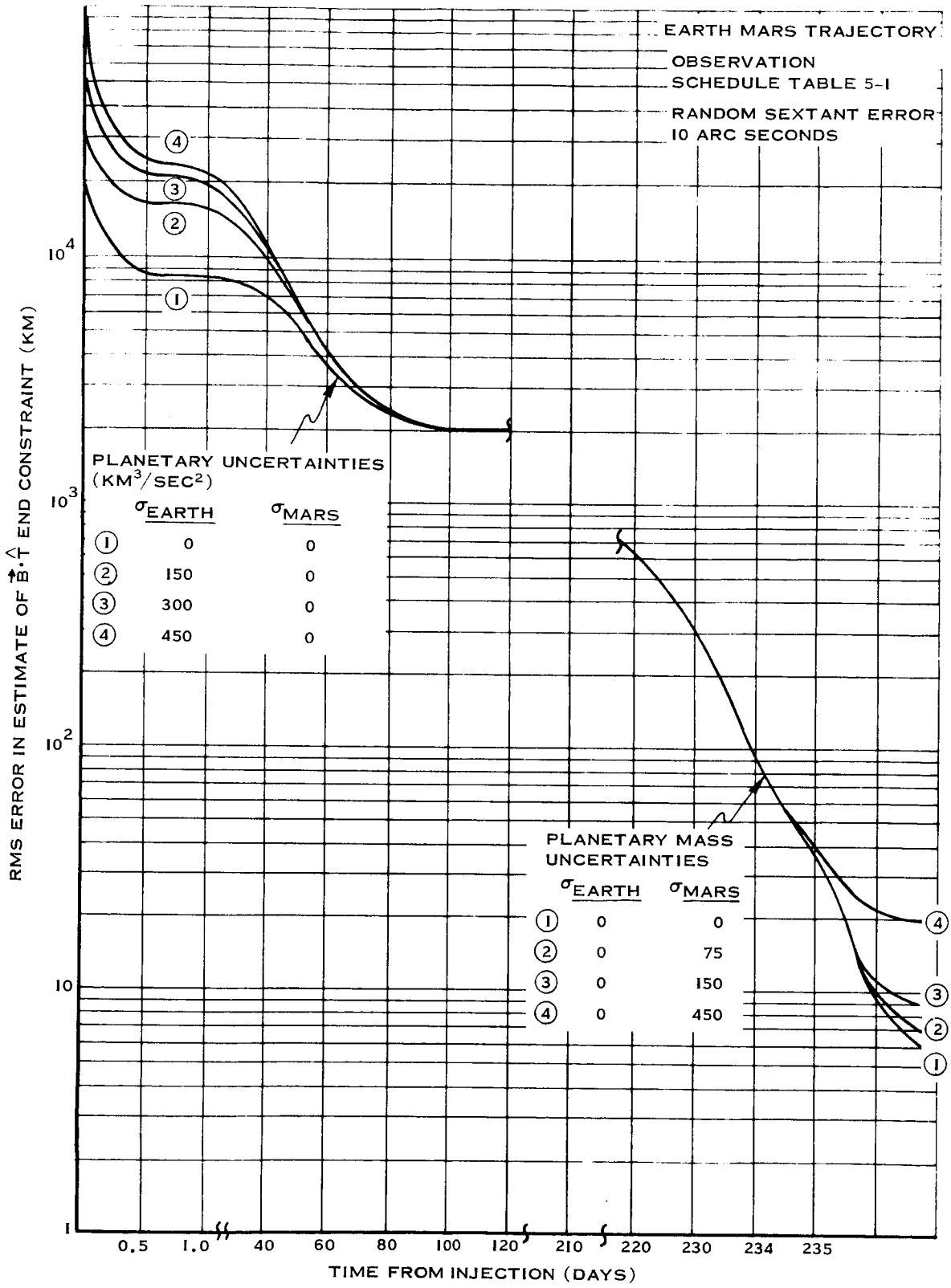

FIGURE 5-16A EFFECT OF PLANETARY MASSES ON $\vec{B}\cdot\hat{T}$ ESTIMATE

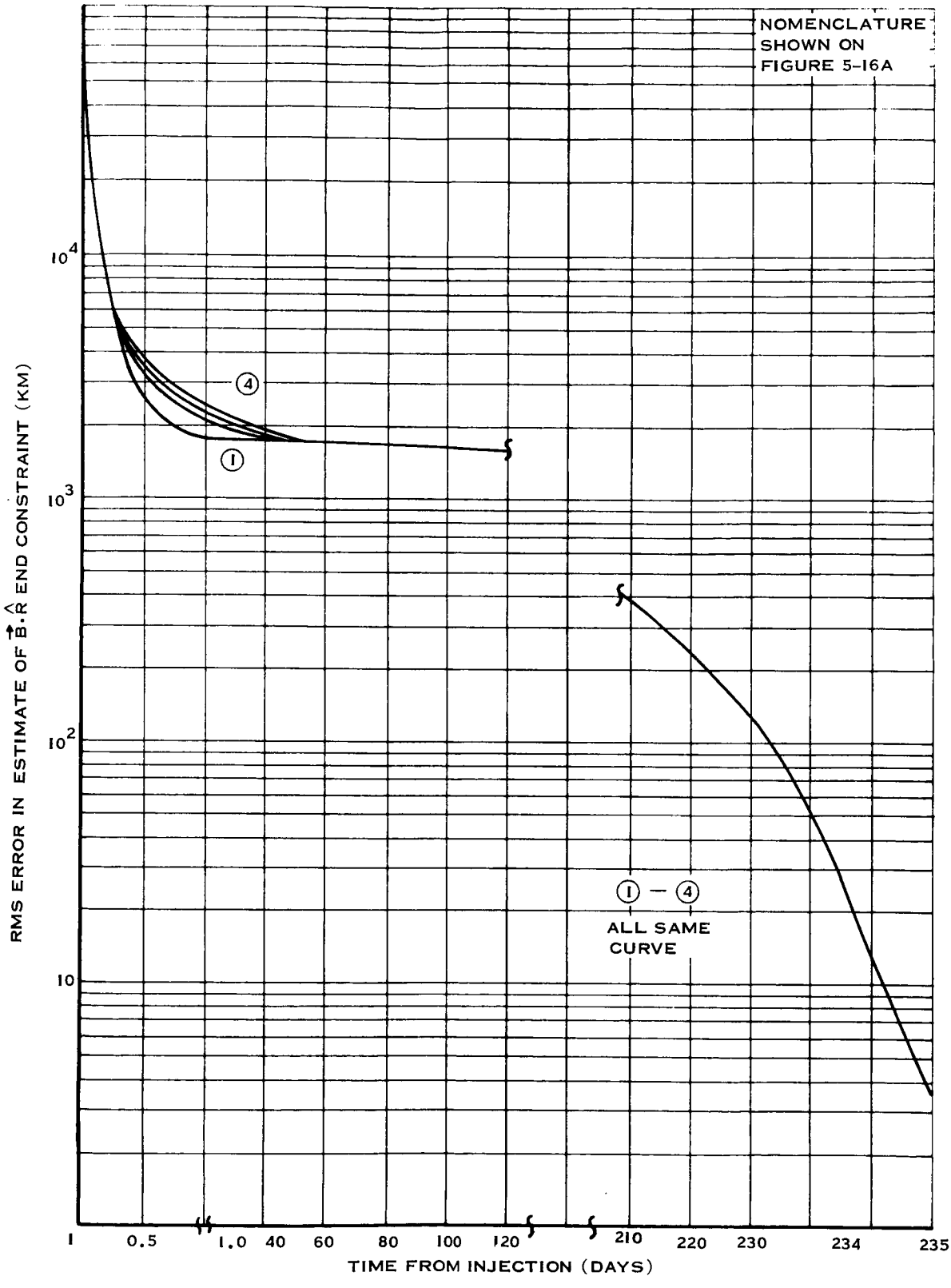

FIGURE 5-16B EFFECT OF PLANETARY MASSES ON $\vec{B}\cdot\hat{R}$ ESTIMATE

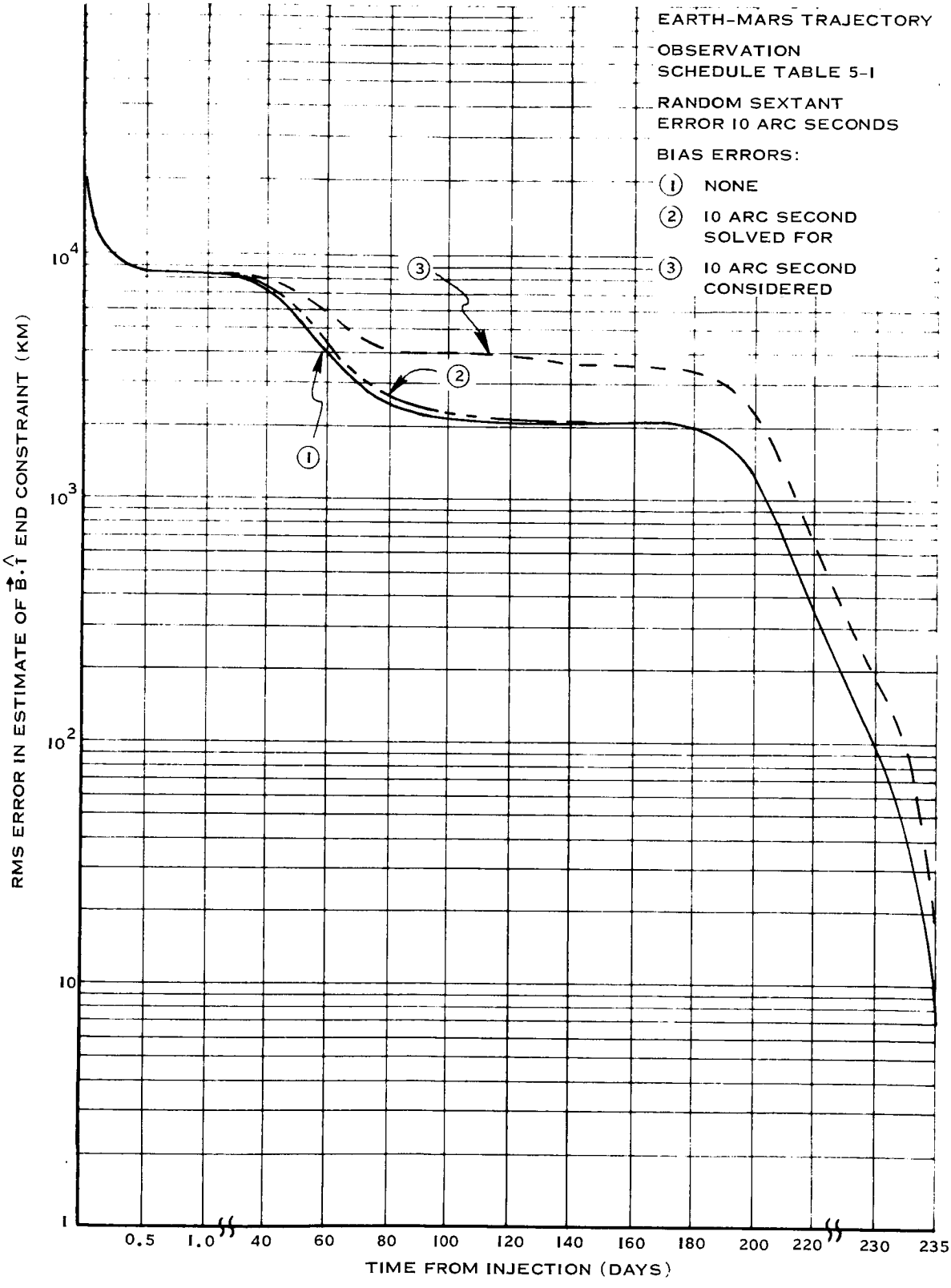

FIGURE 5-17A EFFECT OF SEXTANT ANGLE BIAS ON $\vec{B}\cdot\hat{T}$

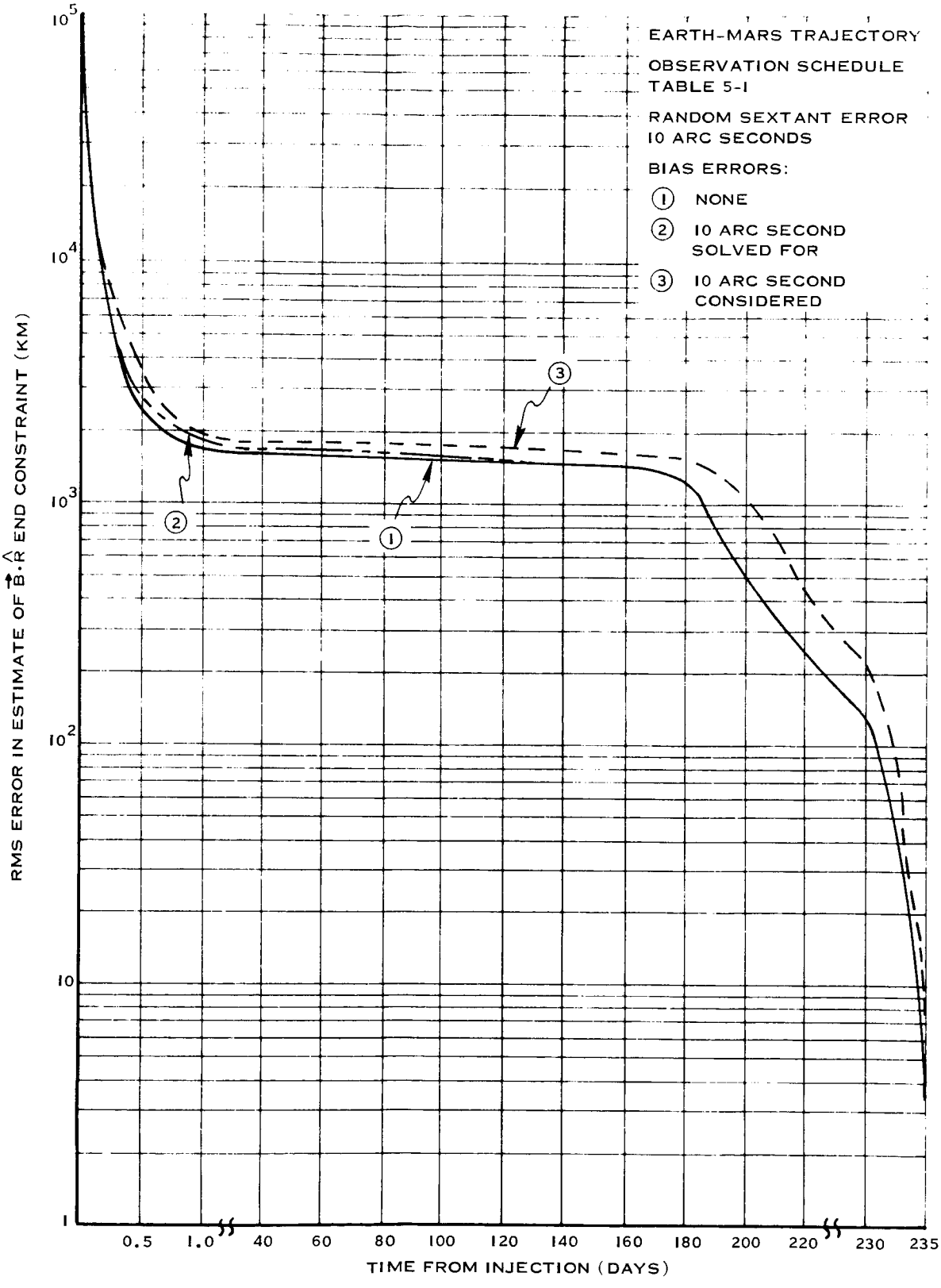

FIGURE 5-17B EFFECT OF SEXTANT ANGLE BIAS ON $\vec{B}\cdot\hat{R}$

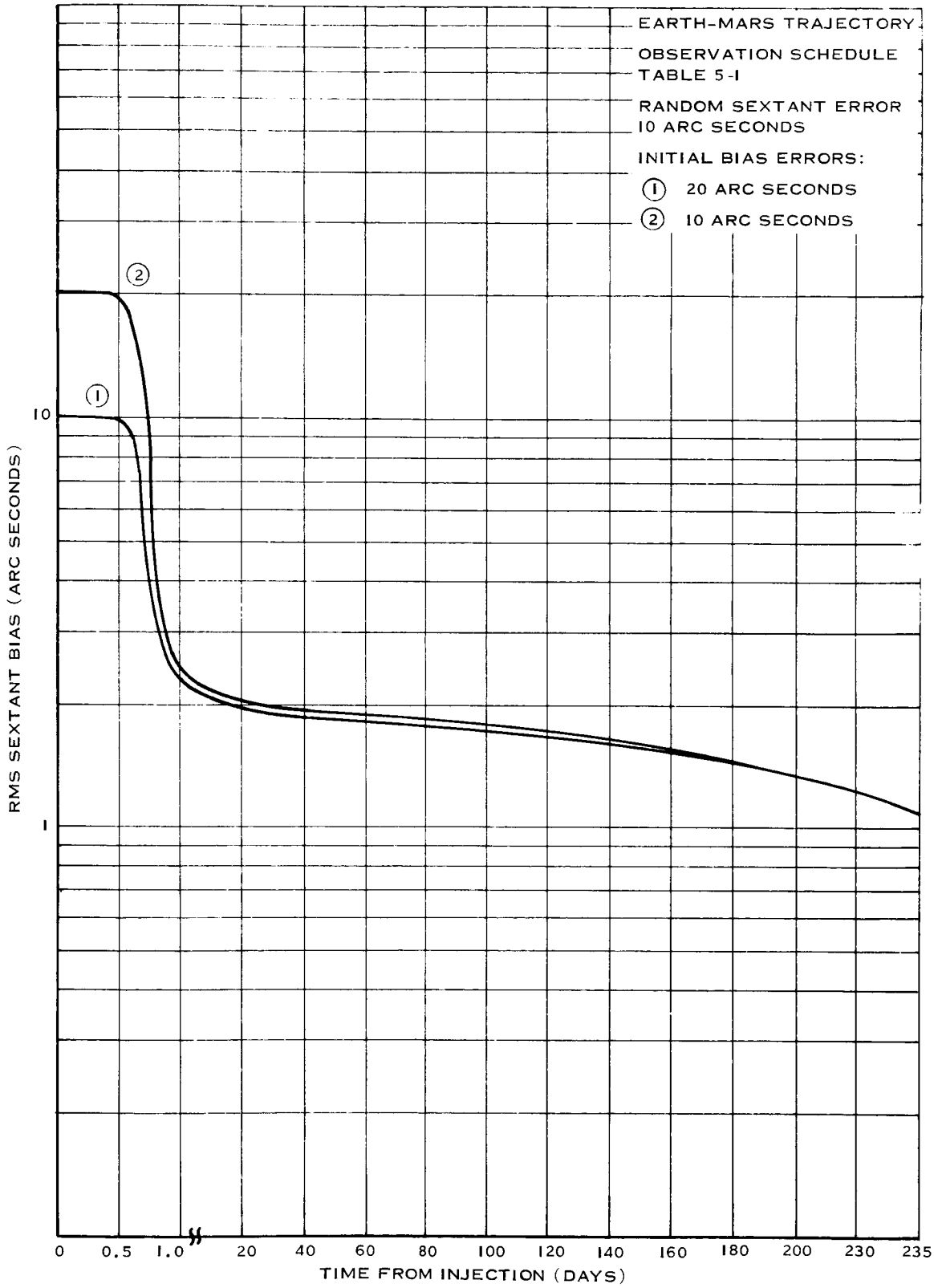

FIGURE 5-18 SOLVED FOR SEXTANT BIAS ERROR

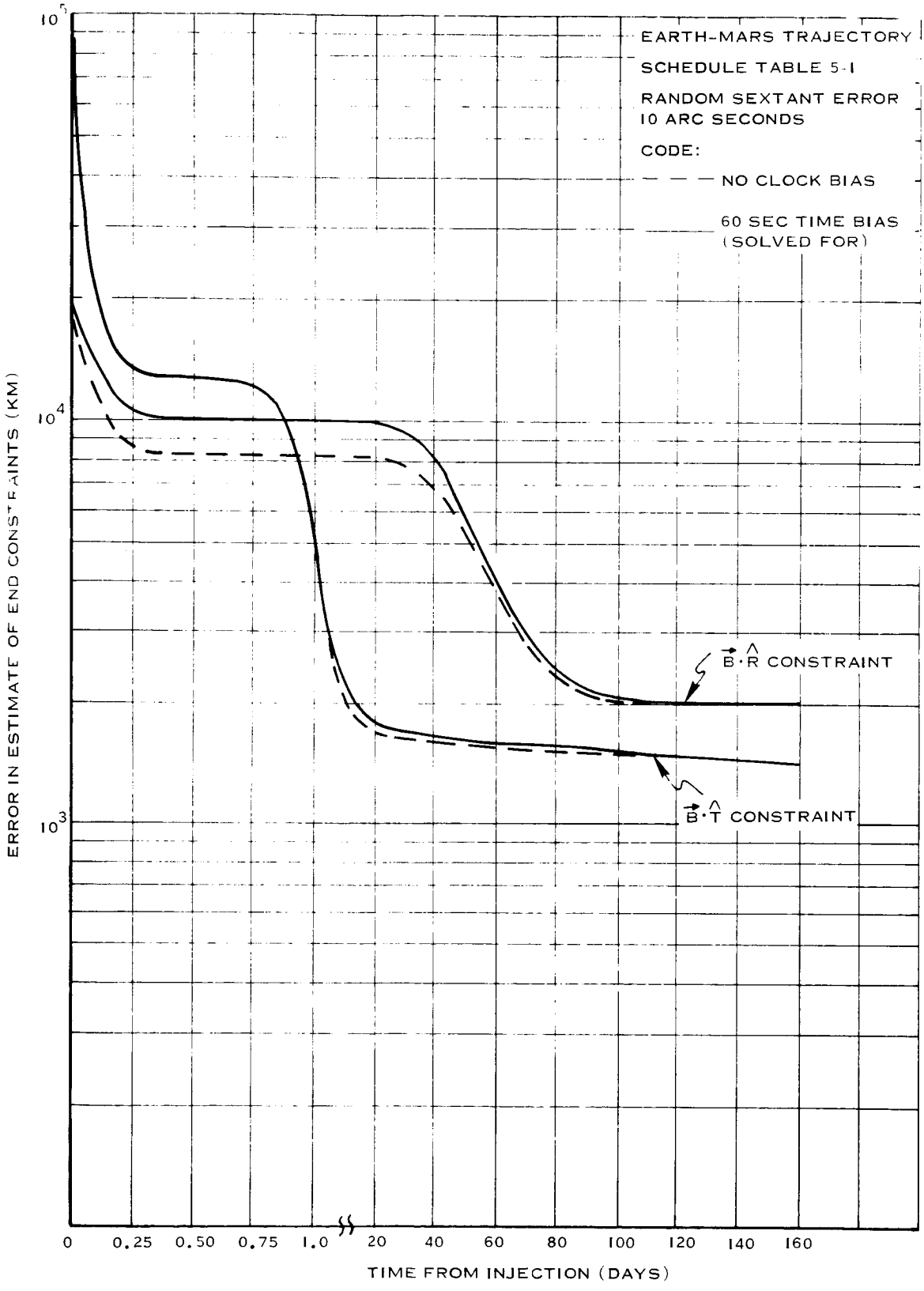

FIGURE 5.19 SOLVED FOR ON-BOARD CLOCK TIME BIAS

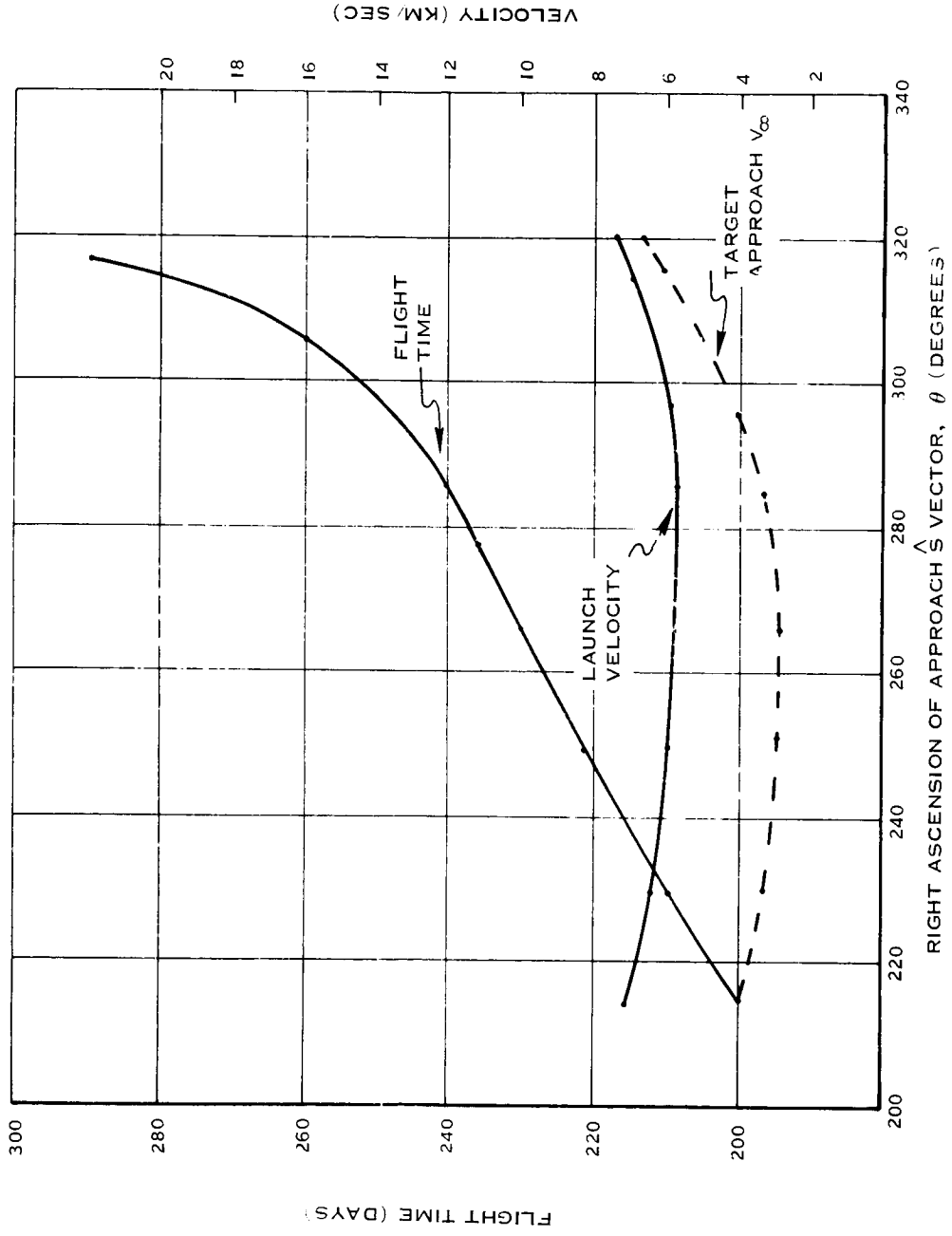

FIGURE 5-20A TRAJECTORY CHARACTERISTICS - 160° TRANSFER, MARS-EARTH

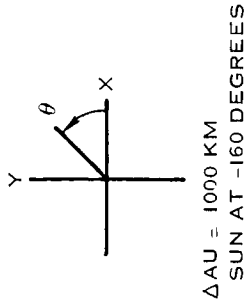

ΔAU = 1000 KM
SUN AT -160 DEGREES

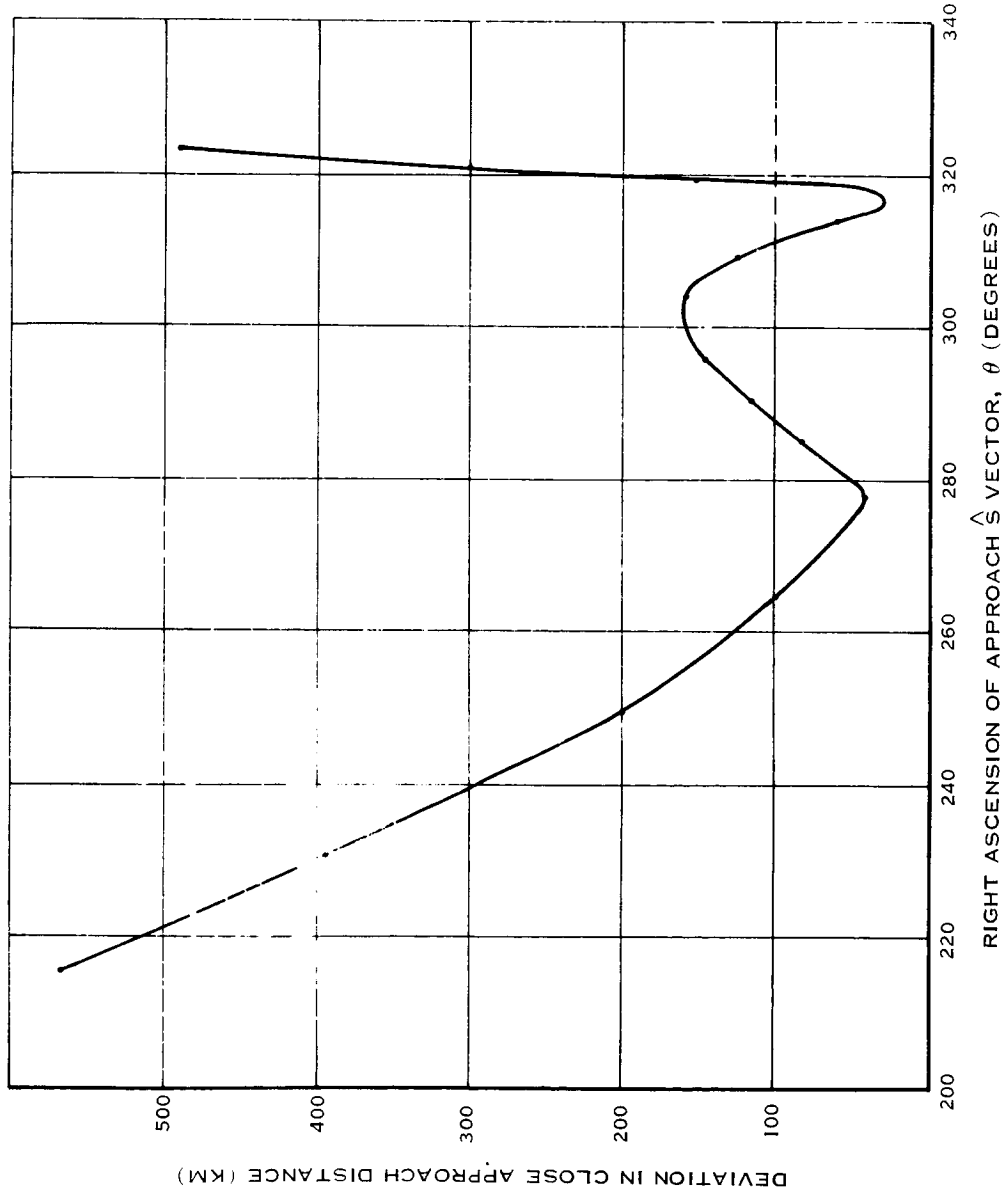

FIGURE 5-20B DEVIATIONS IN CLOSE APPROACH - 160° TRANSFER, MARS-EARTH

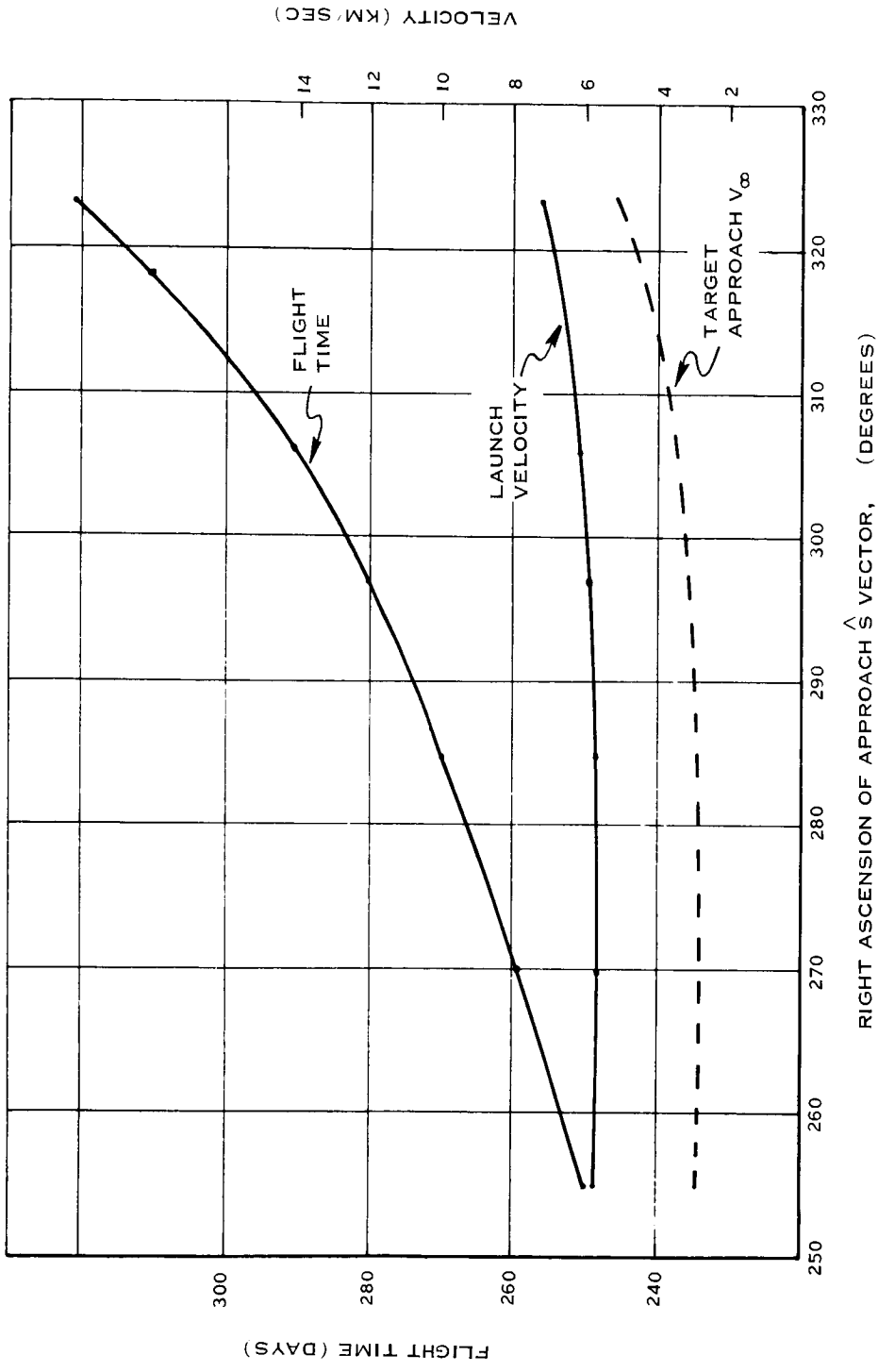

FIGURE 5-21A TRAJECTORY CHARACTERISTICS - 180° TRANSFER, MARS-EARTH

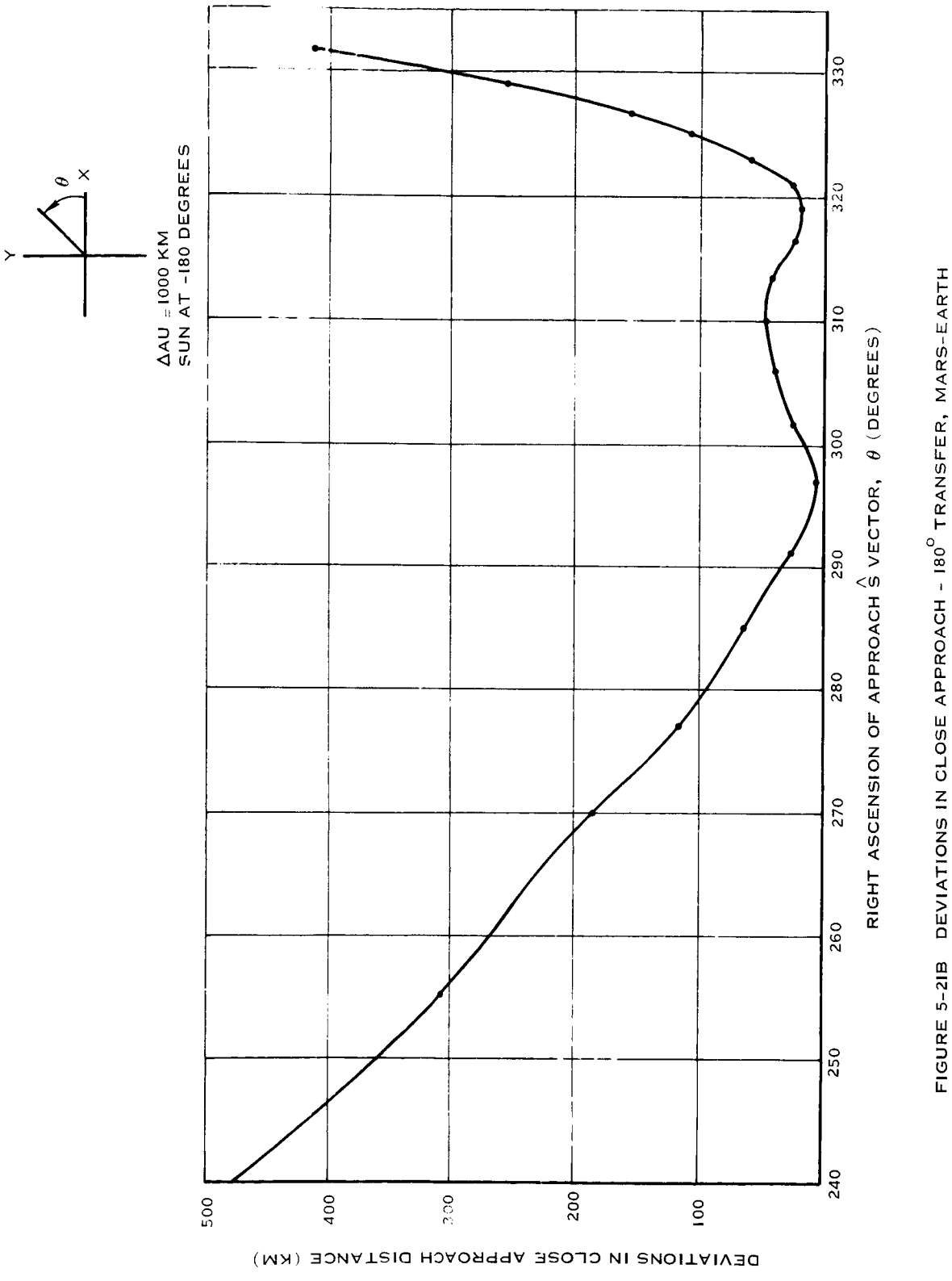

FIGURE 5-21B DEVIATIONS IN CLOSE APPROACH - 180° TRANSFER, MARS-EARTH

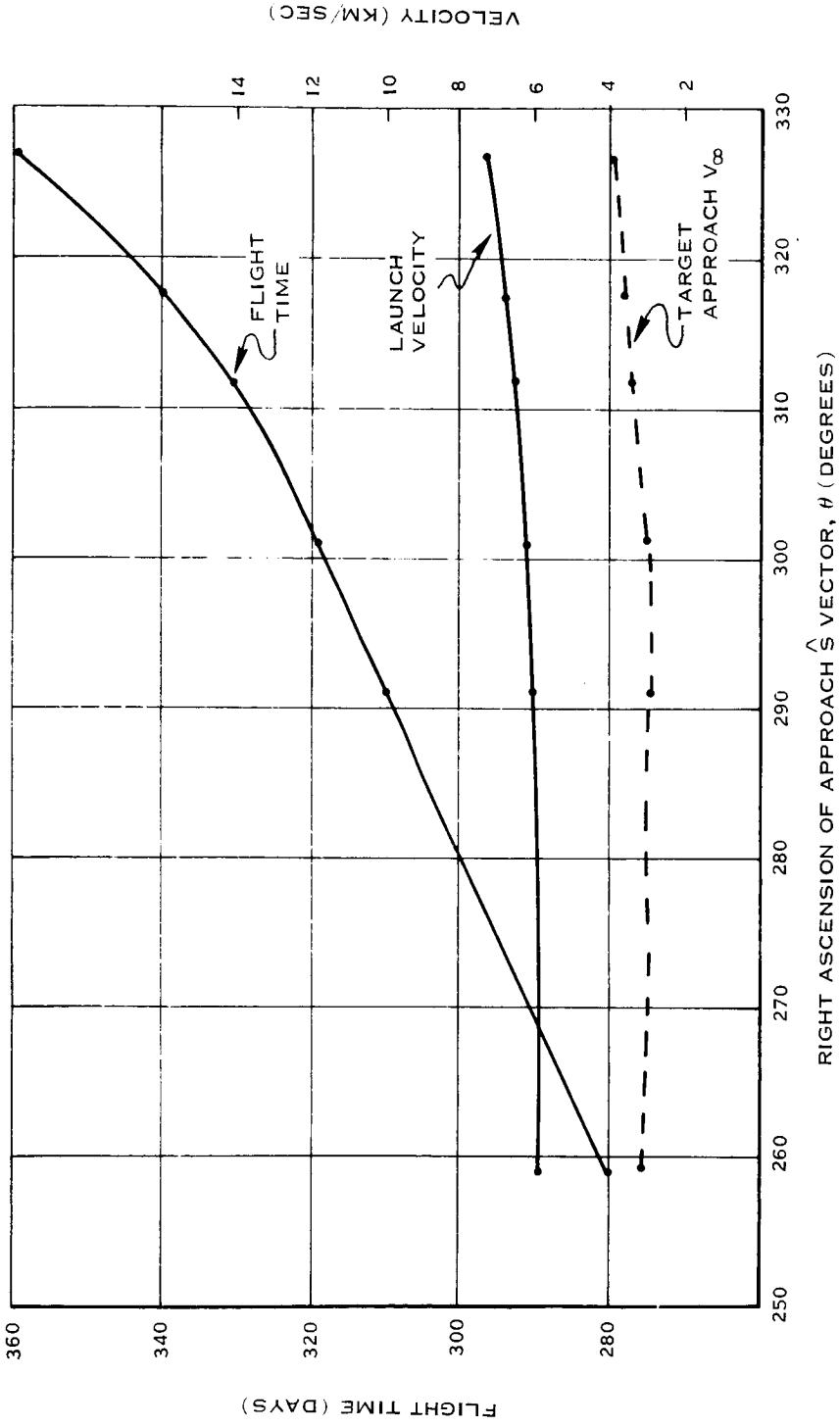

FIGURE 5-22A TRAJECTORY CHARACTERISTICS - 200^{O} TRANSFER, MARS-EARTH

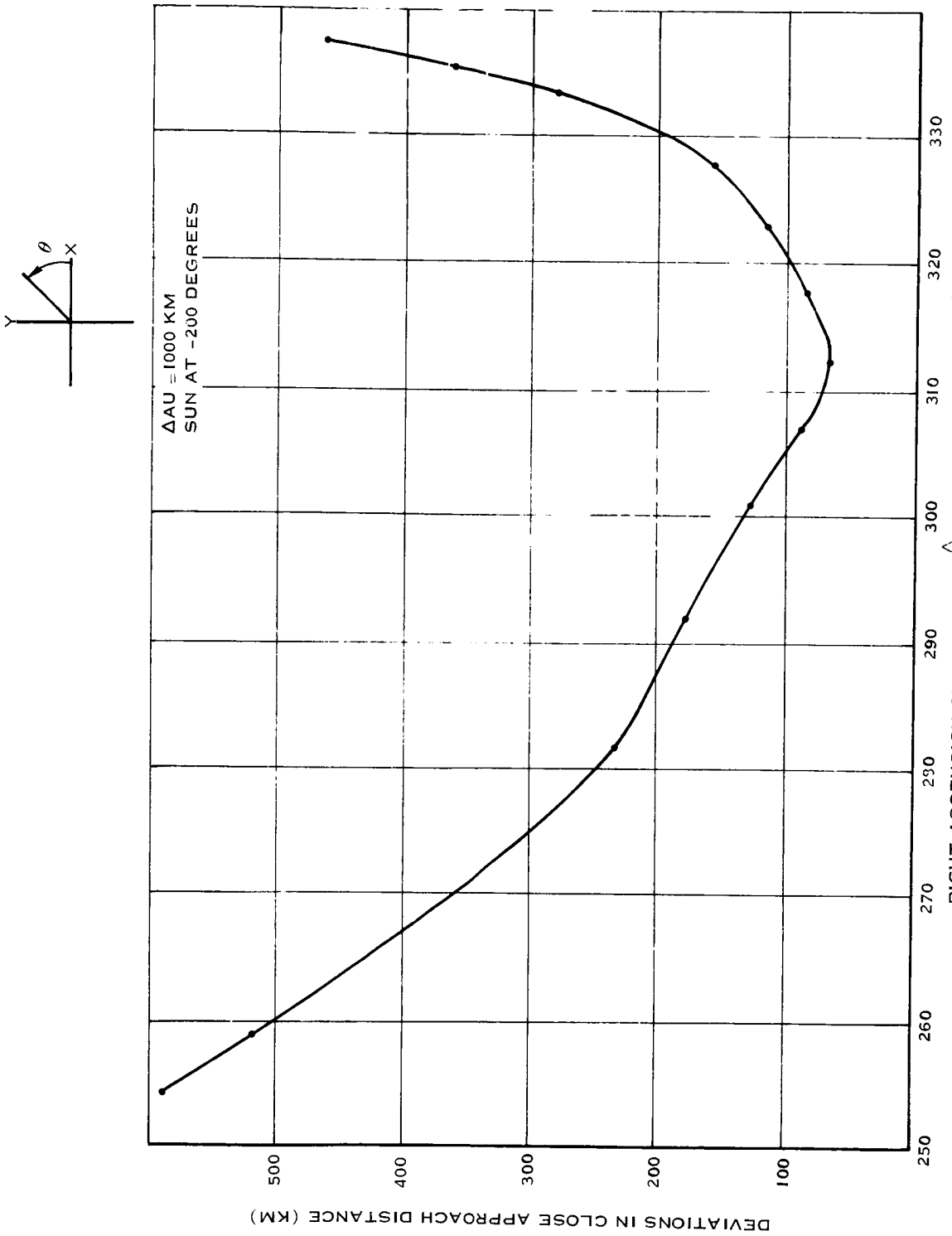

FIGURE 5-22B DEVIATIONS IN CLOSE APPROACH - 200° TRANSFER, MARS-EARTH

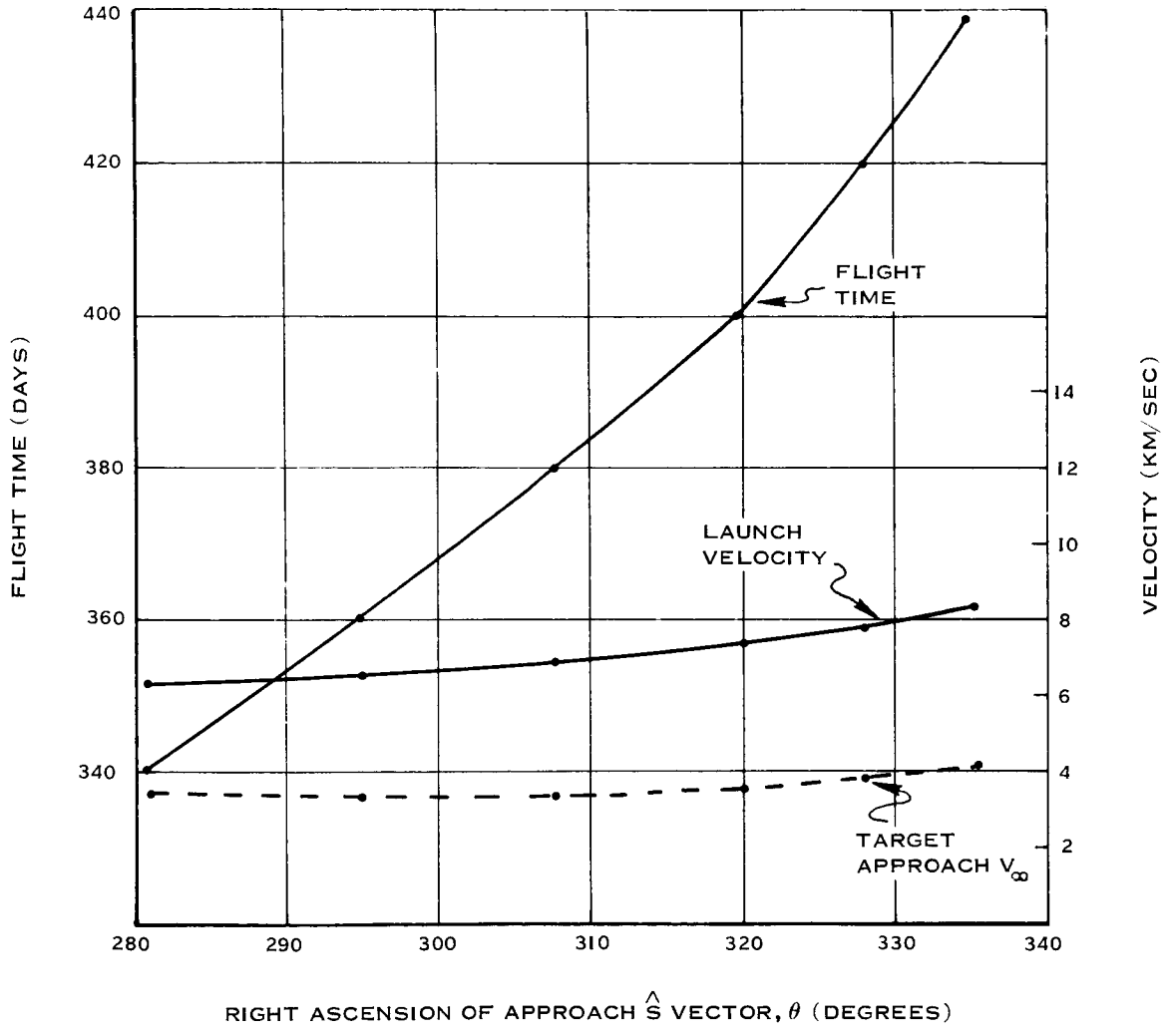

FIGURE 5-23A TRAJECTORY CHARACTERISTICS - 225° TRANSFER, MARS-EARTH

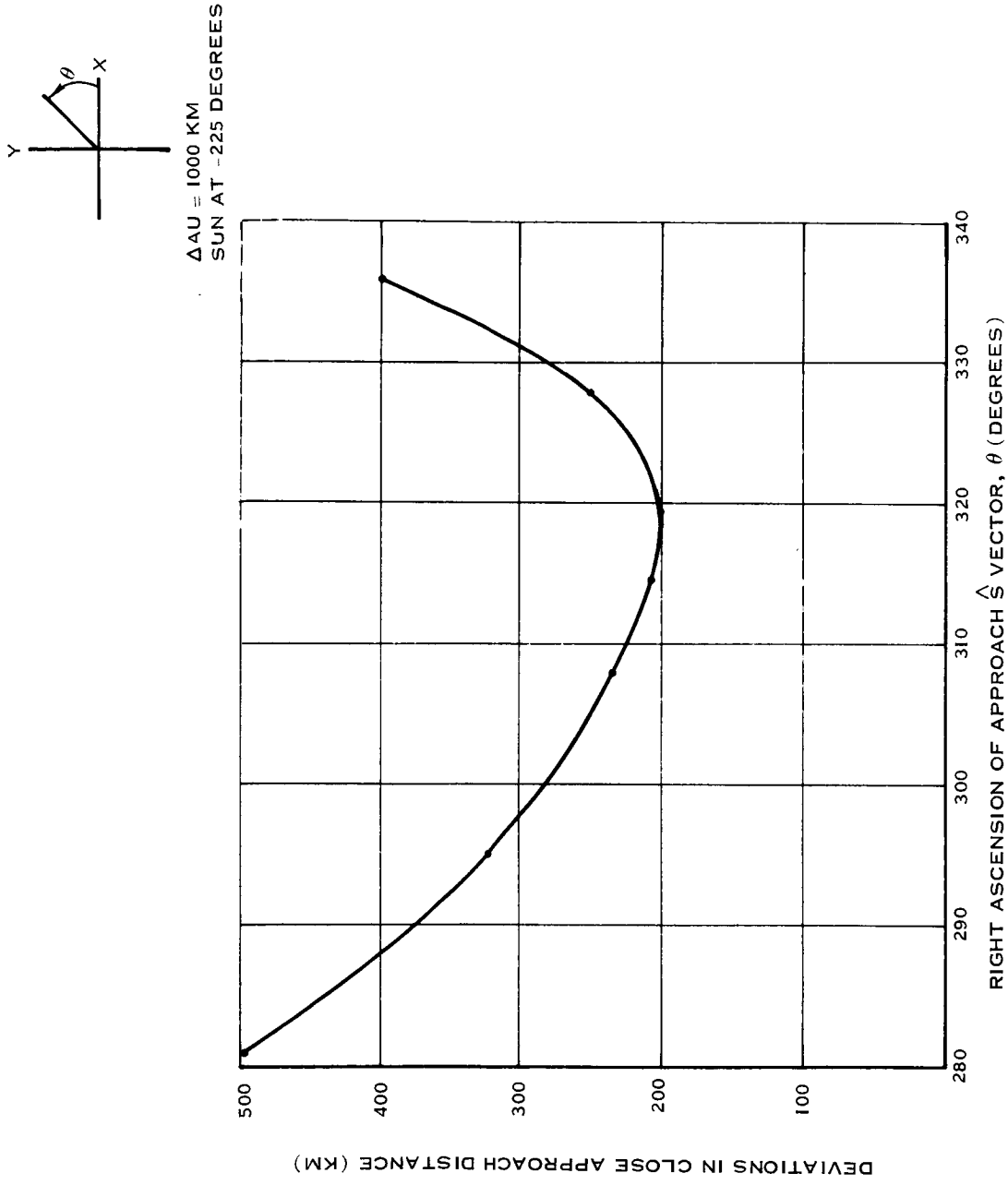

FIGURE 5-23B DEVIATIONS IN CLOSE APPROACH -225° TRANSFER, MARS-EARTH

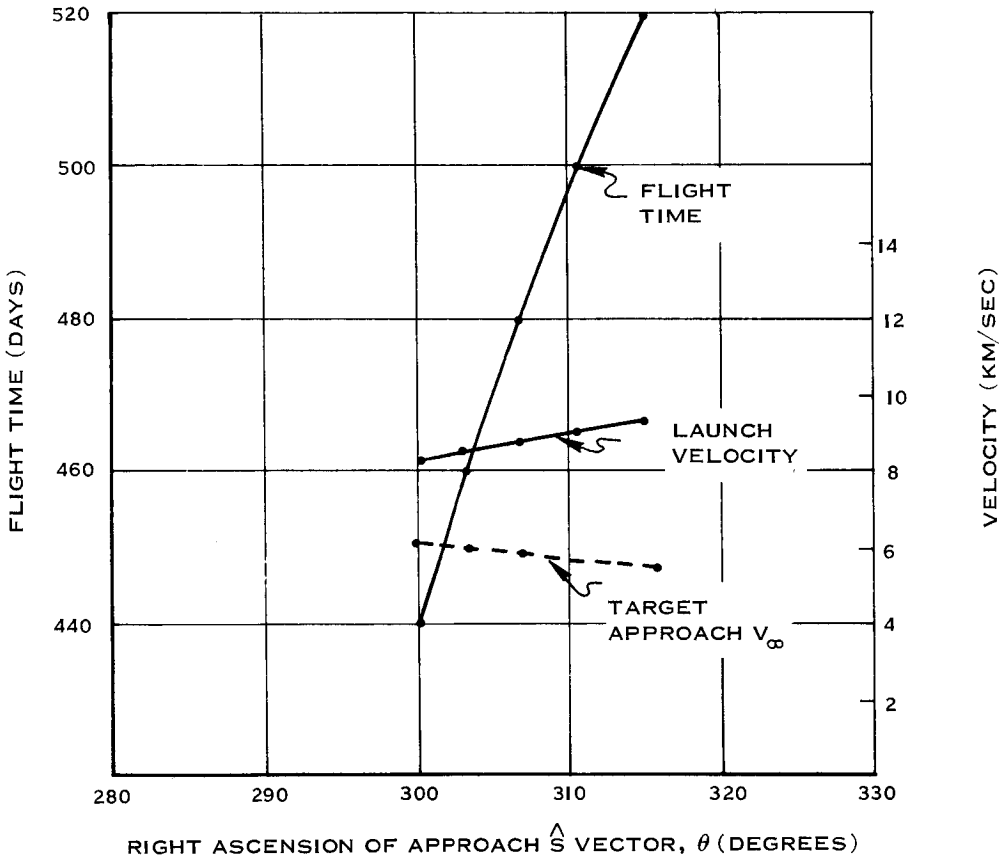

FIGURE 5-24A TRAJECTORY CHARACTERISTICS -270° TRANSFER, MARS-EARTH

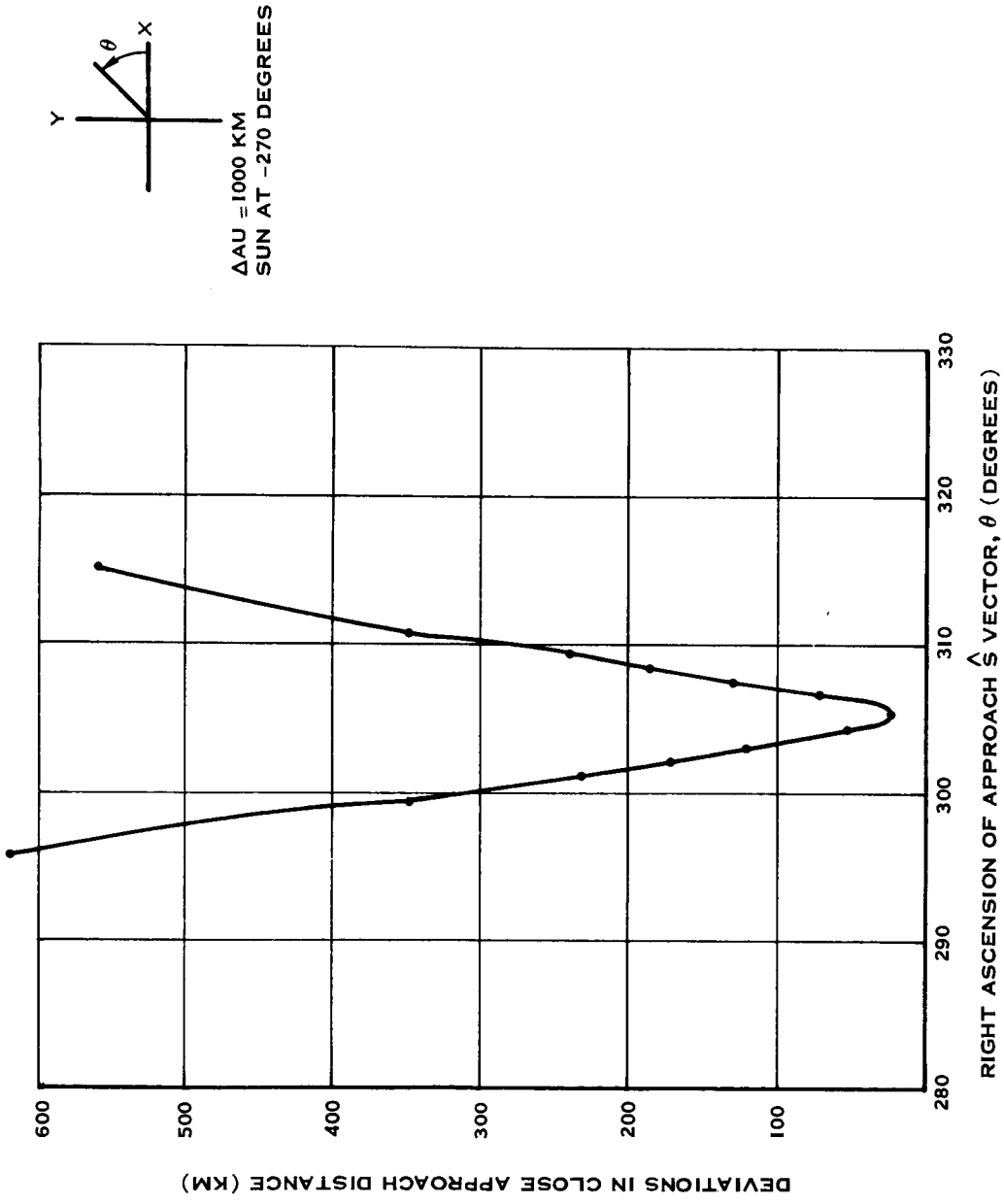

FIGURE 5-24B DEVIATIONS IN CLOSE APPROACH -270° TRANSFER, MARS-EARTH

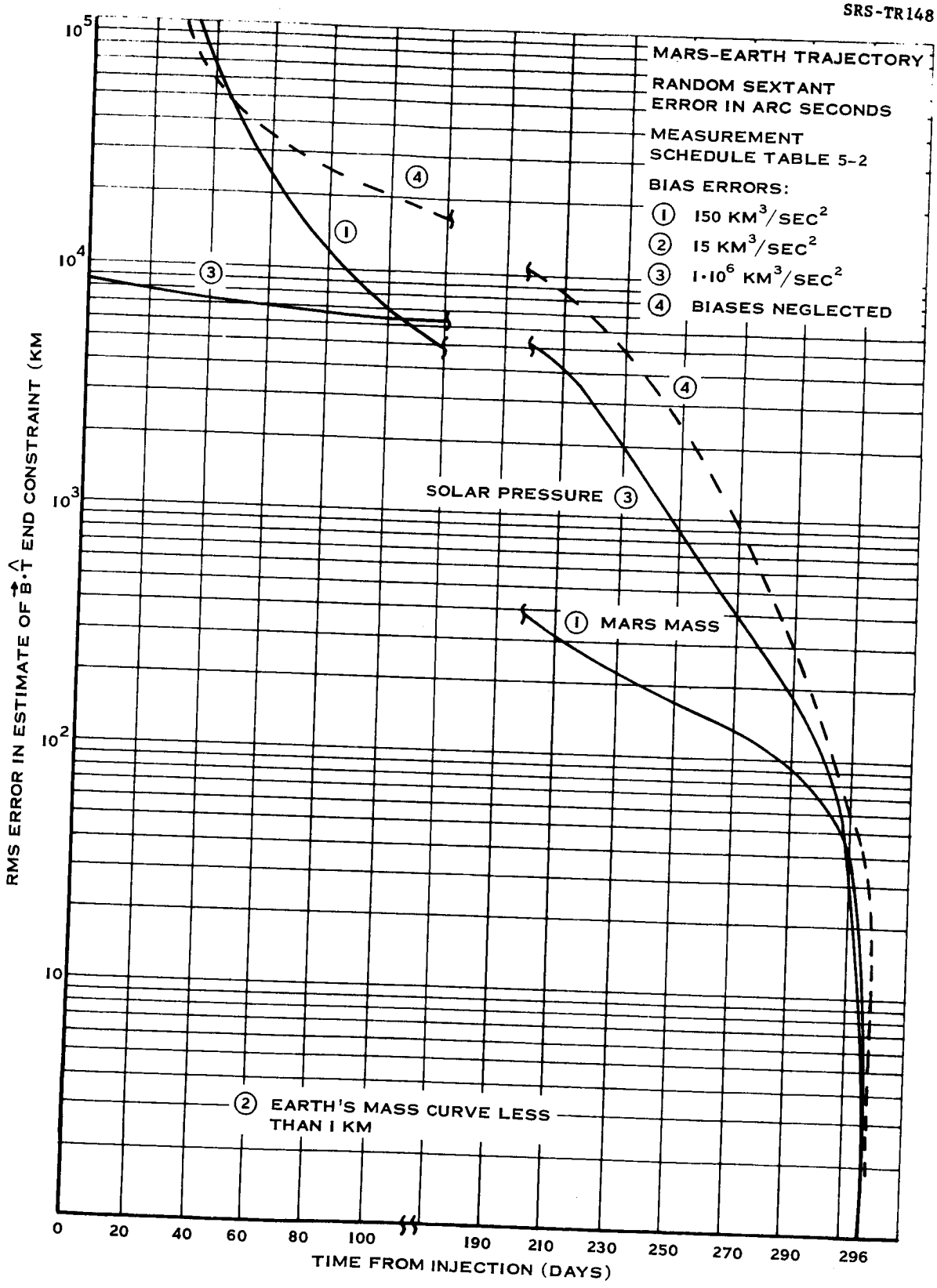

FIGURE 5-25A ERROR IN ESTIMATE OF $\vec{B}\cdot\hat{T}$ DUE TO NEGLECTING BIAS ERRORS

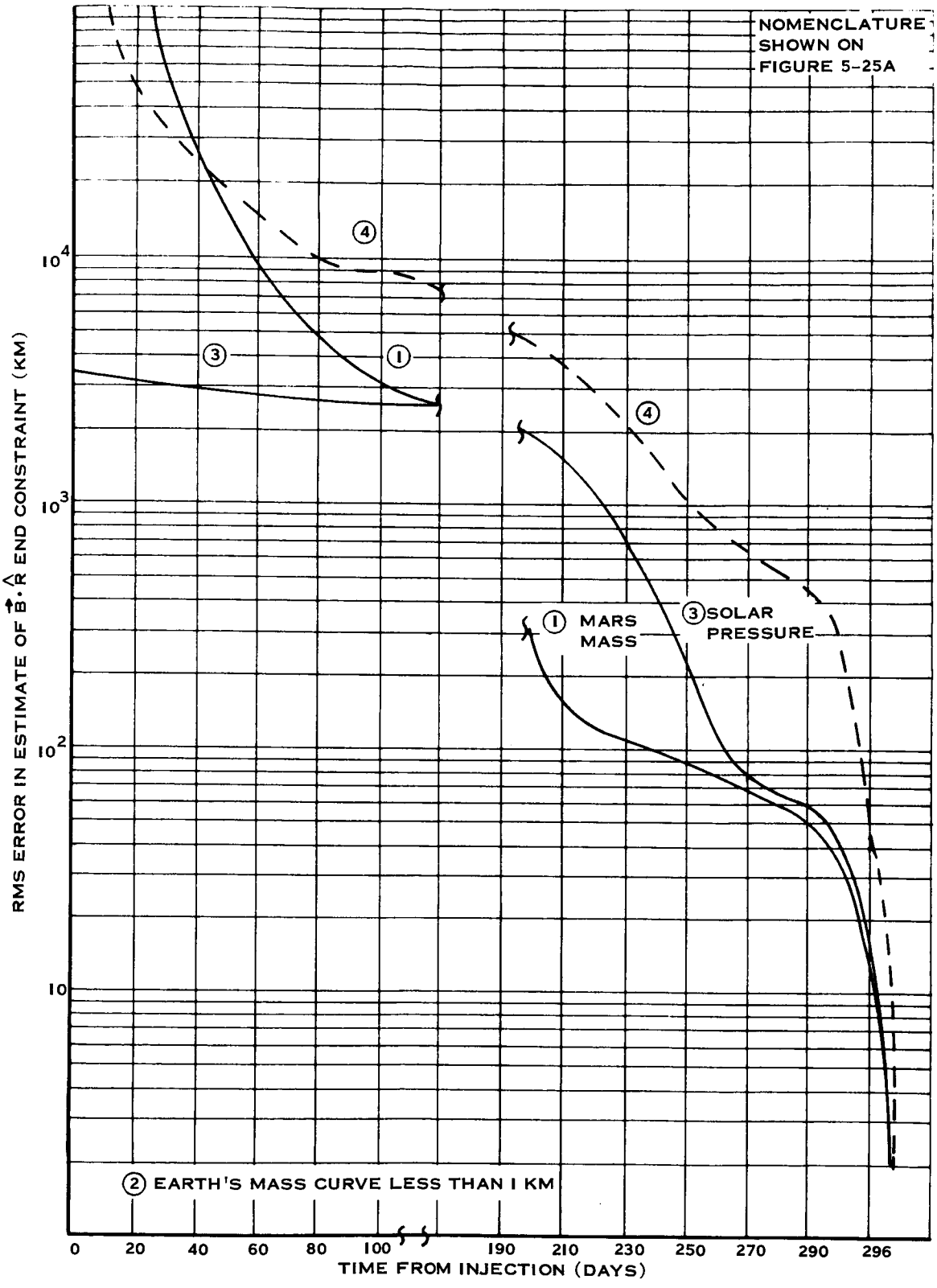

FIGURE 5-25B ERROR IN ESTIMATE OF $\vec{B}\cdot\hat{R}$ DUE TO NEGLECTING BIAS ERRORS

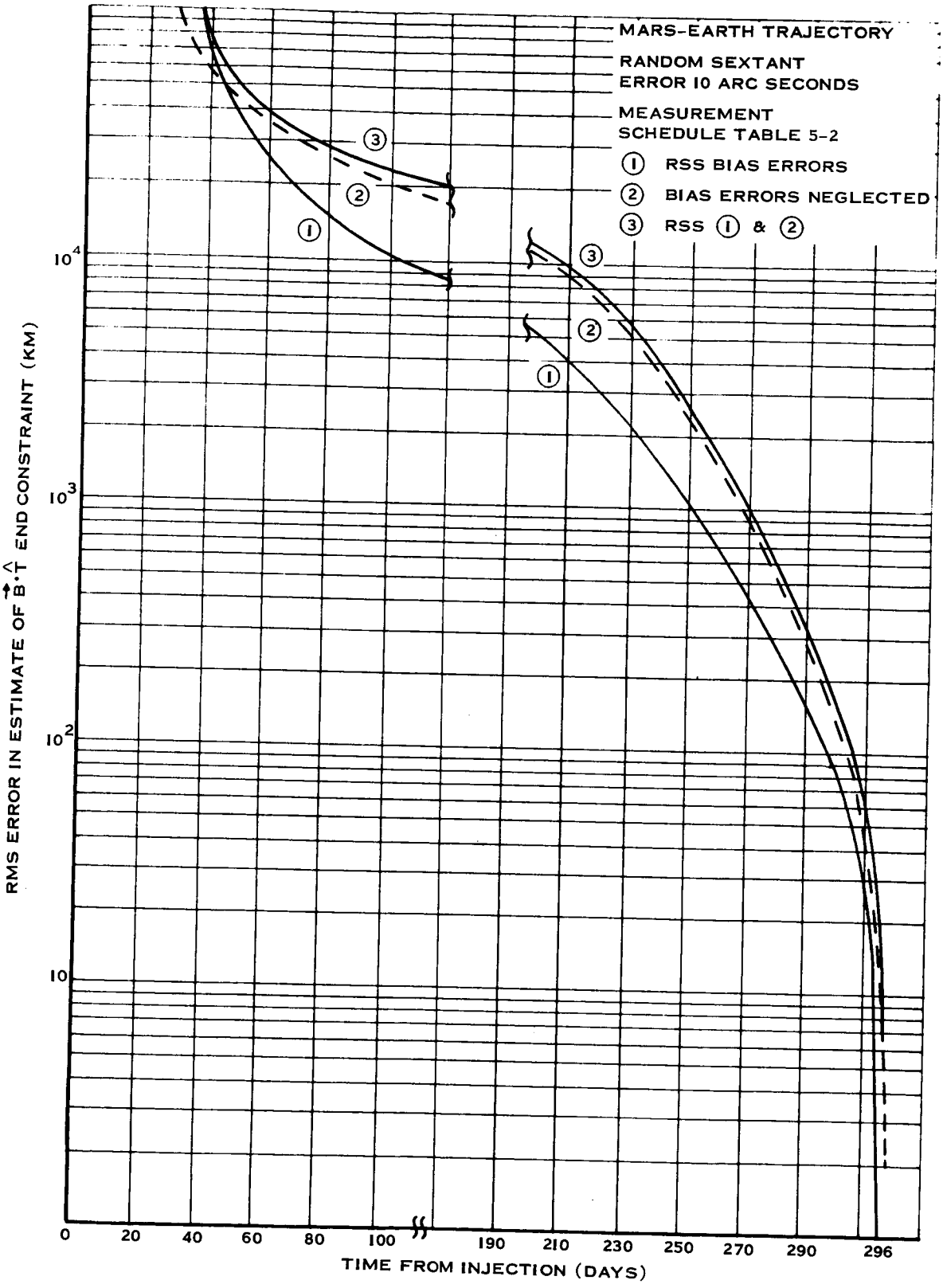

FIGURE 5-26A COMPOSITE EFFECT OF BIAS ERRORS ON $\vec{B}\cdot\hat{T}$ ESTIMATE

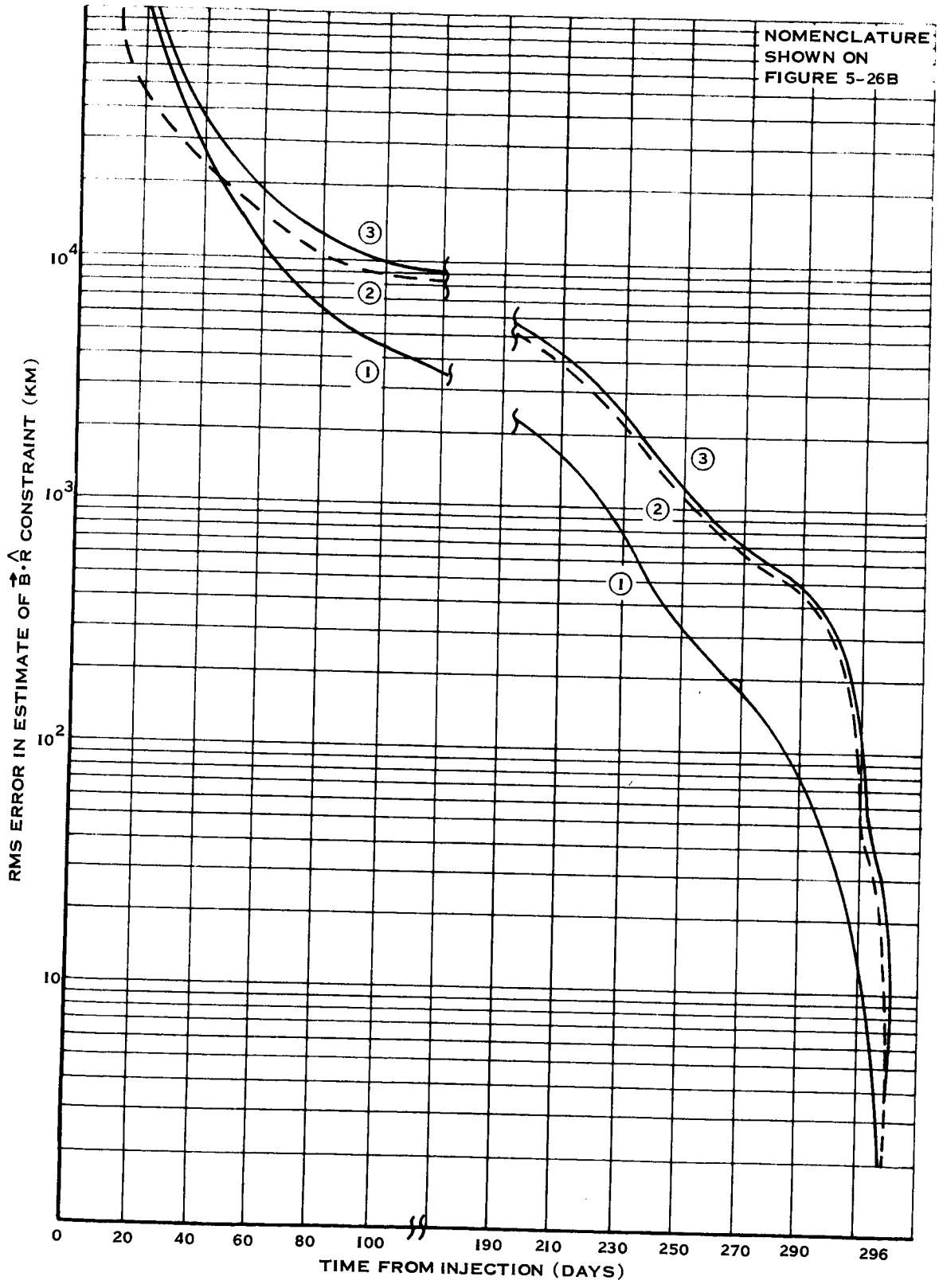

FIGURE 5-26B COMPOSITE EFFECT OF BIAS ERRORS ON $\vec{B}\cdot\hat{R}$ ESTIMATE

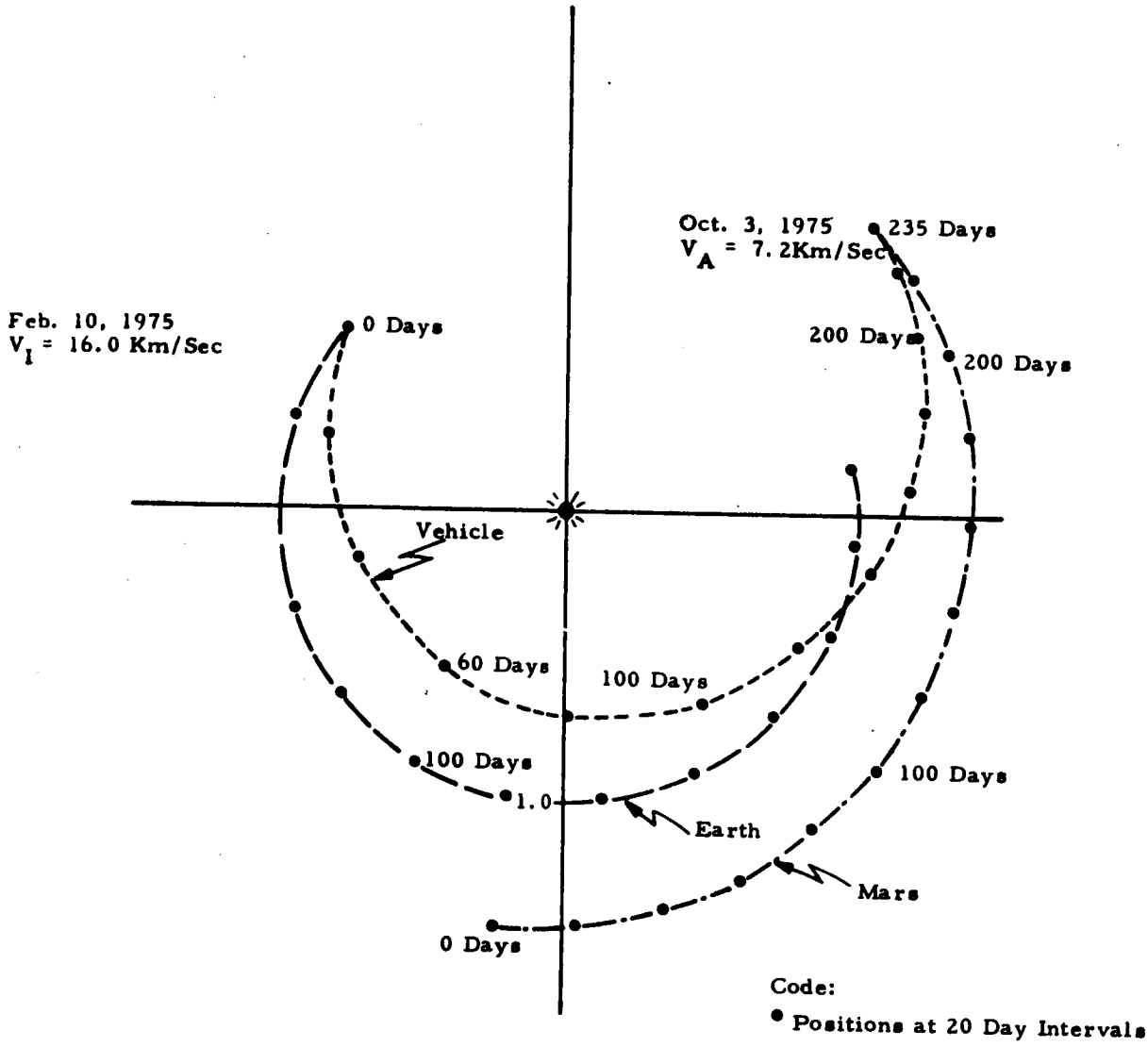

Figure B-1 Ecliptic Projection, Earth-Mars Trajectory

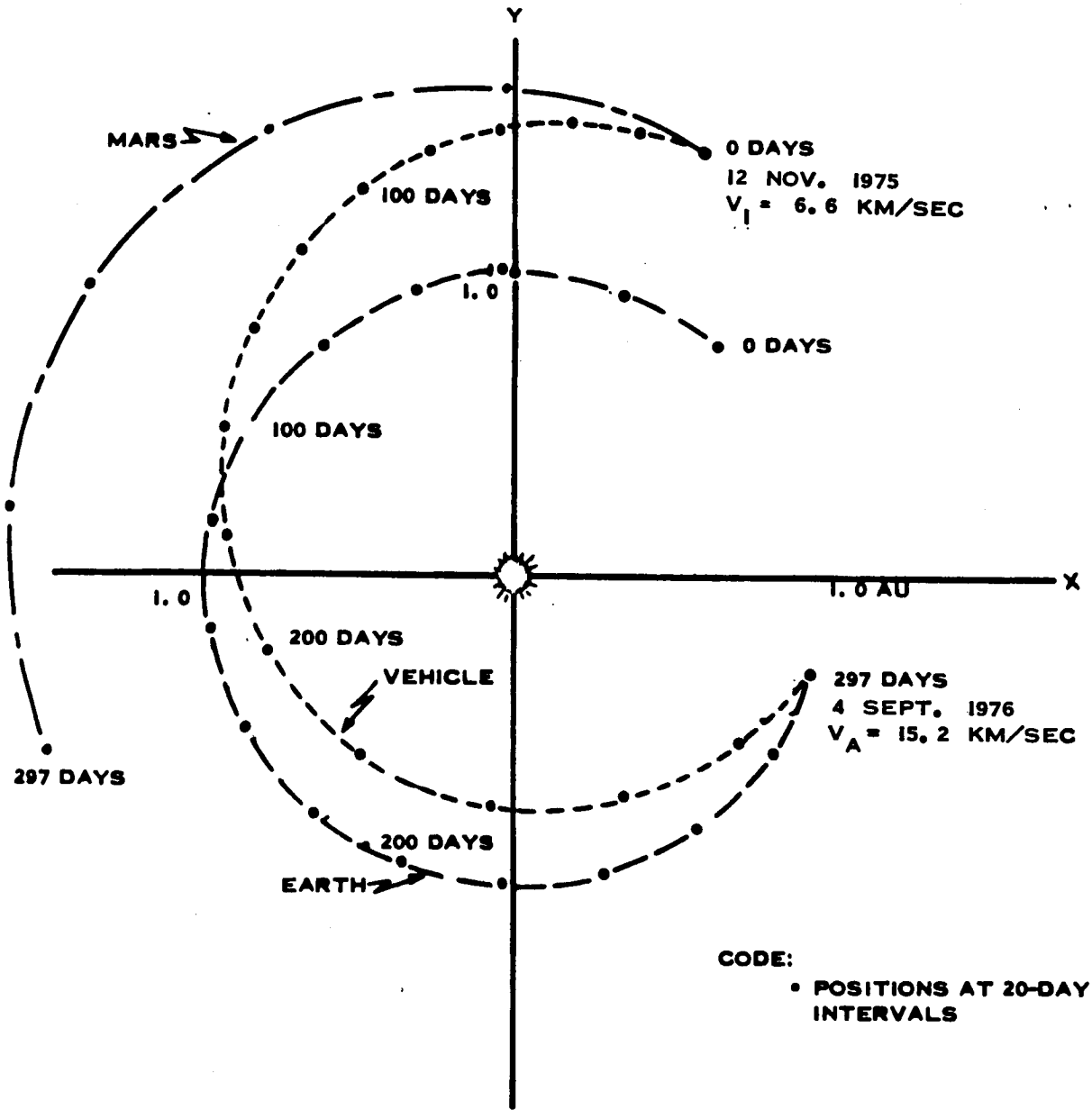

Figure B-2 Ecliptic Projection, Mars-Earth Trajectory

TABLE 3-1

MARS MASS (SUN'S MASS = 1)

Mars Mass (m^{-1})	Method	Author	Reference
3648000	Vesta	Leveau (1890)	(3)
3093500		Newcomb (1895)	(3)
3601280	Vesta	Leveau (1907)	(3)
3085000 ± 5000	Weighted Mean	de Sitter (1938)	(3)
3110000 ± 7700	Eros	Rabe (1949)	(3)
3079000 ± 5700	Deimos	Urey (1952)	(3)
3090000 ± 10000		Adopted (1961)	(3)
3088000 ± 3000	Weighted Mean	Clemence (1961)	(8)
3090000 ± 3000		Adopted (1963)	(8)

TABLE 3-2

EARTH + MOON MASS (Sun's Mass = 1)

Mass (m^{-1})	Method	Author	Reference
329390		Newcomb (1895)	(3)
327900±200	Weighted Mean	de Sitter (1938)	(3)
328390±103	Eros	Witt (1933)	(3)
328452±43	Eros	Rabe (1949)	(3)
328446±43	Eros Revised	E. Rabe (1954)	(3)
328440±40		de Vaucouleurs (1961)	(3)
328450±50		Adopted (1961)	(3)
328905.2±5		Adopted (1963)	(8)

TABLE 3-3

ASTRONOMICAL UNIT

A. U. (KM)	Method	Author	Reference
149662400 ± 25600	Eros (Geometric)	(1941) Jones	(4)
149530300 ± 10200	Eros (Dynamical)	(1950) Rabe	(4)
149598640 ± 250	Venus (Radar)	(1962) Muhleman et.al.	(5)
149597850 ± 400	Venus (Radar)	(1962) Pettingill et.al.	(5)
149598100 ± 400	Venus (Radar)	(1962) Muhleman (Revision of Pettingill's Value)	(5)
149601000 ± 5000	Venus (Radar)	(1961) Thompson,et.al.(GB)	(5)
149599500 ± 800	Venus (Radar)	(1961) Kotelnikov (USSR)	(5)
149599244 ± 278	Mariner II Tracking	(1963) Anderson,et.al.	(7)
149599000 ± 700	Recommended Value	(1963)	(8)

TABLE 5-1

SCHEDULE

TIME	BODY OBSERVED	INTERVAL OF OBS.	TOTAL NUMBER OF OBS.
$0\text{-}3^{h}$	Earth	15 Minutes	12
$3^{h}\text{-}1^{D}$	Earth	1 Hour	21
$1^{D}\text{-}90^{D}$	Sun	5 Days	18
$90^{D}\text{-}180^{D}$	Mars	5 Days	18
$180^{D}\text{-}230^{D}$	Mars	1 Day	50
$230^{D}\text{-}233^{D}$	Mars	6 Hours	12
$233^{D}\text{-}234^{D}$	Mars	1 Hour	24
$234^{D}\text{-}234^{D}18^{h}$	Mars	30 Minutes	36
$234^{D}\text{-}18^{h}\text{-}234^{D}20^{h}$	None	--	--
$234^{D}20^{h}\text{-}234^{D}22^{h}$	Mars	15 Minutes	8
$234^{D}22^{h}\text{-}235^{D}$	None	--	--
		TOTAL	199

TABLE 5-2

SCHEDULE

Time	Body	OBS Interval	Number of OBS
$0\text{-}6^h$	Mars	15 Minutes	24
$6^h\ \text{-}1^d$	Mars	1 Hour	18
$1^d\ \text{-}40^d$	Earth	2 Days	20
$40^d\ \text{-}242^d$	Earth	5 Days	40
$242^d\ \text{-}292^d$	Earth	1 Day	50
$292^d\ \text{-}295^d$	Earth	6 Hours	12
$295^d\ \text{-}296^d$	Earth	1 Hour	24
$296^d\ \text{-}296^d12^h$	Earth	30 Minutes	24
$296^d12^h\ \text{-}296^d14^h$	None	-------	--
$296^d14^h\ \text{-}296^d16^h$	Earth	15 Minutes	
$296^d16^h\ \text{-}296^d18^h$	None	-------	--
		Total Number of OBS	220

σ_N = 3.89 Km σ_V = 11.7 Km σ_W = .841 Km $\sigma_{\dot{N}}$ = 14.5 m/Sec $\sigma_{\dot{V}}$ = 5.02 m/Sec $\sigma_{\dot{W}}$ = 9.03 m/Sec

Normalized Covariance Matrix

	N	V	W	$\dot{N}$	$\dot{V}$	$\dot{W}$
N	1.0	-.723	0	.641	-.915	0
V		1.0	0	-.942	.901	0
W			1.0	0	0	-.011
$\dot{N}$				1.0	-.875	0
$\dot{V}$		Symmetric Matrix			1.0	0
$\dot{W}$						1.0

Table 5-3 Covariance Matrix in NVW Coordinates of State Deviations from Nominal at Injection (30 Minutes Park Time)

TABLE 5-4

INJECTION COVARIANCE MATRIX OF STATE DEVIATIONS FROM NOMINAL

σ_n = 17.3 Km, σ_v = 17.3 Km, σ_w = 17.3 Km,

$\sigma_{\dot{n}}$ = 17.3 m/sec, $\sigma_{\dot{v}}$ = 17.3 m/sec, $\sigma_{\dot{w}}$ = 17.3 m/sec

	n	v	w	$\dot{n}$	$\dot{v}$	$\dot{w}$
n	1	0	0	0	0	0
v		1	0	0	0	0
w			1	0	0	0
$\dot{n}$				1	0	0
$\dot{v}$	Symmetric Matrix				1	0
$\dot{w}$						1

TABLE 5-5

TYPICAL EARTH-MARS TRAJECTORIES

Transfer Trajectory	Flight Time (Days)	Heliocentric Angle (Deg)	Mars Approach Velocity (KM/SEC)
Hohmann	260	180	2.6
Mariner IV	228	160	3.1
Outbound of Round Trip	235	270	6.6

TABLE 6-1

GUIDANCE PERFORMANCE VTA GUIDANCE LAW

Correction	End Constraint Deviations (KM)		Δv Req'd M/Sec	Time
	$\vec{B}\cdot\hat{T}$	$\vec{B}\cdot\hat{R}$		
1	10300	2390	10.56	1^D
2	269	153	8.18	220^D
3	12.8	8.6	3.53	234^D
4	6.54	2.01	.92	$234^D 20^h$

TABLE 6-2

VELOCITY REQUIREMENTS WITH EQUATION OF MOTION UNCERTAINTIES

Correction	Δv Req'd M/Sec
1	10.56
2	8.18
3	3.53 10.00 (AU)
4	0.92 5.00 (μ) 3.00 (AU)
TOTAL	41.19